Differential Chaos Shift Keying Modulation for Cooperative and Spatial Diversity Communication Systems

Atul Kumar

Differential Chaos Shift Keying Modulation for Cooperative and Spatial Diversity Communication Systems

A

Thesis Submitted

in Partial Fulfilment of the Requirements

for the Degree of

DOCTOR OF PHILOSOPHY

By

Atul Kumar

Department of Electronics and Electrical Engineering

Indian Institute of Technology Guwahati

Guwahati - 781 039, INDIA.

April, 2015

To My Family

Certificate

This is to certify that the thesis entitled "**Differential Chaos Shift Keying Modulation for Cooperative and Spatial Diversity Communication Systems**", submitted by **Atul Kumar** (10610227), a research scholar in the *Department of Electronics & Electrical Engineering, Indian Institute of Technology Guwahati*, for the award of the degree of **Doctor of Philosophy**, is a record of an original research work carried out by him under my supervision and guidance. The thesis has fulfilled all requirements as per the regulations of the institute and in my opinion has reached the standard needed for submission. The results embodied in this thesis have not been submitted to any other University or Institute for the award of any degree or diploma.

Dated:

Guwahati.

Dr. Pravas Ranjan Sahu
Associate Professor
Dept. of Electronics & Electrical Engg.
Indian Institute of Technology Guwahati
Guwahati - 781039, Assam, India.

Acknowledgements

I would like to express my sincere gratitude to my supervisor, Dr. Pravas Ranjan Sahu, for his excellent guidance and support throughout the course for this work. His kindness, dedication, friendly accessibility and attention to detail have been a great inspiration to me. My heartfelt thanks to him for the unlimited support and patience shown to me. I would particularly like to thank for all his help in patiently and carefully correcting all my manuscripts.

I would like to thank my doctoral committee members Prof. R. Bhattacharjee, Dr. A. Rajesh and Dr. S. Ranbir Singh for sparing their precious time to evaluate the progress of my work. Their suggestions have been valuable. I would also like to extend my thanks to other faculty members of the department for their kind help during my academic studies. My special thanks to Mr. Sanjib Das and all the members of the Communication Laboratory for maintaining an excellent computing facility and providing various resources useful for the research work.

I had a great time with my many friends at IIT Guwahati, including Vinay, Brijesh, Parveen, Somen, Shivanshu and Anand and the list goes on. I thank them for their support and encouragement. The company of my friends at IIT Guwahati proved to be a great asset which helped me stay relaxed during throughout my research.

I also grateful acknowledge MHRD, Govt. of India for financing my studies at IIT Guwahati. Finally, I would like to thank the Almighty God for bestowing me this opportunity and showering his blessings on me to come out successful against all odds.

Atul Kumar

Abstract

Chaotic signals are unstable and aperiodic, making them naturally harder to identify and predict. It has wideband characteristic, it is resistant against multipath fading and it offers a cheaper solution to traditional spread spectrum systems. In this thesis, the performance of differential chaos shift keying (DCSK) modulation is analyzed in different wireless communication scenarios. First, a relay selection based DCSK cooperative diversity scheme, namely DCSK selection relaying (DCSK-SR) scheme is proposed. The relay which maximizes the total received signal-to-noise ratio (SNR) at the destination is selected from a multiple multiple-input multiple-output (multiple MIMO) relay cluster to cooperate with the source node. Mathematical expression for the probability density function (PDF) of SNR for each hop and end-to-end bit error rate (BER) is derived. Secondly, a spectrum and energy efficient DCSK bidirectional relaying (DCSK-BDR) scheme is proposed in which two source nodes exchange their information through a relay node. The end-to-end BER expression for the DCSK-BDR scheme is derived. Thirdly, DCSK modulation based transmit antenna selection (TAS) schemes are proposed to reduce the effect of signal fading with less hardware complexity at the receiver. Based on receiver structure/specifications, DCSK-TAS, DCSK-joint antenna selection (DCSK-JAS) and DCSK-transmit antenna selection/equal gain combining (DCSK-TAS/EGC) schemes are proposed. BER and throughput of the proposed schemes are derived and evaluated over Nakagami-m fading channels. Finally, a high-data-rate DCSK scheme based on spatial modulation (SM), spatially modulated DCSK (SM-DCSK) is proposed. Analytical expression for the symbol error rate (SER) of the SM-DCSK scheme is derived. All the expressions derived in the thesis are validated by Monte Carlo simulation results.

Contents

List of Figures

List of Tables

Chapter 1

Introduction

The discovery of randomness in apparently predictable physical systems have evolved into a new science, the science of chaos. Chaos is usually referred as state of disorder, however, there is order in chaos; randomness has an underlying geometric form [1]. The phenomenon of chaos emerges from the deterministic nonlinear dynamical systems. Chaos describes the apparently complex behavior of simple, well-behaved systems. Chaotic behavior looks like erratic and almost random; almost like the behavior of a system strongly influenced by outside or random noise [2]. Chaos imposes fundamental limits on prediction, but it also suggests causal relationships where none were previously suspected.

Historically, the study of chaos is strongly rooted in the mathematical study of nonlinear dynamics, going back, at least, to the Poincaré's work [3]. Poincaré discovered the homoclinic trajectories in the state space. It was later proved that Poincaré's homoclinic trajectories are chaotic limit sets. Chaos in electrical circuits was first observed by Van der Pol and Van der Mark. They studied the behavior of a driven neon bulb oscillator circuit and reported the observation as 'often an irregular noise is heard' in the circuit. Lorenz studied a simplified model for thermal convection numerically, known as Lorenz model [4]. Lorenz model consisted of a completely deterministic system of three nonlinearly coupled ordinary differential equations. For this simple deterministic system with bounded solutions, it is found that nonperiodic solutions are ordinarily unstable with respect to small modifications, so that slightly differing initial states can evolve into considerably different

states. Chua discovered a simple electronic circuit, known as Chua's circuit, for synthesizing the specific third-order piecewise-linear ordinary differential equations [5, 6]. In fact, this remarkable circuit is the only physical system for which the presence of chaos has been proven mathematically. Inspired by these results, the behavior of nonlinear systems has been studied in different disciplines including bio-systems, meteorology, cosmology, economics, population dynamics, chemistry, physics, mechanical and electrical engineering, etc.

The application of chaotic signals for communication purpose is possible due to three fundamental research observations. The first was the implementation and characterization of several electronic circuits exhibiting chaotic behavior [7, 8]. This brought chaotic systems from mathematical abstraction into application in electronic engineering. The second was the observation made by Pecora and Carroll that two chaotic systems can be synchronized under suitable coupling or driving conditions [9]. This suggested that chaotic signals could be used for communication, where their noise like broadband nature could improve disturbance rejection and security. The third step was the awareness that chaotic systems exhibit a mixed deterministic/stochastic nature [10–12]. A brief review of the chaos-based communications is presented in the next section.

1.1 Overview of Chaos-Based Communications

1.1.1 Chaos

Chaotic signals are bounded, aperiodic and random-like signals generated from deterministic nonlinear dynamical systems. A dynamical system has a fixed number of independent state variables, whose motions or trajectories are governed by a set of differential equations involving all the state variables. Let us consider discrete-time representation of a dynamical system to understand the generation of chaotic signals. In discrete-time rep-

resentation, the state variables of the system are sampled at fixed time intervals and the dynamics of the system is described by

$$x_n = f\left(x_{n-1}, \mu\right), \tag{1.1}$$

where x_n is the vector of state variables sampled at the nth sampling instant, $f(\cdot)$ is the iterative function that describes the dynamics of the system and μ is the vector of parameters that affect the system's dynamics.

1.1.2 Properties of Chaos

The chaotic signals are typically broadband, noise-like and difficult to predict. Some important properties of chaotic signals are as follows

1. Chaotic signals are very sensitive to initial conditions, i.e., two trajectories starting from nearby initial conditions quickly become uncorrelated. Thus, by changing the initial conditions, theoretically, an infinite number of uncorrelated chaotic signals can be generated.

2. Chaotic signals have impulse-like auto-correlation and very small cross-correlation. The power spectrum of chaotic signals is white wideband.

3. Forecast of long-term behavior of a chaotic signal is not possible.

4. For given conditions or control parameters, chaos is entirely self-generated. No external noise or random variable is required to introduce.

5. Chaotic signals are bounded within a finite range.

1.1.3 Application of Chaos to Communications

Chaotic signals are wideband, aperiodic and unpredictable over long duration of time and hence well suited for spread-spectrum communication. The chaotic signals have all

the advantages of spread-spectrum signals such as mitigation of multipath fading, anti-jamming, suppression of inter-user interference, secure communication, etc. [3]. Furthermore, chaotic signals can be generated using very simple circuitry. Chaotic signals are sensitive to initial conditions and hence by changing the initial condition, a large number of spreading waveforms can be generated. Unlike pseudo-random generator, chaotic system has an infinite number of analog states and hence, the chaotic signal never repeats itself. Chaos based communication does not require additional spreading and de-spreading circuitry. Thus, chaos offers potentially cost-effective alternative for spread-spectrum communications [13].

1.1.4 Chaotic Digital Modulation Techniques

Chaotic digital modulation techniques use chaotic signal as carrier. In particular, the digital information is mapped to chaotic signals. Since chaotic carrier is aperiodic, the sample function for each symbol is different. Thus, the transmitted waveform is never periodic, even if the same symbol is transmitted repeatedly [14].

In chaotic communication systems, detection methods can be broadly classified into two categories; coherent and non-coherent detection. Coherent systems require an exact replica of the chaotic carrier used to modulate the information to be reproduced at the receiver. Through a synchronization process, the replica of chaotic carrier is recovered from the received signal. However, for the required signal-to-noise conditions, the robust chaotic synchronization is not practically possible yet. Thus, the reproduction of replica of chaotic carrier remains major challenge for practical implementation of coherent chaotic systems. If the replica of chaotic carrier is assumed to be available at the receiver, the coherent chaotic systems provide the benchmark performance to other sub-optimum systems under chaotic communication. Non-coherent systems do not require exact replica of the chaotic signals and chaotic synchronization at the receiver and hence represent more

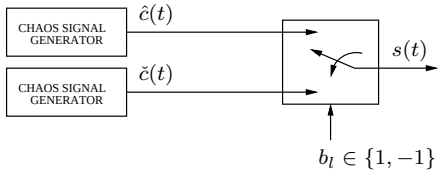

(a) CSK modulator

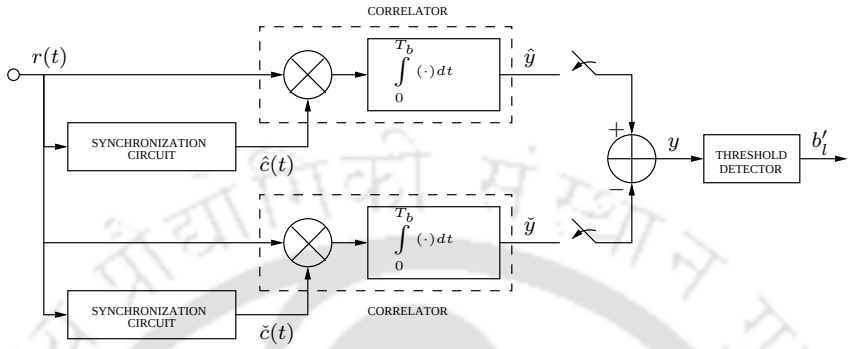

(b) CSK demodulator

Figure 1.1: Block diagram of CSK modulation and demodulation.

practical forms of systems.

In recent years, various chaotic digital modulation schemes have been proposed in literature. Among which chaos shift keying (CSK) and differential chaos shift keying (DCSK) are the most popular. In the following, a brief review of various chaotic digital modulation techniques is presented.

Chaos Shift Keying

CSK maps each symbol to a different chaotic attractor [15]. The attractors are generated either from a set of different dynamical systems or from a dynamical system with different initial conditions. The block diagram of a typical CSK modulator is shown in Figure 1.1(a). The modulator consists of two chaotic signal generators, producing signals $\hat{c}\,(t)$ and $\check{c}\,(t)$. For transmission of '+1' and '−1', the chaotic signals $\hat{c}\,(t)$ and $\check{c}\,(t)$ are

transmitted, respectively. Mathematically

$$s(t) = \begin{cases} \hat{c}(t), & b_l = +1 \\ \check{c}(t), & b_l = -1 \end{cases}. \tag{1.2}$$

Coherent demodulation of CSK uses a correlator-based receiver [16], as shown in Figure 1.1(b). The reproduced chaotic signals are correlated with the received signal and the output of the correlators are compared. If T_s is the acquisition time, the output of the correlators are given by

$$\begin{aligned} \hat{y} &= \int_{T_s}^{T_b} r(t)\,\hat{c}(t)\,dt \\ \check{y} &= \int_{T_s}^{T_b} r(t)\,\check{c}(t)\,dt, \end{aligned} \tag{1.3}$$

where $r(t)$ is the received signal. The input to the threshold detector is

$$y = \hat{y} - \check{y}. \tag{1.4}$$

The decision is taken in favor of '+1' if y is positive otherwise '−1' is decoded.

Some variants of CSK are presented in the literature, as summarized below

■ **Antipodal CSK**

Antipodal CSK modulator uses only one chaotic signal generator, which generates the signal $c(t)$. For transmission of '+1', $c(t)$ is transmitted whereas an inverted version of $c(t)$ is transmitted for '−1' [17, 18]. Hence, the transmitted signal can be expressed as

$$s(t) = \begin{cases} c(t), & b_l = +1 \\ -c(t), & b_l = -1 \end{cases}. \tag{1.5}$$

For coherent demodulation of antipodal CSK, the received signal is correlated with the reproduced chaotic signal. The output of the correlator can be given by

$$y = \int_{T_s}^{T_b} r(t)\,c(t)\,dt. \tag{1.6}$$

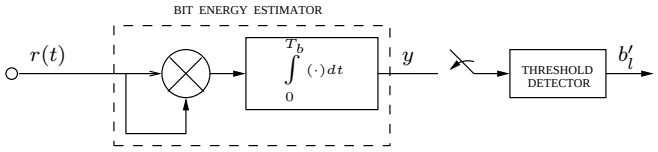

Figure 1.2: Block diagram of non-coherent CSK demodulator.

The output of the correlator is passed through a threshold detector, which is set at zero. If y is greater than zero, '+1' is decoded, otherwise '−1' is decoded.

■ Non-Coherent CSK

Non-coherent detectors are considered as more practical as they do not require an exact replica of the chaotic signals at the receiver [16]. The block diagram of CSK modulator is presented in Figure 1.1(a). Here, the chaotic signals $\hat{c}(t)$ and $\check{c}(t)$ are chosen with different bit energies. The block diagram of non-coherent CSK demodulator is shown in Figure 1.2, which is basically a bit energy estimator. The output of the correlator is given by

$$y = \int_0^{T_b} r^2(t)\,dt. \tag{1.7}$$

For high signal-to-noise ratio (SNR), y can be approximated as

$$y = \begin{cases} \int_0^{T_b} \hat{c}^2(t)\,dt, & b_l = +1 \\ \int_0^{T_b} \check{c}^2(t)\,dt, & b_l = -1 \end{cases}. \tag{1.8}$$

By setting the threshold of the detector at the mid-value of the bit energies, the received symbols can be decoded correctly. However, the threshold will shift with the noise level in a noisy environment and this threshold-shift problem remains a major drawback of non-coherent CSK systems.

Differential Chaos Shift Keying

Differential chaos shift keying modulation scheme uses a differential shift keying modulator and non-coherent detection [19]. The block diagram of binary DCSK modulator is shown in Figure 1.3(a). In DCSK modulation, each bit period is divided into two equal time slots. In the first time slot, the reference segment of chaotic signal is transmitted whereas in the second time slot, the data segment is transmitted. The data segment is same as the reference segment for transmitting bit '1', and an inverted version of reference segment is transmitted for transmitting bit '0' [14], i.e.,

$$s(t) = \begin{cases} c(t), & 0 \leq t \leq \frac{T_b}{2} \\ \pm c(t - \frac{T_b}{2}), & \frac{T_b}{2} \leq t \leq T_b \end{cases}, \tag{1.9}$$

where T_b is the bit duration and $c(t)$ is the chaotic signal.

The block diagram of binary DCSK demodulator is shown in Figure 1.3(b), which uses a suboptimal autocorrelation receiver (AcR). At the demodulator, the reference segments are correlated with the corresponding data segments. The output of the correlator at the end of the bit duration is

$$y = \int_{T_b/2}^{T_b} r\,(t)\, r\left(t - \frac{T_b}{2}\right) dt, \tag{1.10}$$

where $r(t)$ is the received signal at the input of AcR. The output of the correlator is passed through a threshold detector whose threshold value is set to zero. The decision is made in favor of bit '1' or '0' depending on whether y is greater or less than zero.

Other Modulation Techniques

Several variations of CSK and DCSK schemes are proposed in literature. A brief review on some important CSK or DCSK variants is presented here.

■ **Chaotic On-Off Keying**

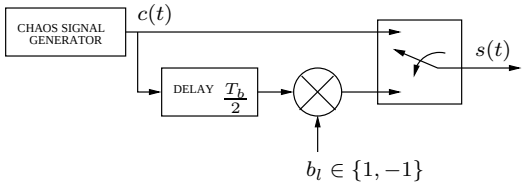

(a) DCSK modulator

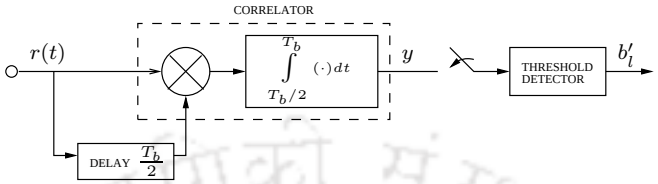

(b) DCSK demodulator

Figure 1.3: Block diagram of DCSK modulation and demodulation.

Chaotic on-off keying (COOK) requires only one chaotic signal for modulation. The transmission of '+1' and '−1' are simply represented by transmission of chaotic carrier and no transmission, respectively [16]. COOK demodulation can be accomplished by using a coherent or non-coherent receiver. The methodology of coherent and non-coherent detection is discussed in the previous section.

■ **Frequency-Modulated DCSK**

To overcome the problem of varying bit energies of DCSK signal, frequency-modulated DCSK (FM-DCSK) modulation scheme is proposed by Kolumbán *et al.* in [20]. In this scheme, the chaotic signal is first passed through a frequency modulator to generate a chaotic FM signal. DCSK modulation is then performed using this chaotic FM signal. Since, chaotic FM signal has a constant amplitude, the energy of FM-DCSK signal remains the same for all bits. FM-DCSK demodulator is same as the DCSK demodulator. Because of constant bit energy, the FM-DCSK scheme achieves a better bit error performance than the DCSK scheme.

■ **Correlation Delay Shift Keying**

In DCSK modulation, the reference signal and the information-bearing signal are transmitted separately, which results in reduced data-rate. Correlation delay shift keying

(CDSK) modulation is proposed by Sushchik *et al.* in [21], to transmit the information continuously and enhance the bandwidth efficiency. In CDSK, the transmitted signal is the sum of the chaotic reference signal and information-bearing signal. Furthermore, the delay is not necessarily equal to half the symbol period.

The CDSK demodulator is similar to the DCSK demodulator. Because of non-zero correlation between the chaotic signal and the delayed version of it, there is more uncertainty at the correlator output and the bit error performance degrades in comparison to the DCSK scheme.

■ **Symmetric Chaos Shift Keying**

Symmetric chaos shift keying (SCSK) can be considered as a subclass of antipodal chaos shift keying [21]. SCSK uses a matched nonlinear system to reconstruct the reference signal, thus eliminating the need for transmitting it over the communication channel and simplifying the transmitter design. The chaotic system in the transmitter is represented by

$$\mathrm{x}_{i+1} = \mathrm{F}(\mathrm{x}_\mathrm{i}), \tag{1.11}$$

where x_i is the internal state vector. The transmitted signal is the first component of this vector multiplied by the information signal $b_l = \pm 1$, i.e., $s_i = b_l x_i$.

At the receiver, s_i is used to drive a matched chaotic system

$$\mathrm{y}_{i+1} = \mathrm{G}(|\mathrm{s}_\mathrm{i}|, \mathrm{y}_\mathrm{i}). \tag{1.12}$$

Thus, the systems $\mathrm{F}(\cdot)$ and $\mathrm{G}(\cdot)$ form a drive-response system with $\mathrm{x_i}$ and $\mathrm{y_i}$ being the coupling pair. In a noise-free case, the output of the chaotic system in the receiver is the same as the output of the chaotic system in the transmitter. Thus, by correlating the received signal with reconstructed reference signal, the transmitted symbol can be decoded by observing the sign of the correlator output at the end of each symbol period.

■ **Quadrature Chaos Shift Keying**

Quadrature chaos shift keying (QCSK) is a multilevel version of DCSK, characterized by an increased data-rate with respect to DCSK, with the same bandwidth occupation [22]. In QCSK, to send a symbol, the chaotic reference signal is transmitted in first half symbol period and in the second half the information-bearing chaotic signal is transmitted. The Hilbert filter is used to generate the orthogonal signal of the chaotic reference signal. The QCSK transmitted signal can be expressed as

$$s(t) = \begin{cases} c_x(t), & 0 \leq t \leq \frac{T}{2} \\ a_s c_x(t - \frac{T}{2}) + b_s c_y(t - \frac{T}{2}), & \frac{T}{2} \leq t \leq T \end{cases}, \tag{1.13}$$

where $c_x(t)$ is the chaotic signal generated from chaos generator, $c_y(t)$ is the corresponding orthogonal chaotic signal generated by Hilbert filter, T is the symbol period, a_s and b_s depend on signal constellation.

At the receiving end, $\tilde{c}_x(t)$ and $\tilde{c}_y(t)$ are first recovered from the received signal. Then, the demodulation can be done by correlating the information-bearing received signal with recovered signals $\tilde{c}_x(t)$ and $\tilde{c}_y(t)$. Based on correlator outputs, the symbol can be decoded by an appropriate decision making algorithm.

1.2 Motivation

DCSK modulation has been shown to possess some unique advantages over other chaotic modulation techniques, such as

- DCSK demodulation is based on non-coherent detection and hence, an exact replica of chaotic sequence and chaotic synchronization are not required at the receiver.
- There is no threshold-shift problem in DCSK demodulation. The threshold of the detector is independent of the noise level.
- DCSK is less sensitive to channel distortion as the channel usually does not vary

much within a symbol period and thus, both the reference and data samples get subjected to same distortion.

- Using a simple AcR, DCSK obtains the multipath diversity without requiring channel state information (CSI).

Motivated by the above mentioned advantages, we investigated the performance of DCSK modulation in different wireless communications scenarios.

1.3 Literature Survey

The performance of DCSK system under an additive white Gaussian noise (AWGN) environment has been studied in [21,23–25]. Sushchik *et al.* analyzed the bit-error-rate (BER) of DCSK modulation in [21], assuming decision variable was Gaussian approximated. An exact analysis of BER for DCSK modulation is reported in [23], which describes the decision variable as non-central F distributed. To improve the accuracy of the BER estimation, [24] proposed a method based on variable bit energy of the chaotic sequence in the calculation. By using the non-central F distribution of the decision variable and assuming variable bit energy of the chaotic sequence in the calculation, an accurate analysis of BER for DCSK system is proposed in [25].

Multiple access DCSK system has been widely studied in [26–31]. In [26], a time-delay-based multiple access DCSK (MA-DCSK) system is proposed. A Walsh function based multiple access DCSK system is proposed in [27]. Lau *et al.* studied a multiple access DCSK technique which is based on different separation between the reference and data samples for different users [28, 29]. In [30], a permutation-based multiple access DCSK system is proposed. For more accurate performance analysis of multi-user DCSK system, a dynamically improved Gaussian approximation (DIGA) is developed in [31].

Performance of DCSK modulation is analyzed over Rayleigh and Ricean fading chan-

nels in [32]. The authors considered a frequency-nonselective slowly fading channel for analysis. An exact BER analysis of DCSK system is reported in [33, 34], for frequency-nonselective fading channel, considering the non-central F distribution of the decision variable. The performance is investigated in Nakagami-m, Rayleigh and Rician fading channels. BER of DCSK modulation in a multipath fading channel incorporating multipath fading for each path with delay spread is derived in [35].

Multiple antenna system or generally called multiple-input multiple-output (MIMO) system improves the capacity and reliability of wireless communication significantly. Recently, many research works addressing DCSK modulation in MIMO system are reported in literature. In [36], a novel MIMO-DCSK scheme is proposed, in which the BER performance of DCSK modulation is investigated in MIMO wireless channels by implementing Alamouti space-time codes. Analysis of DCSK modulation with Alamouti space-time codes is further explored in [37, 38]. In [39], multicode transmission with equal gain combining (MC-EGC) and stochastic gradient method based beamforming (SG-BF) schemes are proposed. By combining the benefits of space-time block code (STBC) and DCSK modulation, a novel analog STBC-DCSK scheme is proposed in [40], which offers better system performance and robustness against multipath fading delay spread.

Application of DCSK modulation in cooperative communication systems with decode-and-forward (DF) protocol can be found in [41–44]. In [42], DCSK cooperative communication (DCSK-CC) system is proposed in which co-mobile users' antenna is used to achieve the space diversity. Compared to DCSK-CC which is based on user-cooperation, a better BER performance can be obtained using DCSK cooperative diversity (DCSK-CD) systems [43], which employ a MIMO relay to cooperate with the source node. In [44], the BER performance of DCSK modulation is analyzed for opportunistic relaying system in a two-ray Rayleigh fading environment. In [45], a low-complexity amplify-and-forward (AF) relaying scheme is proposed for DCSK system.

In DCSK, half of the bit duration is used in sending the reference sequences. This

results in the reduced data rate compared to other modulation techniques having same bandwidth. Various methods have been proposed in literature to improve the data rate of DCSK [21, 22, 46–51]. Multilevel version of DCSK, quadrature chaos shift keying (QCSK) is proposed to achieve the higher data rate [22]. Correlation delay shift keying (CDSK) [21] and generalized-CDSK [46] obtain double data rate since they do not send the reference sequence for each bit. In [47], High-data-rate code-shifted DCSK (HCS-DCSK) is designed to increase data rate by using the orthogonal property of different chaotic sequences. By recycling the reference sequences in DCSK, high-efficiency DCSK (HE-DCSK) [48] is able to get increased data rate. Reference-modulated DCSK (RM-DCSK) [49] achieves double attainable bit rate by using the chaotic sequence sent in each time slot as the reference sequence for the next data bit to be transmitted. Multi-carrier DCSK (MC-DCSK) proposed in [50] obtains a higher data rate by using multiple orthogonal subcarrier. In [51], a phase-separated DCSK (PS-DCSK) modulation scheme is proposed, which is a simple delay-component-free version of DCSK modulation. In PS-DCSK, the reference and information-bearing signals are transmitted simultaneously after being separated by orthogonal sinusoidal carriers and thus, achieves a doubled attainable data-rate.

1.4 Problem Formulation

Based on the discussion presented in the previous section, we feel that analysis of DCSK modulation in different wireless communication systems can be a potential area of research. Hence, in this thesis, we consider the following problems for analysis, as stated below.

1. Performance analysis of relay selection based DCSK cooperative diversity scheme in which the best relay is selected from a MIMO relay cluster to cooperate with the source node.

2. Performance analysis of spectrum and energy efficient DCSK bidirectional relaying (DCSK-BDR) scheme.

3. Performance analysis of DCSK modulation based transmit antenna selection (TAS) schemes.

4. Improving the data-rate of DCSK system using spatial modulation (SM) transmission strategy.

For the above stated problems, we focus on the performance evaluation of DCSK modulation in different wireless communication systems.

1.5 Thesis Contributions

The important contributions of the thesis are stated below:

1. Performance of DCSK modulation with post-detection equal gain combiner (EGC) at the receiver, i.e., DCSK-EGC, is analyzed.
   (a) The conditional error probability expression for DCSK-EGC is derived.
   (b) The average BER expression of DCSK-EGC is presented and evaluated in Nakagami-m fading channels.

2. A DCSK modulation based cooperative communication scheme, DCSK selection relaying (DCSK-SR), is analyzed in Nakagami-m fading channels.
   (a) Mathematical expressions for the probability density function (PDF) of SNR for each hop and end-to-end BER are derived.

3. A spectrum and energy efficient DCSK-BDR scheme is analyzed in Nakagami-m fading channels.

(a) The end-to-end BER expression is derived.

(b) Performance of the scheme is investigated for the parameters of interest. The BER performance of DCSK-BDR is compared with that of the DCSK traditional transmission scheme and CDMA-BDR system.

4. DCSK modulation based transmit antenna selection schemes are proposed.

   (a) DCSK-TAS, DCSK joint-antenna selection (DCSK-JAS) and DCSK-TAS/EGC schemes are presented and analyzed in Nakagami-m fading channels.

   (b) BER and throughput of the proposed schemes are numerically evaluated.

5. A high data-rate spatially modulated DCSK (SM-DCSK) scheme is proposed.

   (a) The conditional BER expression for the transmit bit estimation is derived.

   (b) The SER expression is presented.

1.6 Organization

There are four chapters in the thesis. Brief description about the content of each chapter is given below.

Chapter 2 gives an overview of DCSK modulation technique. It describes the discrete-time baseband model of the DCSK system and presents the performance analysis of DCSK modulation in multipath fading channels. This chapter also presents the performance analysis of DCSK modulation with post-detection EGC at the receiver, i.e., DCSK-EGC system. This chapter provides some useful notations to be used in subsequent chapters.

Chapter 3 presents the performance analysis of DCSK modulation in different wireless communication systems. This chapter is divided in four sections. The performance analysis of DCSK-SR, DCSK-BDR, DCSK-TAS schemes and SM-DCSK are presented in

section one, two, three and four, respectively. Each section is divided in different subsections describing system model, BER analysis and discussion on numerical and simulation results for each system.

Chapter 4 presents the conclusion of the thesis with a brief summary of the work presented. Besides, it introduces some research problems for future work.

Chapter 2

Overview of DCSK Communication System

Being wideband and aperiodic, chaotic signals are well suited for spread-spectrum communication. Among various proposed chaotic modulation techniques in literature, differential chaos shift keying (DCSK) is the most popular [14, 21, 52]. DCSK system is based on non-coherent detection and does not require chaos synchronization at the receiver. Thus, DCSK represents more practical form of chaotic modulation technique. DCSK has some unique advantages over other chaotic modulation techniques such as non-coherent detection, no threshold-shift problem, less sensitive to channel distortion, etc., as discussed in the previous chapter. Furthermore, by using a simple autocorrelation receiver (AcR), DCSK gains the benefit of multipath diversity and hence, does not require any channel state information (CSI). On the contrary, the conventional direct-sequence spread-spectrum (DS-SS) techniques need to employ a RAKE receiver to get the advantage of multipath diversity, which requires the full CSI and hence increases the circuit complexity. Because of its simple structure, DCSK is widely used in various wireless communication applications [37, 38, 41, 53, 54].

In this chapter, an overview of DCSK communication system is presented. In section 2.1, a brief discussion on the generation of chaotic signal is presented. The discrete-time

baseband model for DCSK system is presented in section 2.2. Multiple access DCSK system based on Walsh codes is presented in section 2.3. In section 2.4, the performance of DCSK modulation is investigated in multipath fading channel. Performance analysis of DCSK modulation with post-detection equal-gain combiner (EGC) at the receiver is presented in section 2.5.

2.1 Chaotic Signal Generation

In this thesis, logistic map and cubic map are used to generate the chaotic signals. In this section, A brief discussion on the statistical properties of logistic map and cubic map is presented.

Consider the Chebyshev map of degree M, defined as [55]

$$g_M(x) = \cos\left(M \cos^{-1}(x)\right), \qquad -1 \leq x \leq 1, \tag{2.1}$$

where x is a variable. For $M = 2$ and 3, we have logistic and cubic map, respectively,

$$g_2(x) = 2x^2 - 1. \tag{2.2}$$

$$g_3(x) = 4x^3 - 3x. \tag{2.3}$$

The invariant probability density function (PDF) of x is given as [56]

$$\rho(x) = \begin{cases} \frac{1}{\pi\sqrt{1-x^2}}, & \text{if } |x| < 1 \\ 0, & \text{otherwise} \end{cases}. \tag{2.4}$$

According to Eq. 2.4, the statistical properties of x can be derived as

$$\begin{aligned} &E[x_k] = 0, \\ &\text{var}[x_k] = E\left[x_k^2\right] = \frac{1}{2}, \\ &\text{var}\left[x_k^2\right] = \frac{1}{8}, \\ &\text{cov}\left[x_k^2, x_q^2\right] = 0, \qquad k \neq q, \end{aligned}$$

$$E\left[x_k x_q\right] = 0, \qquad k \neq q, \tag{2.5}$$

where $E\left[\cdot\right]$ and $\mathrm{var}\left[\cdot\right]$ represent the expectation and variance operators, respectively, and $\mathrm{cov}\left[X, Y\right]$ represents the covariance of X and Y.

The statistical properties given in Eq. 2.5 show that logistic map and cubic map are well suited for chaotic communication. The waveforms of chaotic signals generated using logistic map and cubic map are shown in Figure 2.1(a) and Figure 2.1(b), respectively. The waveforms are generated from a first-order discrete-time dynamical system defined in Eq. 2.1 and plotted against the normalized time. In the figure, time is normalized with respect to the number of samples. The waveforms of the signals are aperiodic and random but bounded within the range $[-1, +1]$.

2.2 DCSK Modulation and Demodulation

DCSK modulation uses chaotic sequences as the carrier, with a differential shift keying modulator. The block diagram of binary DCSK modulator is shown in Figure 2.2. Each bit period is divided into two equal time slots. In the first time slot, the reference segment of chaotic sequence x_k is transmitted and in the second time slot, the data segment is transmitted. The data segment is same as the reference segment, x_k for transmitting bit '1', and an inverted version of reference segment, $-x_k$ is transmitted for bit '0' [14]. Thus, the transmitter output sequence s_k over the lth bit duration can be given as

$$s_k = \begin{cases} x_k, & k = 2(l-1)\beta + 1, \ldots, (2l-1)\beta \\ b_l x_{k-\beta}, & k = (2l-1)\beta + 1, \ldots, 2l\beta \end{cases}, \tag{2.6}$$

where β is the length of chaotic sequence, x_k and thus 2β is the spreading factor, i.e., the number of chaotic sequences required to transmit an information bit.

A block diagram of binary DCSK demodulator is shown in Figure 2.3, which uses a

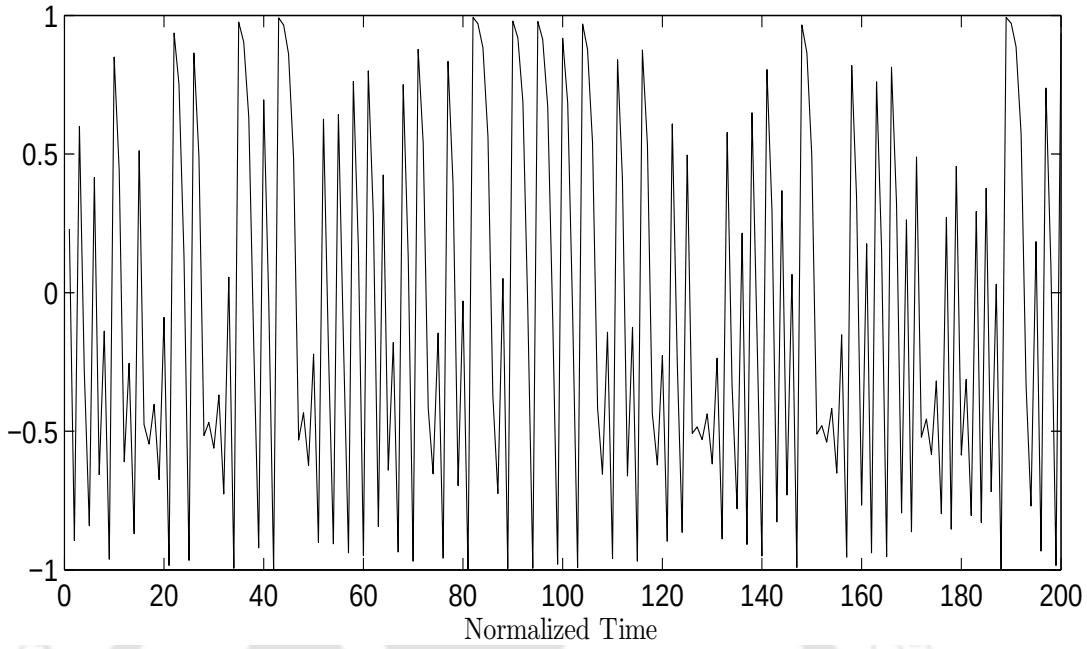

(a) Waveform of chaotic signal from logistic map (initial value = 0.23).

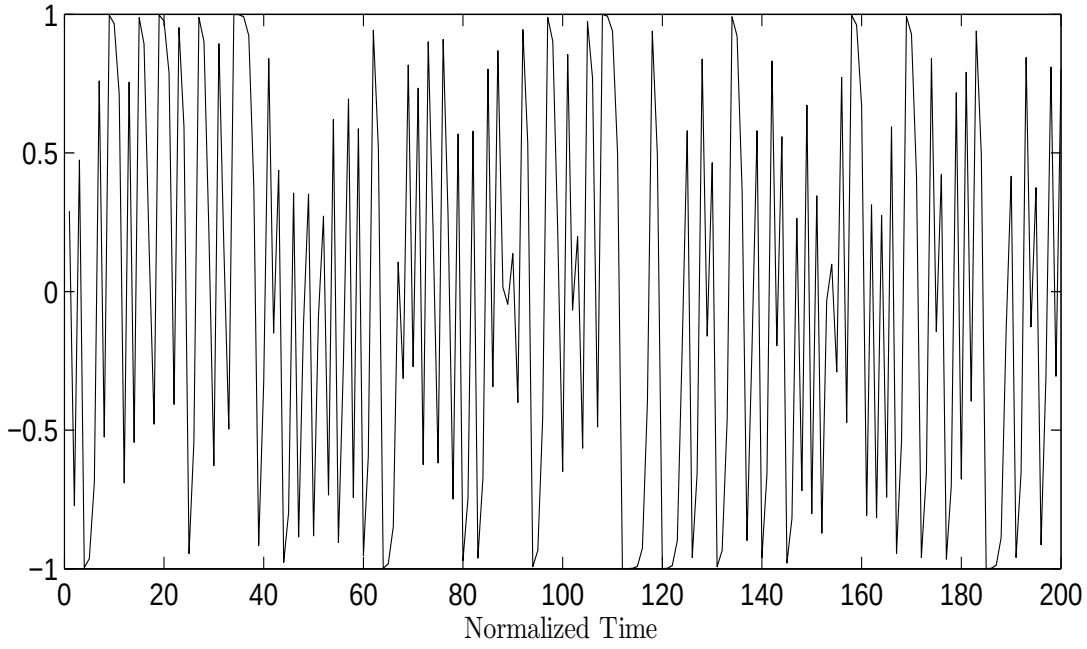

(b) Waveform of chaotic signal from cubic map (initial value = 0.29).

Figure 2.1: Chaotic signal waveforms.

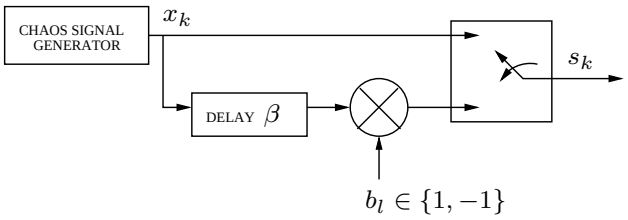

Figure 2.2: Block diagram of the DCSK modulator.

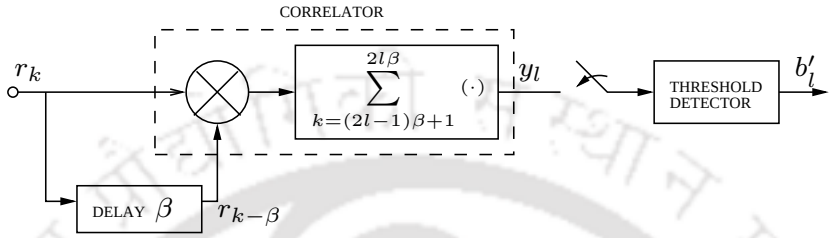

Figure 2.3: Block diagram of the DCSK demodulator.

suboptimal AcR. The reference segments of the received sequence $r_k, k = 2(l-1)\beta + 1, \ldots, (2l-1)\beta, (2l-1)\beta+1, \ldots, 2l\beta$, is correlated with the corresponding data segments. The output of the correlator over lth bit duration can be given as

$$y_l = \sum_{k=(2l-1)\beta+1}^{2\beta l} r_k r_{k-\beta}. \tag{2.7}$$

The output of the correlator is passed through a threshold detector whose threshold value is set to zero. The decision is made in favor of bit '1' or '0' depending on whether y_l is greater or less than zero.

Illustrative Example of DCSK Modulation

Let the samples of chaotic signal, x_k, are given as

$$x_k = \Big\{0.2900, -0.7724, 0.4738, -0.9959, -0.9637, -0.6886, 0.7598, -0.5247, \ldots\Big\}.$$

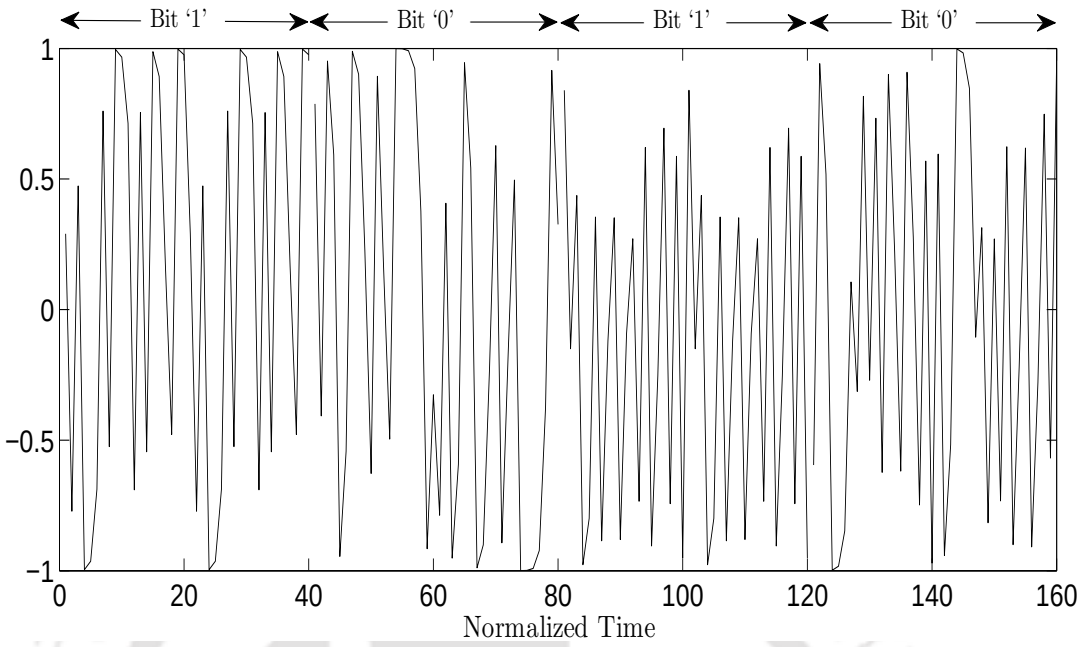

Figure 2.4: A typical DCSK modulated signal sample

For $\beta = 5$, the DCSK modulated signal for the bit '1' and '0' can be represented, respectively, as

$$s_k^{(1)} = \underbrace{0.2900, -0.7724, 0.4738, -0.9959, -0.9637}_{\text{reference segment}}, \underbrace{0.2900, -0.7724, 0.4738, -0.9959, -0.9637}_{\text{data segment}}, \tag{2.8}$$

$$s_k^{(0)} = \underbrace{0.2900, -0.7724, 0.4738, -0.9959, -0.9637}_{\text{reference segment}}, \underbrace{-0.2900, 0.7724, -0.4738, 0.9959, 0.9637}_{\text{data segment}}, \tag{2.9}$$

where $k = 1, \ldots, 5, 6, \ldots, 10$.

A graphical representation of DCSK modulated signal is shown in Figure 2.4. In the figure, binary sequence {1 0 1 0} is DCSK modulated with $\beta = 20$. For transmission of first bit, i.e., '1', the reference segment of 20 samples is transmitted followed by the data segment of 20 samples. Thus, in this example, a total of 40 samples are required to transmit a bit. It is to be noted that data segment is same as reference segment for transmission of bit '1'. However, for transmission of second bit, i.e., '0', data segment is inverted version of reference segment.

2.3 Multiple-User DCSK System Based on Walsh Codes

Orthogonal Walsh code sequences are used for a multiple-user DCSK communication system [27]. The 2^n-order Walsh code sequences can be generated as

$$W_{2^n} = \begin{bmatrix} W_{2^{n-1}} & W_{2^{n-1}} \\ W_{2^{n-1}} & -W_{2^{n-1}} \end{bmatrix}, \tag{2.10}$$

where $n = 1, 2, \ldots$ and $W_1 = [+1]$.

For example, a 4th-order Walsh code sequence can be constructed as follows

$$\begin{aligned} W_4 = \begin{bmatrix} W_2 & W_2 \\ W_2 & -W_2 \end{bmatrix} &= \left[\begin{bmatrix} W_1 & W_1 \\ W_1 & -W_1 \end{bmatrix} \quad \begin{bmatrix} W_1 & W_1 \\ W_1 & -W_1 \end{bmatrix} \right. \\ &\quad \left. \begin{bmatrix} W_1 & W_1 \\ W_1 & -W_1 \end{bmatrix} - \begin{bmatrix} W_1 & W_1 \\ W_1 & -W_1 \end{bmatrix} \right] \\ &= \begin{bmatrix} +1 & +1 & +1 & +1 \\ +1 & -1 & +1 & -1 \\ +1 & +1 & -1 & -1 \\ +1 & -1 & -1 & +1 \end{bmatrix} = \begin{bmatrix} w_1 \\ w_2 \\ w_3 \\ w_4 \end{bmatrix} \end{aligned} \tag{2.11}$$

For a binary DCSK system, $2U$-order Walsh code is used to accommodate U users. If 2β is the global spreading factor, $SF = 2\beta/2U$ denotes the length of each carrier segment. For lth bit, $b_l \in \{1, 0\}$, the transmitted signal of the uth user can be given as

$$s_{u,b_l} = \sum_{z=0}^{2U-1} w_{2u-b_l,z+1} c\left(t - z\frac{T_b}{2U}\right), \quad 0 < t < T_b, \tag{2.12}$$

where w_χ, $\chi = 1, 2, \ldots, 2U$, is a row vector of the $2U$-order Walsh code.

A generalized maximum likelihood (GML) detector is used for detection process [57]. The block diagram of the demodulator for the uth user is shown in Figure 2.5. The weighted energy for the lth bit of the uth user can be given as

$$E_{u,b_l} = \int_{T_b - T_b/2U}^{T_b} \left[\sum_{z=0}^{2U-1} r\left(t - z\frac{T_b}{2U}\right) w_{2u-b_l,2U-z} \right]^2 dt. \tag{2.13}$$

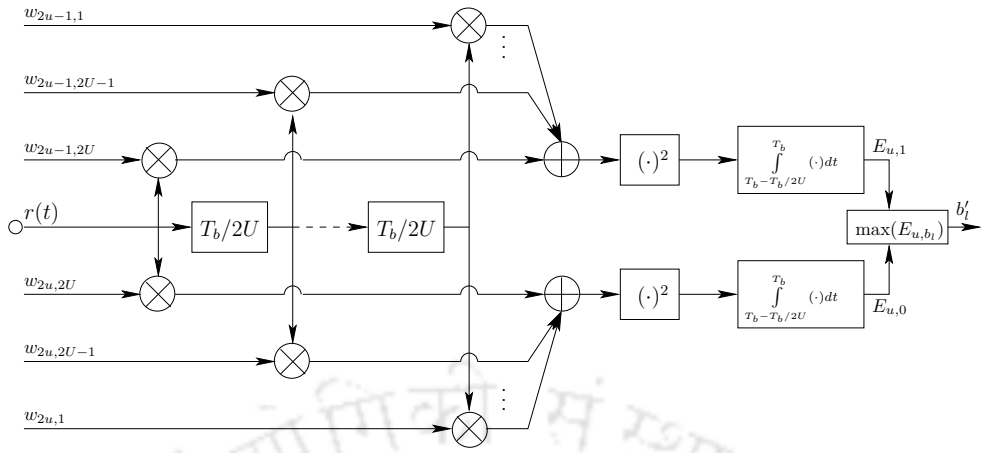

Figure 2.5: Block diagram of the uth user receiver.

The decision statistic of the uth user is denoted as $\max(E_{u,1}, E_{u,0})$. It is assumed that Walsh codes are synchronized in order to keep the interference minimum among different users.

2.4 Performance of DCSK over Fading Channels

It is well known that spread-spectrum systems perform better in multipath fading environment [58]. Since DCSK is a spread-spectrum system, so its performance in wireless multipath fading channels has important consideration. The performance analysis of DCSK communication systems over a multipath fading channel with delay spread is presented in [35]. However, the analysis presented in [35] is for *two-ray* fading channel. Here, we present the performance analysis for a generalized case of multipath fading, i.e., L-path fading channels.

2.4.1 System Model

The transmitter and receiver structure for DCSK systems are presented in previous section. At time instant k, the received signal, r_k, is given by

$$r_k = \sum_{i=1}^{L} \alpha_i s_{k-\tau_i} + n_k, \tag{2.14}$$

where α_i and τ_i are the channel coefficient and time delay for the ith path, respectively, and L is the number of independent fading paths. n_k is the additive white Gaussian noise (AWGN) with zero mean and $N_0/2$ variance.

The channel is assumed to be static block frequency-selective fading channel, meaning that the channel state remains constant during each transmission period. The channel multipath impulse response h can be modeled by a linear time-invariant process, i.e., $h(k) = \sum_{i=1}^{L} \alpha_i \delta(k - \tau_i)$, where the channel coefficients α_i are assumed to be independent and Nakagami-m distributed random variables with PDF given as [59]

$$f(\alpha_i) = \frac{2{m_i}^{m_i} \alpha_i^{2m_i-1}}{\Omega_i^{m_i} \Gamma(m_i)} \exp\left(-\frac{m_i \alpha_i^2}{\Omega_i}\right), \quad \alpha_i \geq 0, \tag{2.15}$$

where $\Omega_i = E[\alpha_i^2]$, m_i is the fading parameter which ranges from $\frac{1}{2}$ to ∞ and $\Gamma(\cdot)$ is the Gamma function. For simplicity, it is assumed that each fading channel has a uniform scale parameter, i.e., Ω_i/m_i is constant for all paths.

2.4.2 BER Analysis

In the following BER analysis, the multipath time delays are assumed to be negligible as compared to the bit duration, i.e., $\tau_i \ll 2\beta$, to avoid inter symbol interference (ISI).

Conditional BER

Using Eq. 2.7 and Eq. 2.14, the output of the correlator over lth bit duration can be given as

$$y_l = \sum_{k=(2l-1)\beta+1}^{2\beta l} \left(\sum_{i=1}^{L} \alpha_i s_{k-\tau_i} + n_k\right)\left(\sum_{i=1}^{L} \alpha_i s_{k-\beta-\tau_i} + n_{k-\beta}\right). \tag{2.16}$$

Let τ_1, τ_2, ..., τ_{L-1} represents the time delay for the 2nd, 3rd, ..., Lth path with respect to the first path, respectively, and $\tau_1 < \tau_2 < \ldots, < \tau_{L-1}$. Thus, Eq. 2.16 can be simplified as

$$\begin{aligned}
y_l = &\sum_{k=(2l-1)\beta+1}^{(2l-1)\beta+\tau_1} \Big\{ \left(\alpha_1 b_l x_{k-\beta} + \alpha_2 x_{k-\tau_1} + \ldots + \alpha_L x_{k-\tau_{L-1}} + n_k\right) \\
&\times \left(\alpha_1 x_{k-\beta} + \alpha_2 b_{l-1} x_{k-2\beta-\tau_1} + \ldots + \alpha_L b_{l-1} x_{k-2\beta-\tau_{L-1}} + n_{k-\beta}\right) \Big\} \\
&+ \sum_{k=(2l-1)\beta+\tau_1+1}^{(2l-1)\beta+\tau_2} \Big\{ \left(\alpha_1 b_l x_{k-\beta} + \alpha_2 b_l x_{k-\beta-\tau_1} + \alpha_3 x_{k-\tau_2} + \ldots + \alpha_L x_{k-\tau_{L-1}} + n_k\right) \\
&\times \left(\alpha_1 x_{k-\beta} + \alpha_2 x_{k-\beta-\tau_1} + \alpha_3 b_{l-1} x_{k-2\beta-\tau_2} + \ldots + \alpha_L b_{l-1} x_{k-2\beta-\tau_{L-1}} + n_{k-\beta}\right) \Big\} \\
&+ \ldots \\
&+ \sum_{k=(2l-1)\beta+\tau_{L-2}+1}^{(2l-1)\beta+\tau_{L-1}} \Big\{ \left(\alpha_1 b_l x_{k-\beta} + \alpha_2 b_l x_{k-\beta-\tau_1} + \ldots + \alpha_{L-1} b_l x_{k-\beta-\tau_{L-2}} + \alpha_L x_{k-\tau_{L-1}} + n_k\right) \\
&\times \left(\alpha_1 x_{k-\beta} + \alpha_2 x_{k-\beta-\tau_1} + \ldots + \alpha_{L-1} x_{k-\beta-\tau_{L-2}} + \alpha_L b_{l-1} x_{k-2\beta-\tau_{L-1}} + n_{k-\beta}\right) \Big\} \\
&+ \sum_{k=(2l-1)\beta+\tau_{L-1}+1}^{2l\beta} \Big\{ \left(\alpha_1 b_l x_{k-\beta} + \alpha_2 b_l x_{k-\beta-\tau_1} + \ldots + \alpha_L b_l x_{k-\beta-\tau_{L-1}} + n_k\right) \\
&\times \left(\alpha_1 x_{k-\beta} + \alpha_2 x_{k-\beta-\tau_1} + \ldots + \alpha_L x_{k-\beta-\tau_{L-1}} + n_{k-\beta}\right) \Big\}.
\end{aligned} \tag{2.17}$$

Since, $\tau_\xi \ll 2\beta$, $\xi = 1, 2, \ldots, L-1$, Eq. 2.17 can be approximated as

$$\begin{aligned}
y_l \approx \sum_{k=(2l-1)\beta+1}^{2l\beta} \Big\{ &\left(\alpha_1 b_l x_{k-\beta} + \alpha_2 b_l x_{k-\beta-\tau_1} + \ldots + \alpha_L b_l x_{k-\beta-\tau_{L-1}} + n_k\right) \\
&\times \left(\alpha_1 x_{k-\beta} + \alpha_2 x_{k-\beta-\tau_1} + \ldots + \alpha_L x_{k-\beta-\tau_{L-1}} + n_{k-\beta}\right) \Big\}.
\end{aligned} \tag{2.18}$$

For large β and a given chaotic map, $\sum_{k=(2l-1)\beta+1}^{2l\beta} x_{k-\beta}x_{k-\beta-\tau_\xi} \approx 0$ and $\sum_{k=(2l-1)\beta+1}^{2l\beta} x_{k-\beta-\tau_\xi}x_{k-\beta-\tau_\zeta} \approx 0$, where $\xi, \zeta = 1, 2, \ldots, L-1$, $\xi \neq \zeta$. Thus, Eq. 2.18 can be simplified as

$$\begin{aligned} y_l \approx \sum_{k=(2l-1)\beta+1}^{2l\beta} \Bigg[& \left(\alpha_1^2 b_l x_{k-\beta}^2 + \alpha_2^2 b_l x_{k-\beta-\tau_1}^2 + \ldots + \alpha_L^2 b_l x_{k-\beta-\tau_{L-1}}^2\right) \\ & + \left(\alpha_1 x_{k-\beta} + \alpha_2 x_{k-\beta-\tau_1} + \ldots + \alpha_L x_{k-\beta-\tau_{L-1}}\right)(n_k + b_l n_{k-\beta}) \\ & + n_k n_{k-\beta} \Bigg]. \end{aligned} \tag{2.19}$$

For large spreading factor, i.e., 2β, y_l can be approximated to be Gaussian [60]. Thus, assuming $b_l = +1$, mean and variance of the decision variable y_l can be given, respectively, as

$$\begin{aligned} E\left[y_l|_{\alpha_i, b_l=+1}\right] &= \left(\sum_{i=1}^{L} \alpha_i^2\right) \beta E\left[x_k^2\right] \\ \text{var}\left[y_l|_{\alpha_i, b_l=+1}\right] &= \left(\sum_{i=1}^{L} \alpha_i^4\right) \beta \text{var}\left[x_k^2\right] + \left(\sum_{i=1}^{L} \alpha_i^2\right) \beta N_0 \text{var}\left[x_k\right] + \beta \frac{N_0^2}{4}. \end{aligned} \tag{2.20}$$

Similarly, for $b_l = -1$, mean and variance can be obtained as $E\left[y_l|_{\alpha_i, b_l=-1}\right] = -E\left[y_l|_{\alpha_i, b_l=+1}\right]$ and $\text{var}\left[y_l|_{\alpha_i, b_l=-1}\right] = \text{var}\left[y_l|_{\alpha_i, b_l=+1}\right]$.

Thus, the conditional BER may be computed as

$$\begin{aligned} \text{BER} &= \frac{1}{2} erfc\left(\frac{E\left[y_l|_{\alpha_i, b_l=+1}\right]}{\sqrt{2\text{var}\left[y_l|_{\alpha_i, b_l=+1}\right]}}\right) \\ &= \frac{1}{2} erfc\left(\left[\frac{2\left(\sum_{i=1}^{L} \alpha_i^4\right) \text{var}\left[x_k^2\right]}{\left(\sum_{i=1}^{L} \alpha_i^2\right)^2 \beta E^2\left[x_k^2\right]} + \frac{2N_0 \text{var}\left[x_k\right]}{\left(\sum_{i=1}^{L} \alpha_i^2\right) \beta E^2\left[x_k^2\right]} + \frac{2\beta N_0^2}{\left(\sum_{i=1}^{L} \alpha_i^2\right)^2 4\beta^2 E^2\left[x_k^2\right]}\right]^{-\frac{1}{2}}\right), \end{aligned} \tag{2.21}$$

where $erfc(u) = \frac{2}{\sqrt{\pi}} \int_u^\infty e^{-z^2} dz$ is the complementary error function.

For a given chaotic signal, x_k, with zero mean, the variance of x_k can be defined as $\text{var}\left[x_k\right] = E\left[x_k^2\right]$. If the logistic map is used, $\text{var}\left[x_k^2\right] = \frac{1}{8}$ and $E\left[x_k^2\right] = \frac{1}{2}$. Thus, Eq. 2.21

can be further simplified as

$$\text{BER} = \frac{1}{2} erfc \left(\left[\frac{\left(\sum_{i=1}^{L} \alpha_i^4 \right)}{\left(\sum_{i=1}^{L} \alpha_i^2 \right)^2 \beta} + \frac{4N_0}{\left(\sum_{i=1}^{L} \alpha_i^2 \right) E_b} + \frac{2\beta N_0^2}{\left(\sum_{i=1}^{L} \alpha_i^2 \right)^2 E_b^2} \right]^{-\frac{1}{2}} \right), \tag{2.22}$$

where E_b is the bit energy and is defined as $E_b = 2\beta E\left[x_k^2\right]$.

For large β, the first term in Eq. 2.22 may be neglected and thus, conditional BER can be approximated as

$$\text{BER} \approx \frac{1}{2} erfc \left(\left[\frac{4}{\left(\sum_{i=1}^{L} \gamma_i \right)} + \frac{2\beta}{\left(\sum_{i=1}^{L} \gamma_i \right)^2} \right]^{-\frac{1}{2}} \right) = \frac{1}{2} erfc \left(\left[\frac{4}{\gamma} + \frac{2\beta}{\gamma^2} \right]^{-\frac{1}{2}} \right), \tag{2.23}$$

where $\gamma_i = \frac{E_b}{N_0} \alpha_i^2$ is the instantaneous signal-to-noise ratio (SNR) of the ith path.

PDF of SNR

The instantaneous SNR at the output of the correlator can be given from Eq. 2.23, as

$$\gamma = \sum_{i=1}^{L} \gamma_i, \tag{2.24}$$

where $\gamma_i = \frac{E_b}{N_0} \alpha_i^2$. From Eq. 2.24, the average SNR can be defined as $\overline{\gamma} = E\left[\gamma\right] = E_b/N_0$, assuming $\sum_{i=1}^{L} E\left[\alpha_i^2\right] = 1$. Assuming α_i is Nakagami-m distributed as the PDF given in Eq. 2.15, it can be shown using the transformation of random variables that γ_i follows gamma distribution, i.e., $\gamma_i \sim G\left(m_i, \frac{E_b/N_0}{m_i}\Omega_i\right)$, with PDF given as

$$f_{\gamma_i}(x) = \frac{x^{m_i - 1} e^{-x \frac{m_i}{(E_b/N_0)\Omega_i}}}{\left(\frac{E_b/N_0}{m_i}\Omega_i\right)^{m_i} \Gamma\left(m_i\right)}. \tag{2.25}$$

Assuming $m_i = m$, for $i = 1, \ldots, L$, the distribution of γ can be obtained using the moment generating function (MGF) approach as [61]

$$\gamma \sim G\left(\sum_{i=1}^{L} m_i, \frac{E_b \sum_{i=1}^{L} \Omega_i}{N_0 \sum_{i=1}^{L} m_i}\right) = G\left(mL, \frac{E_b/N_0}{mL}\right). \tag{2.26}$$

Thus, PDF of γ is given as

$$f_\gamma(x) = \frac{x^{mL-1} e^{-x\frac{mL}{(E_b/N_0)}}}{\left(\frac{E_b/N_0}{mL}\right)^{mL} \Gamma(mL)}. \tag{2.27}$$

Average BER

The average BER for DCSK system can be obtained by averaging the conditional BER, as

$$\text{BER}_{\text{av}} = \int_0^\infty \text{BER}(\gamma) f(\gamma) d\gamma, \tag{2.28}$$

where $\text{BER}(\gamma) = \frac{1}{2} erfc\left(\left[\frac{4}{\gamma} + \frac{2\beta}{\gamma^2}\right]^{-\frac{1}{2}}\right)$ is the conditional BER defined in Eq. 2.23. By substituting Eq. 2.23 and Eq. 2.27 in Eq. 2.28, the average BER can be numerically evaluated. Since, the $erfc$ function in Eq. 2.23 has a quadratic argument function, it is not possible to solve the integration in Eq. 2.28 to get a closed form expression. Hence, BER_{av} needs to be evaluated numerically.

2.4.3 Numerical and Simulation Results

The derived BER_{av} expression is numerically evaluated using Eq. 2.28 and compared with the MATLAB simulation results. Monte Carlo simulations are carried out to evaluate the performance of DCSK system over Nakagami fading environment. The cubic map is used to generate the chaotic samples. In the simulation, we assume $\beta = 64$ and $L = 2$. The two paths have identical average power gain. The time delay between two path is assumed to be $\tau_1 = 1$.

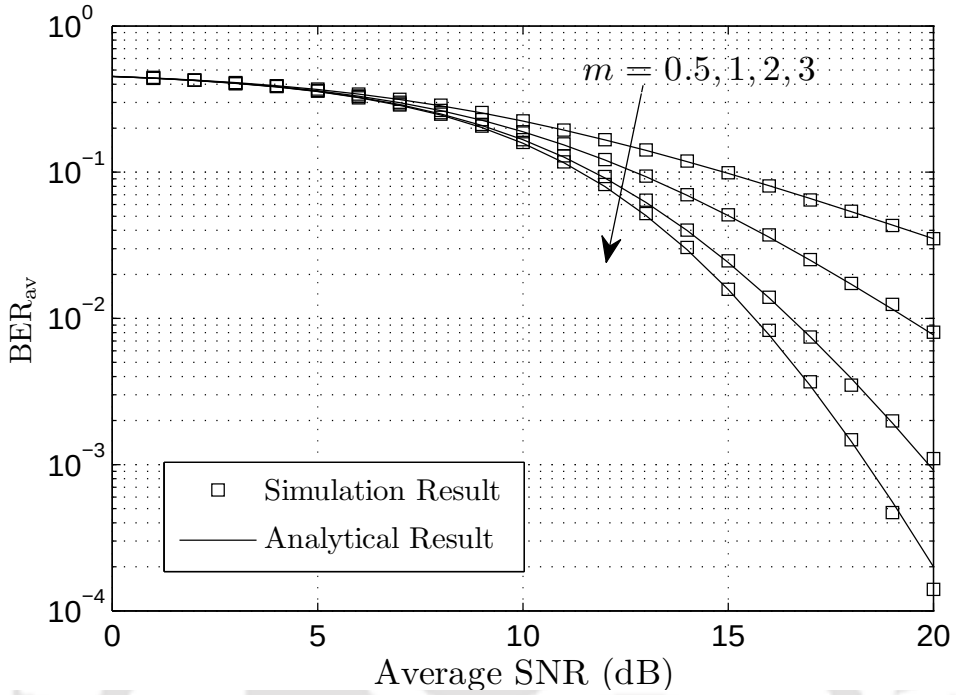

(a) BER performance of DCSK for varying m.

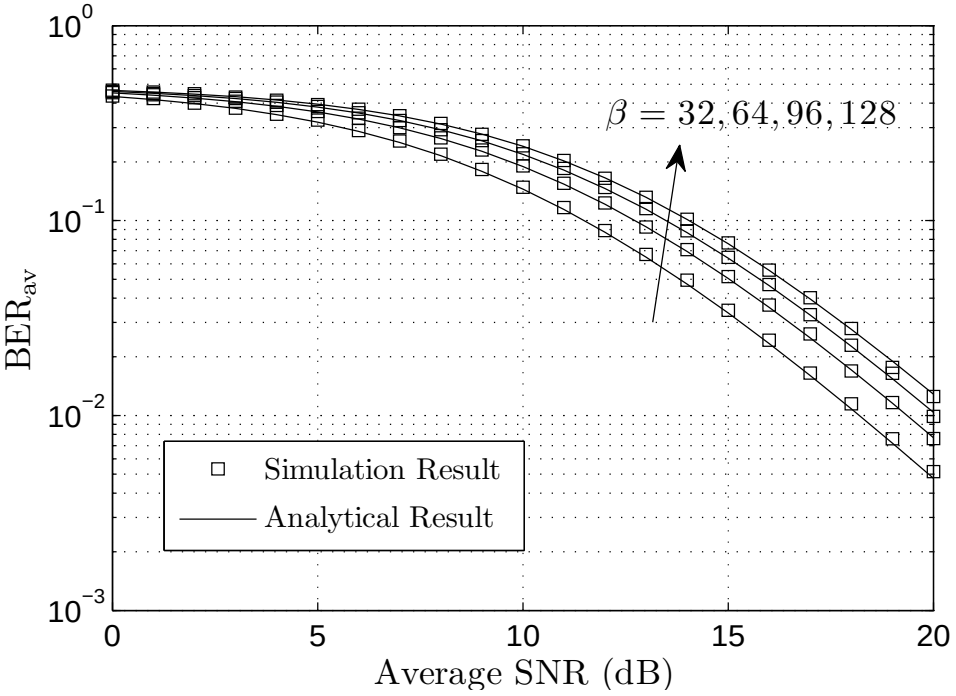

(b) BER performance of DCSK for varying β.

Figure 2.6: BER performance of the DCSK scheme.

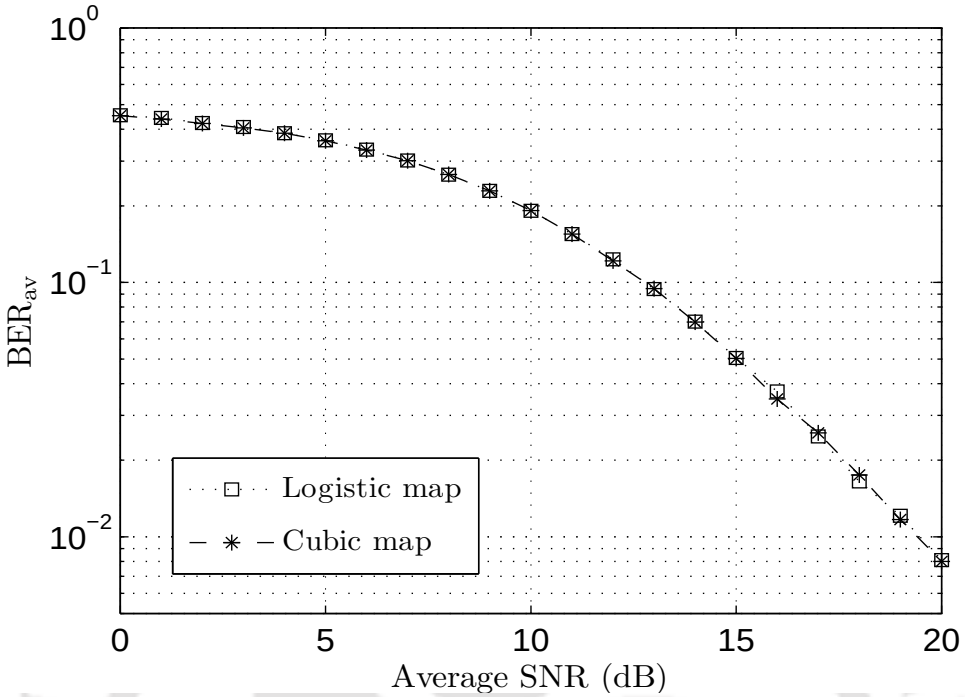

(a) BER performance of the DCSK scheme for different chaotic map.

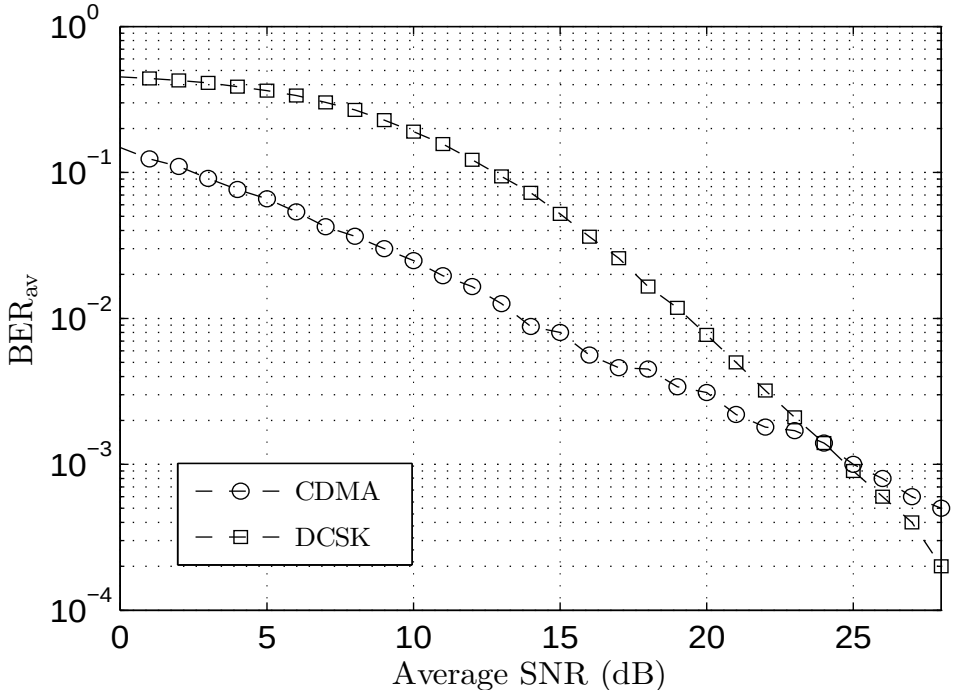

(b) Performance comparison of the CDMA and DCSK scheme.

Figure 2.7: BER performance of the DCSK scheme.

Average BER of DCSK modulation is numerically evaluated using Eq. 2.28. BER_{av} versus average SNR curves are shown in Figure 2.6(a), for fading parameter $m = 0.5$, 1, 2 and 3. The numerical result matches closely with the simulation result. An improvement in BER with increase in m can be observed from the figure, as expected. This is because the fading is less severe at higher m. For example, at 17 dB average SNR, the average BER is $\approx 6.5 \times 10^{-2}$ for $m = 0.5$. However, the average BER is improved to $\approx 2.5 \times 10^{-2}$, $\approx 8.0 \times 10^{-3}$ and $\approx 4.0 \times 10^{-3}$ when m increased to 1, 2 and 3, respectively. BER performance of DCSK modulation over Rayleigh fading (which is a special case of Nakagami-m fading at $m = 1$) is presented in [35].

Figure 2.6(b) illustrates the effect of the spreading factor (2β) on the BER performance of the DCSK system. BER_{av} is plotted against the average SNR, for $\beta = 32$, 64, 96 and 128. With fixed transmitted energy per bit, we observe from the figure that the curves with lower β have the better BER performance. The reason behind this is that the noise component in the decision variable is proportional to β. However, in order to obtain the benefits of spread-spectrum, β should be sufficiently large. Thus, a trade-off is required for selecting β.

Performance of Different Chaotic Maps

BER performance of the DCSK system is investigated and compared for different chaotic maps in Figure 2.7(a). The following maps are used in the simulation studies.

1. Logistic map

$$x_{k+1} = 1 - 2x_k^2. \tag{2.29}$$

2. Cubic map

$$x_{k+1} = 4x_k^3 - 3x_k. \tag{2.30}$$

It can be observed from the figure that logistic map and cubic map have the same BER performance. This is because logistic and cubic map have the same statistical properties [14]. However, the chaotic maps with different statistical properties have the different BER performance [14, 42, 62].

Comparison with CDMA Systems

In Figure 2.7(b), BER performance of DCSK is compared with that of the CDMA system for $m = 1$. For CDMA system simulation, Gold-sequences are adopted as spreading sequences. To ensure the same bandwidth of the two systems, an extra '0' is added at the end of each Gold-sequence as the length of a Gold-sequence is always odd and the spreading factor (2β) of DCSK system is always even. A simple correlation receiver is adopted at the receiver. It is observed from the figure that CDMA system has lower BER than DCSK system at the low SNR range. However, at high SNR range, DCSK scheme completely outperforms CDMA scheme. The reason behind the low BER of DCSK system at high SNR is that the DCSK system by default exploits the multipath diversity by using AcR whereas the CDMA system needs to employ a RAKE receiver to get the advantage of multipath diversity. It is to be noted that RAKE receiver requires the full CSI and hence increases the circuit complexity.

2.5 Performance Analysis of DCSK-EGC

Wireless transmission is often affected by multipath fading. This results in the system performance degradation and hence, making reliable communication difficult. Antenna diversity is a practical, effective and thus, very popular technique to combat the effect of multipath fading. Among various proposed diversity techniques, maximal ratio combining (MRC) is the optimal linear combining technique [63]. However, it does not make sense

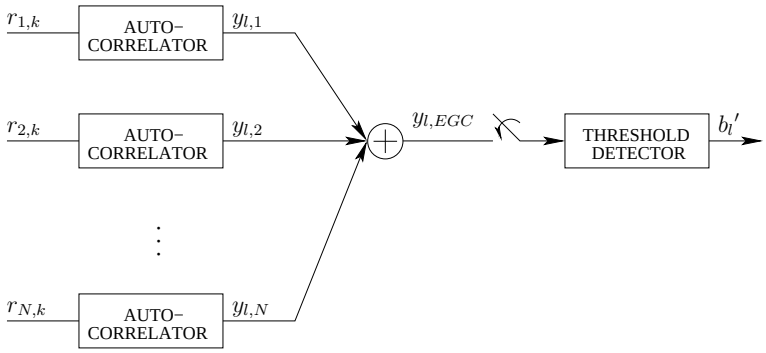

Figure 2.8: Post-detection equal-gain-combining receiver.

to use MRC with differential detection as MRC is a coherent combining technique [64]. For differential detectors, post-detection equal gain combining (EGC), i.e., differential detection followed by equal gain combiner, gives the best performance.

In this section, the performance analysis of DCSK modulation in multipath fading with post-detection EGC at the receiver, i.e., (DCSK-EGC), is presented. In particular, the conditional BER expression is derived for DCSK modulation when receiver utilizes post-detection EGC.

2.5.1 System Model

Consider a communication system in which the transmitter uses DCSK modulation and the receiver employs multiple correlators followed by an equal-gain-combiner, i.e., post-detection EGC. In post-detection EGC, the received signals are demodulated first and then equal gain combined. The block diagram of a post-detection EGC receiver is shown in Figure. 2.8.

The signal received at the input of the jth correlator, where $1 \leq j \leq N$, is given by

$$r_{j,k} = \sum_{i=1}^{L} \alpha_{j,i} s_{k-\tau_{j,i}} + n_{j,k}, \tag{2.31}$$

where $\alpha_{j,i}$ and $\tau_{j,i}$ are the channel coefficient and time delay for the ith path at the jth correlator, respectively, and L is the number of multipath components. $n_{j,k}$ is AWGN at

the jth correlator with zero mean and $N_0/2$ variance.

The channel model is same as assumed in the previous section. The channel coefficients $\alpha_{j,i}$ are assumed to be independent and Nakagami-m distributed random variables with the PDF defined in Eq. 2.15.

The output of correlators can be obtained using Eq. 2.7. If $y_{l,j}$ is the output of the jth correlator, the output of EGC can be given as

$$y_{l,EGC} = \sum_{j=1}^{N} y_{l,j}. \tag{2.32}$$

The output of post-detection EGC is passed through a threshold detector to make decision.

2.5.2 BER Analysis

It is assumed that the multipath time delays are negligible as compared to the bit duration, i.e., $\tau_{j,i} \ll 2\beta$, to avoid ISI.

Conditional BER

From Eq. 2.19, the output of the jth correlator can be given as

$$\begin{aligned} y_{l,j} \approx \sum_{k=(2l-1)\beta+1}^{2l\beta} \Bigg[& \left(\alpha_{j,1}^2 b_l x_{k-\beta}^2 + \alpha_{j,2}^2 b_l x_{k-\beta-\tau_{j,1}}^2 + \ldots + \alpha_{j,L}^2 b_l x_{k-\beta-\tau_{j,L-1}}^2\right) \\ & + \left(\alpha_{j,1} x_{k-\beta} + \alpha_{j,2} x_{k-\beta-\tau_{j,1}} + \ldots + \alpha_{j,L} x_{k-\beta-\tau_{j,L-1}}\right)\left(n_{j,k} + b_l n_{j,k-\beta}\right) \\ & + n_{j,k} n_{j,k-\beta} \Bigg]. \end{aligned} \tag{2.33}$$

The output of N correlators are equal gain combined and thus, the final decision variable can be given using Eq. 2.32. For large spreading factor 2β, $y_{l,EGC}$ can be approximated to be Gaussian [60]. Thus, assuming $b_l = +1$, mean and variance of the decision variable $y_{l,EGC}$ can be given as

$$E\left[y_{l,EGC}|_{\alpha_{j,i},b_l=+1}\right] = \left[\sum_{j=1}^{N}\left(\sum_{i=1}^{L}\alpha_{j,i}^2\right)\right]\beta E\left[x_k^2\right]$$

$$\text{var}\left[y_{l,EGC}|_{\alpha_{j,i},b_l=+1}\right] = \left[\sum_{j=1}^{N}\left(\sum_{i=1}^{L}\alpha_{j,i}^4\right)\right]\beta\text{var}\left[x_k^2\right] + \left[\sum_{j=1}^{N}\left(\sum_{i=1}^{L}\alpha_{j,i}^2\right)\right]\beta N_0\text{var}\left[x_k\right] + N\beta\frac{N_0^2}{4}. \tag{2.34}$$

Using Eq. 2.34 and following the steps as in previous section, the conditional BER can be given as

$$\begin{aligned}\text{BER} &\approx \frac{1}{2}erfc\left(\left[\frac{4}{\left[\sum_{j=1}^{N}\left(\sum_{i=1}^{L}\gamma_{j,i}\right)\right]} + \frac{2N\beta}{\left[\sum_{j=1}^{N}\left(\sum_{i=1}^{L}\gamma_{j,i}\right)\right]^2}\right]^{-\frac{1}{2}}\right)\\ &= \frac{1}{2}erfc\left(\left[\frac{4}{\left[\sum_{j=1}^{N}\gamma_j\right]} + \frac{2N\beta}{\left[\sum_{j=1}^{N}\gamma_j\right]^2}\right]^{-\frac{1}{2}}\right)\\ &= \frac{1}{2}erfc\left(\left[\frac{4}{\gamma_{eq}} + \frac{2N\beta}{\gamma_{eq}^2}\right]^{-\frac{1}{2}}\right),\end{aligned} \tag{2.35}$$

where, $\gamma_{j,i} = \frac{E_b}{N_0}\alpha_{j,i}^2$ is the instantaneous SNR of the ith path of the jth correlator, $\gamma_j = \sum_{i=1}^{L}\gamma_{j,i}$ is the instantaneous SNR at the output of the jth correlator and $\gamma_{eq} = \sum_{j=1}^{N}\gamma_j$ is the equivalent instantaneous SNR available at the output of post-detection EGC.

It is to be noted that the conditional BER derived in Eq. 2.35 is different from the conditional BER in Eq. 2.23. Hence, the conditional BER derived in Eq. 2.23 cannot be used to evaluate the average BER for DCSK modulation with post-detection EGC at the receiver.

PDF of SNR

The equivalent instantaneous SNR available at the output of post-detection EGC is

$$\gamma_{eq} = \sum_{j=1}^{N}\gamma_j. \tag{2.36}$$

The distribution of γ_j can be given From Eq. 2.26, as $\gamma_j \sim G\left(mL, \frac{E_b/N_0}{mL}\right)$. Thus, the distribution of γ_{eq} can be given as $\gamma_{eq} \sim G\left(NmL, \frac{E_b/N_0}{mL}\right)$ with PDF

$$f_{\gamma_{eq}}(x) = \frac{x^{NmL-1} e^{-x\frac{mL}{(E_b/N_0)}}}{\left(\frac{E_b/N_0}{mL}\right)^{NmL} \Gamma(NmL)}. \tag{2.37}$$

Average BER

The average BER for DCSK modulation with post-detection EGC at the receiver can be obtained by averaging the conditional BER, as

$$\text{BER}_{\text{av}} = \int_0^\infty \text{BER}(\gamma_{eq})\, f(\gamma_{eq})\, d\gamma_{eq}, \tag{2.38}$$

where $\text{BER}(\gamma_{eq}) = \frac{1}{2} erfc\left(\left[\frac{4}{\gamma_{eq}} + \frac{2N\beta}{\gamma_{eq}^2}\right]^{-\frac{1}{2}}\right)$ is the conditional BER defined in Eq. 2.35. Substituting Eq. 2.35 and Eq. 2.37 in Eq. 2.38, the average BER for DCSK-EGC can be numerically evaluated.

2.5.3 Numerical and Simulation Results

The derived BER_{av} expression is numerically evaluated and compared with the MATLAB simulation results. Monte Carlo simulations are carried out to evaluate the performance of DCSK-EGC system. The cubic map is used to generate the chaotic samples. In the simulation, we assume $\beta = 64$ and $L = 2$. The two paths have identical average power gain. The time delay between two path is assumed to be $\tau_1 = 1$.

Average BER of DCSK-EGC is evaluated by numerical integration of Eq. 2.38. In Figure 2.9, BER_{av} is plotted against the average SNR per branch at $m = 1$, for $N = 1$, 2 and 3. The figure demonstrates an improvement in BER_{av} with increase in N, as expected. For example, at 15 dB average SNR, BER_{av} improves from $\approx 5.0 \times 10^{-2}$ to $\approx 9.0 \times 10^{-3}$ when N increases from 1 to 2. Further, BER_{av} improves from $\approx 9.0 \times 10^{-3}$ to $\approx 2.0 \times 10^{-3}$ on the increment of N from 2 to 3.

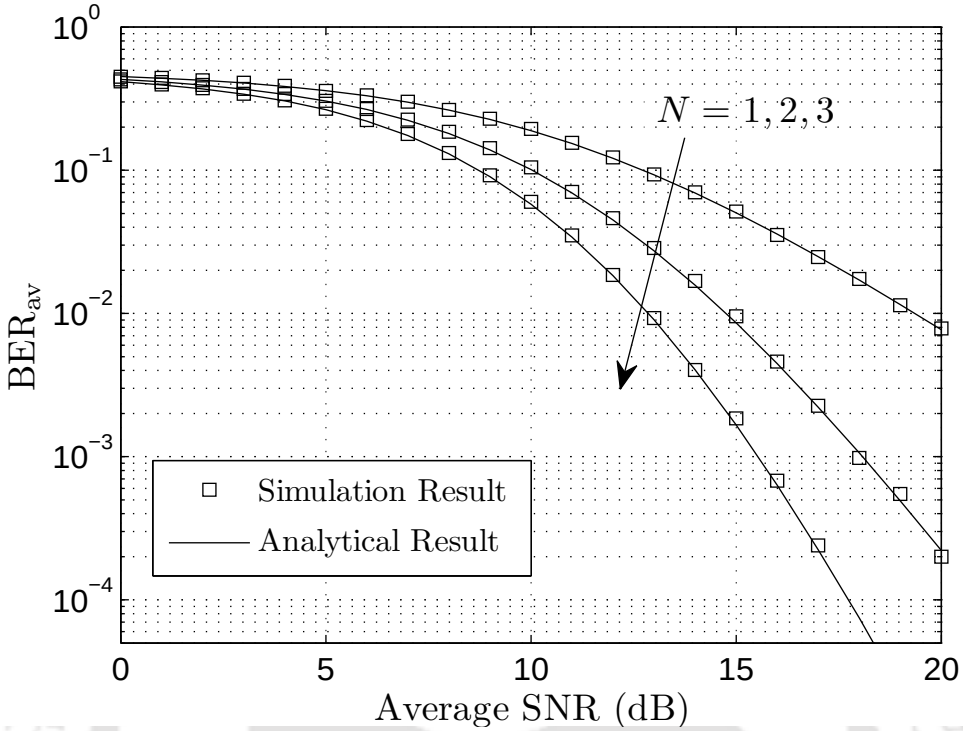

Figure 2.9: BER performance of the DCSK-EGC scheme for varying N.

2.6 Summary

In this chapter, an overview of DCSK communication system is presented. This chapter contains the survey works as well as original contributions of thesis. The survey works include the discussion on chaotic signal generation, DCSK modulation and demodulation, and Walsh codes based multiple access DCSK system. The original contributions include the performance analysis of DCSK communication system. In particular, the BER performance of DCSK system is analyzed in multipath fading channels. BER of DCSK is evaluated in Nakagami-m fading channels. Numerical and simulation results are obtained and plotted for the parameters of interest. Performance analysis of DCSK systems with post-detection equal gain combiner at the receiver, i.e., DCSK-EGC, is also presented. An improvement in the BER is observed when the receiver employs multiple correlators followed by post-detection EGC diversity combining technique.

Chapter 3

DCSK Modulation: Application to Wireless Communication Systems

In the past decades, differential chaos shift keying (DCSK) system has been a topic of interest in the field of wireless communications due to its excellent capacity to counter multipath fading and time delay. Because of its simple and easy to implement structure, DCSK can be recommended for various wireless communication applications. Many research works addressing DCSK modulation in multiple-input multiple-output (MIMO) systems are reported in [36–40]. Application of DCSK modulation in the cooperative communication systems can be found in [41–45]. To improve the data-rate of DCSK, various methods have been proposed in literature [21, 22, 46–51]. Recently, the performance of DCSK modulation is analyzed in ultra-wideband (UWB) systems [53]. A Walsh code based reliable chaotic modulation transmission technique, differentially DCSK Walsh Coding (DDCSK-WC) is proposed in [65]. In [54], analog network coding based multi-user multi-carrier DCSK communication system is analyzed.

In this chapter, performance of DCSK modulation is analyzed in different wireless communication systems. In section 3.1, a relay selection based DCSK cooperative diversity scheme, DCSK selection relaying (DCSK-SR) is presented. A spectrum and energy efficient DCSK bidirectional relaying (DCSK-BDR) scheme is presented in section 3.2.

In section 3.3, the performance analysis of DCSK modulation with transmit antenna selection (DCSK-TAS) is presented. A high-data-rate DCSK scheme based on spatial modulation (SM), i.e., spatially modulated DCSK (SM-DCSK), is proposed in section 3.4.

3.1 DCSK Selection Relaying Systems

Cooperative diversity offers a promising solution to overcome the degradation due to signal fading, where the spatial diversity cannot be implemented [66], [67]. In this scheme, the relaying terminals cooperate in the transmission of source data to destination. For two-hop wireless networks, different cooperative transmission protocols are proposed in [68], among which amplify-and-forward (AF) and decode-and-forward (DF) are more popular. Recently, the performance of DCSK modulation is evaluated using DF protocol in cooperative diversity systems [41–44].

The use of multiple antennas at transmitting/receiving nodes ensure the link reliability and spectrum efficiency. In [69], different relaying protocols for MIMO relay networks are discussed and compared. Motivated by the considerable benefits, in [43], Fang *et al.* have proposed the implementation of MIMO relay in DCSK cooperative diversity systems and investigated its performance. However, intuitively it is also appealing that by implementing the relay selection scheme in multiple MIMO relay environment can also further enhance the system performance significantly.

In this section, we propose a cooperative diversity scheme, named as DCSK selection relaying (DCSK-SR), in which the transmitting nodes use DCSK modulation to transmit its information and the best relay is selected from a MIMO relay cluster to cooperate with the source. The source node employs single antenna whereas the destination and all the relays employ multiple antennas. DF protocol is adopted by all the relays and the relay which maximizes the total received SNR at the destination is selected to cooperate with

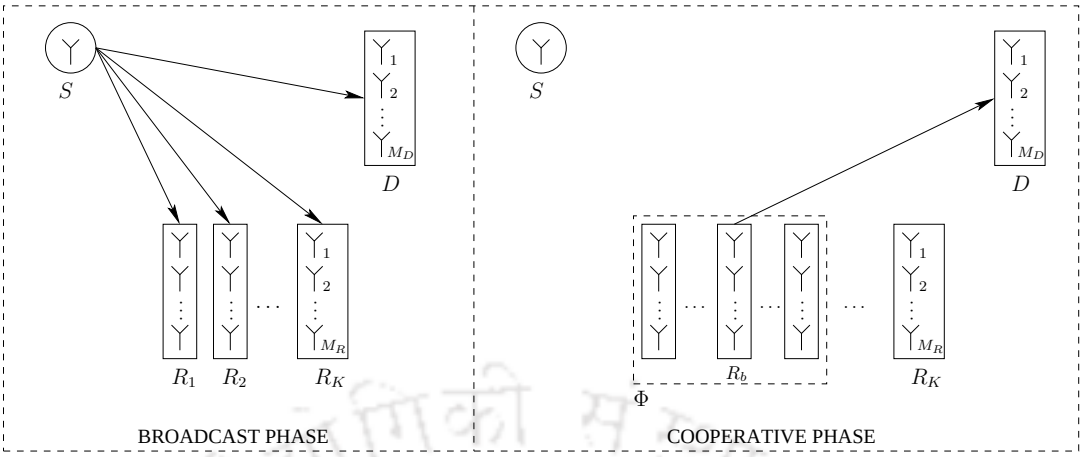

Figure 3.1: DCSK-SR System Model.

the source. Assuming fading occurs in the channel, post-detection equal gain combiners (EGC) are used to combine the received signals at the relay and the destination node. An expression for the probability density function (PDF) of the signal-to-noise ratio (SNR) at the output of EGC combiner for each hop is presented. The BER performance of the proposed system is evaluated in Nakagami-m fading channels. Numerical and simulation results show that the proposed scheme can provide a significant improvement in the BER. The effect of the system parameters on the BER performance is also studied.

3.1.1 System Model

A dual-hop network with one source node (S), one destination node (D), and K MIMO relays (R_r, $r = 1, 2, \ldots, K$) is under consideration as shown in Figure 3.1. It is assumed that S has one antenna, D has M_D antennas and each relay has M_R antennas. All the K relays adopt DF protocol. Each transmission period is divided into two phases: *Broadcast phase* and *Cooperative phase*. In the broadcast phase, the source node broadcasts message to all nodes (D and all R_rs). The relays that are able to decode the message correctly, constitute the set Φ. If set Φ is non-empty, the relay which maximizes the total received SNR at the destination is selected to cooperate with the source. If set Φ is empty, the

decision is taken on the signal received in broadcast phase. The following assumptions are made for simplicity

1. Equal power is allocated to each phase,
2. Relays transmit the message only if they are able to decode it correctly,
3. Each relay knows if it has correctly decoded the message by using a cyclic redundancy check (CRC) bit,
4. The destination D possesses CSI of the channel $R_r \rightarrow D$ and the decoding statement of every relay before selection, by sending some pilot bits in advance.

In the broadcast phase, S broadcasts a DCSK modulated signal $s(t)$, while all the relays and D keep listening. The received signals from S at jth antenna of D and rth relay can be given, respectively, as [70]

$$y_{SD-j}(t) = \sum_{i=1}^{L} \sqrt{\frac{E_b}{2}} \alpha_{SD-j,i} s(t - \tau_{SD-j,i}) + n_{SD-j}(t), \qquad j = 1, 2, \ldots, M_D, \tag{3.1}$$

$$y_{SR_r-j}(t) = \sum_{i=1}^{L} \sqrt{\frac{E_b}{2}} \alpha_{SR_r-j,i} s(t - \tau_{SR_r-j,i}) + n_{SR_r-j}(t), \qquad j = 1, 2, \ldots, M_R, \tag{3.2}$$

where $n_{SD-j}(t)$ and $n_{SR_r-j}(t)$ are the additive white Gaussian noise (AWGN) at the jth antenna pair of the links $S \rightarrow D$ and $S \rightarrow R_r$, respectively, with zero mean and variance $N_0/2$. The variables $\alpha_{XY-j,i}$ and $\tau_{XY-j,i}$ are the channel coefficient and time delay of the ith path of the jth antenna pair of the $X \rightarrow Y$ link, respectively, and L is the number of independent fading paths in one link. The signals received at the relays are combined using a post-detection EGC followed by decoding.

In the cooperative phase, when the relays form the decoding set Φ, the best relay R_b can be chosen as

$$R_b = \arg \max_{r \in \Phi} \{\gamma_{R_r D}\}, \tag{3.3}$$

where $\gamma_{R_r D}$ is the instantaneous SNR of the rth relay to the destination link. The chosen relay performs DCSK demodulation and transmits M_R DCSK modulated signals to the destination in the cooperative phase. The signals received at the jth antenna pair of the $R_b \rightarrow D$ link, can be expressed as

$$y_{R_b D-j}(t) = \sum_{i=1}^{L} \sqrt{\frac{E_b}{2M_r}} \alpha_{R_b D-j,i} \hat{s}\left(t - \tau_{R_b D-j,i}\right) + n_{R_b D-j}(t), \tag{3.4}$$

where $n_{R_b D-j}$ is AWGN at the jth antenna pair of the $R_b \rightarrow D$ (best relay to destination) link. The signals received at the destination in cooperative phase are combined using a post-detection EGC followed by decoding.

When set Φ is empty, i.e., no relay is able to decode the message correctly, the decision is taken on the signal received in the broadcast phase. Note that, in the cooperative phase, the received signal at each antenna of D is the sum of signals from M_R antennas. However, the implementation of Walsh codes ensure that the signals from the multiple antennas of the relay can be separated at the receiving end and hence, the inter-antenna interference can be neglected. It is assumed that Walsh codes are synchronized in order to keep the inter-antenna interference minimum.

Channel Model

The channels between $S \rightarrow D$, $S \rightarrow R_r$ and $R_r \rightarrow D$ are independent and are subjected to static block frequency-selective fading, meaning that the channel state remains constant during each transmission period. The channel multipath impulse response $h(t)$ can be modeled by a linear time-invariant process, i.e., $h(t) = \sum_{i=1}^{L} \alpha_i \delta(t - \tau_i)$, where the channel coefficient α_i is assumed to be Nakagami-m distributed with the PDF given in Eq. 2.15.

It is further assumed that all independent channels are under similar channel conditions, all the nodes are located in a two dimensional plane and negligible link distance between any two relays. Let d_{SD}, d_{SR} and d_{RD} be the normalized distances of $S \rightarrow D$,

$S \rightarrow R$ and $R \rightarrow D$ links, respectively. The path-loss is modeled as $PL_{SD} = (d_{SD})^{-\eta}$, $PL_{SR} = (d_{SR})^{-\eta}$ and $PL_{RD} = (d_{RD})^{-\eta}$, where η is the path-loss exponent [43]. The delay is assumed to be negligible as compared to the bit duration, i.e., $\tau_i \ll T_b$, to avoid inter symbol interference (ISI).

Using Eq. 2.37, the distribution of the received instantaneous SNR at the jth antenna pair of the $S \rightarrow R_r$, $R_r \rightarrow D$ and $S \rightarrow D$ links are $\gamma_{SR_{r-j}} \sim G\left(mL, \frac{E_b/N_0}{2d_{SR}^{\eta} mL}\right)$, $\gamma_{R_rD-j} \sim G\left(mL, \frac{E_b/N_0}{2M_R d_{RD}^{\eta} mL}\right)$ and $\gamma_{SD-j} \sim G\left(mL, \frac{E_b/N_0}{2d_{SD}^{\eta} mL}\right)$, respectively. Hence, the distribution of $\gamma_{SR_r} = \sum_{j=1}^{M_R} \gamma_{SR_r-j}$, $\gamma_{R_rD} = \sum_{j=1}^{M_R M_D} \gamma_{R_rD-j}$ and $\gamma_{SD} = \sum_{j=1}^{M_D} \gamma_{SD-j}$ can be obtained as

$$\begin{aligned}
\gamma_{SR_r} &\sim G\left(M_R mL, \frac{E_b/N_0}{2d_{SR}^{\eta} mL}\right) = G\left(a_1, b_1\right) \\
\gamma_{R_rD} &\sim G\left(M_R M_D mL, \frac{E_b/N_0}{2M_R d_{RD}^{\eta} mL}\right) = G\left(a_2, b_2\right) \\
\gamma_{SD} &\sim G\left(M_D mL, \frac{E_b/N_0}{2d_{SD}^{\eta} mL}\right) = G\left(a_3, b_3\right),
\end{aligned} \tag{3.5}$$

where $a_1 = M_R mL$, $b_1 = \frac{E_b/N_0}{2d_{SR}^{\eta} mL}$, $a_2 = M_R M_D mL$, $b_2 = \frac{E_b/N_0}{2M_R d_{RD}^{\eta} mL}$, $a_3 = M_D mL$ and $b_3 = \frac{E_b/N_0}{2d_{SD}^{\eta} mL}$ are used for simplicity.

3.1.2 Performance Analysis

The end-to-end error probability of the system with K MIMO relays can be given as

$$P_e = p^K P_1 + \sum_{\psi=1}^{K} \binom{K}{\psi} (1-p)^{\psi} p^{K-\psi} P_2, \tag{3.6}$$

where ψ is the number of relays in Φ, p is the probability that a relay decodes the message incorrectly, P_1 is the error probability of the $S \rightarrow D$ link of the broadcast phase and P_2 is the probability of error when the best relay cooperates with the source node. Thus, to obtain BER performance from Eq. 3.6, we need expressions for p, P_1 and P_2 as discussed below.

For DCSK modulation, p can be expressed as

$$p = \int_0^\infty P_{DCSK-SR}(x)\, f_{\gamma_{SR}}(x)\, dx, \tag{3.7}$$

where $f_{\gamma_{SR}}(x)$ is defined in Eq. 3.5 and $P_{DCSK-SR}(x) = \frac{1}{2} erfc\left(\left[\frac{4}{x} + \frac{2M_R\beta}{x^2}\right]^{-\frac{1}{2}}\right)$ is the conditional error probability of DCSK with a post-detection equal gain combiner at the relays, defined in Eq. 2.35. Below we present the derivations for P_1 and P_2.

Derivation For P_1

When the decoding set Φ is empty, the decision is taken on the signal received at D in the broadcast phase. The error probability of the $S \rightarrow D$ link can be given as

$$P_1 = \int_0^\infty P_{DCSK-SD}(x)\, f_{\gamma_{SD}}(x)\, dx, \tag{3.8}$$

where $P_{DCSK-SD}(x) = \frac{1}{2} erfc\left(\left[\frac{4}{x} + \frac{2M_D\beta}{x^2}\right]^{-\frac{1}{2}}\right)$ and $f_{\gamma_{SD}}(x)$ is the PDF of SNR of the $S \rightarrow D$ link, defined in Eq. 3.5. Thus, substituting these expressions in Eq. 3.8, P_1 can be numerically evaluated.

Derivation For P_2

When the decoding set Φ is non-empty, the best relay cooperates with the source. The probability of error of the $R_b \rightarrow D$ link can be given as

$$P_2 = \int_0^\infty P_{DCSK-RD}(x)\, f_{\gamma_{R_bD}}(x)\, dx, \tag{3.9}$$

where $P_{DCSK-RD}(x) = \frac{1}{2} erfc\left(\left[\frac{4}{x} + \frac{2M_RM_D\beta}{x^2}\right]^{-\frac{1}{2}}\right)$ and $f_{\gamma_{R_bD}}(x)$ is the PDF of SNR of the best relay to destination ($R_b \rightarrow D$) link. Evaluation of Eq. 3.9 requires an expression for PDF $f_{\gamma_{R_bD}}(x)$, which is derived below.

According to the selection criterion stated in Eq. 3.3, the cumulative distribution

function (CDF) of SNR of the $R_b \rightarrow D$ can be derived as (for integer m)

$$F_{\gamma_{R_bD}}(x) = \prod_{r=1}^{\psi} F_{\gamma_{R_rD}}(x) = \left[\int_0^x f_{\gamma_{R_rD}}(\vartheta)\, d\vartheta\right]^{\psi}$$
$$= \left[1 - \sum_{M=0}^{a_2-1} \frac{\left(x/b_2\right)^M}{M!} e^{-x/b_2}\right]^{\psi}, \tag{3.10}$$

where $f_{\gamma_{R_rD}}(\vartheta) = \frac{\vartheta^{a_2-1}e^{-\vartheta/b_2}}{b_2^{a_2}\Gamma(a_2)}$ is the PDF of SNR of the $R_r \rightarrow D$ link. The integration involved in Eq. 3.10 can be solved using [71, (3.351.2)]. Thus, taking the derivative of Eq. 3.10 w.r.t. x and simplifying the resulting expression, an expression for $f_{\gamma_{R_bD}}(x)$ can be obtained as

$$f_{\gamma_{R_bD}}(x) = \psi \frac{x^{a_2-1}e^{-x/b_2}}{b_2^{a_2}\Gamma(a_2)} \left[1 - \sum_{M=0}^{a_2-1} \frac{\left(x/b_2\right)^M}{M!} e^{-x/b_2}\right]^{\psi-1}$$
$$= \frac{\psi}{b_2^{a_2}\Gamma(a_2)} \sum_{\nu=0}^{\psi-1} \binom{\psi-1}{\nu} (-1)^{\nu} \left\{\sum_{M=0}^{\nu(a_2-1)} \frac{\mu_{M\nu}}{b_2^M} x^{M+a_2-1} e^{-(1+\nu)\frac{x}{b_2}}\right\}, \tag{3.11}$$

where $\mu_{\chi\omega}$ is the coefficient of λ^{ω} in the expansion of $\left(\sum_{\chi=0}^{T} \frac{\lambda^{\chi}}{\chi!}\right)^{\omega}$, given as [72]

$$\mu_{\chi\omega} = \begin{cases} \sum_{v=\chi-T}^{\chi} \frac{\mu_{v(\omega-1)}}{(\chi-v)!}, & 0 \le v \le (\omega-1)\,T \\ 0, & \text{else} \end{cases}$$

and $\mu_{00} = \mu_{0\omega} = 1$. Thus, substituting Eq. 3.11 in Eq. 3.9, P_2 can be numerically evaluated.

Finally, substituting Eq. 3.7, Eq. 3.8 and Eq. 3.9 in Eq. 3.6, probability of error of the system can be evaluated.

3.1.3 Numerical and Simulation Results

The derived probability of error expression is numerically evaluated and compared with the MATLAB simulation results. Monte Carlo simulations are carried out to evaluate the performance of the proposed scheme. The cubic map is used to generate the chaotic samples. In the simulation, we assume $\eta = 2$, $2\beta = 128$ and $L = 2$ with both paths

having identical average power gain and path-loss model. The path delay parameters τ_i are assumed to be $(\tau_1, \tau_2) = (0, 1)$. In the figures, $(d_{SD} : d_{SR} : d_{RD})$ represents the geometric position of the source, relays and destination, respectively. These distances are normalized with d_{SD}.

BER vs. average SNR curves are shown in Figure. 3.2(a), for $m = 1$, 2 and 4, for two MIMO relays ($K = 2$). The parameters $(d_{SD} : d_{SR} : d_{RD})$ and (M_R, M_D) are set to $(1 : 1 : 1)$ and $(2, 1)$, respectively. An improvement in BER with increase in m can be observed from the figure, as expected. For example, at 19 dB average SNR, BER improves from $\approx 7.0 \times 10^{-3}$ to $\approx 4.0 \times 10^{-3}$ when m increases from 1 to 2. Further, the BER improves to $\approx 3.0 \times 10^{-3}$ when m is increased to 4.

Figure. 3.2(b) shows the effect of the number of relays (K) on the system performance, at $m = 1$. The geometric position is set to $(1 : 1 : 1)$ and $(M_R, M_D) = (2, 1)$. It can be observed from the figure that the BER improves with increase in K. When the number of relays is more, there is a high probability for relays to make the decoding set Φ non-empty and hence best relay is selected to cooperate instead of no-cooperation. The figure compares the BER performance of the system when single MIMO relay cooperates with the source and when the best relay is selected from multiple MIMO relays to cooperate with the source. It can be observed from the figure that at 19 dB average SNR, the system has a BER of $\approx 3.0 \times 10^{-2}$ when single relay is used to cooperate whereas the BER decreases to $\approx 7.0 \times 10^{-3}$ when the best relay is selected ($K = 2$) to cooperate with the source. However, the performance improvement falls if the relays are further increased, i.e., BER becomes $\approx 3.0 \times 10^{-3}$ and $\approx 1.5 \times 10^{-3}$ if K is increased to 3 and 4, respectively.

The effect of the number of relays and destination antennas (M_R, M_D) on the BER performance of the system is shown in Figure. 3.3(a). The geometric position is set to $(1 : 1 : 1)$ with $K = 2$ and $m = 1$. The curves demonstrate the significance of using multiple antennas at relays and the destination. The BER of the system degrades

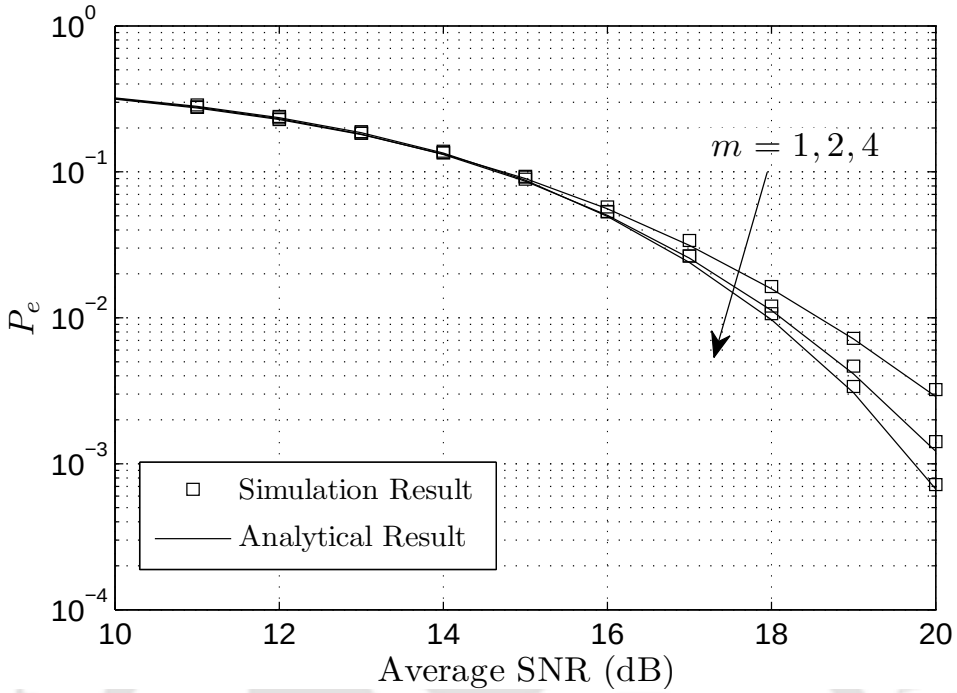

(a) BER with varying fading parameter m.

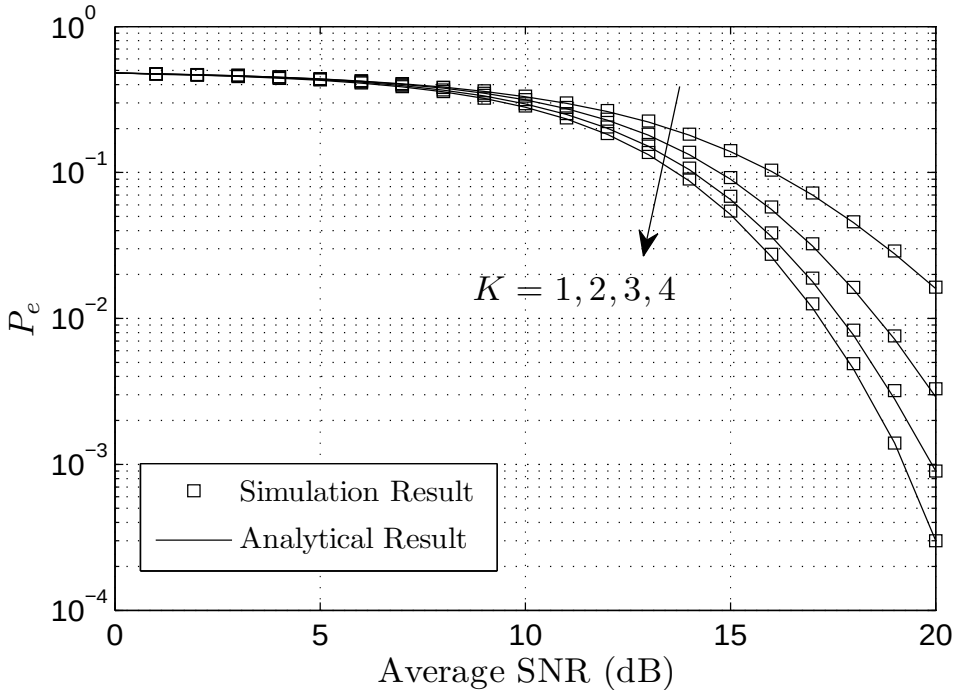

(b) BER with varying relays K.

Figure 3.2: BER performance of the DCSK-SR scheme.

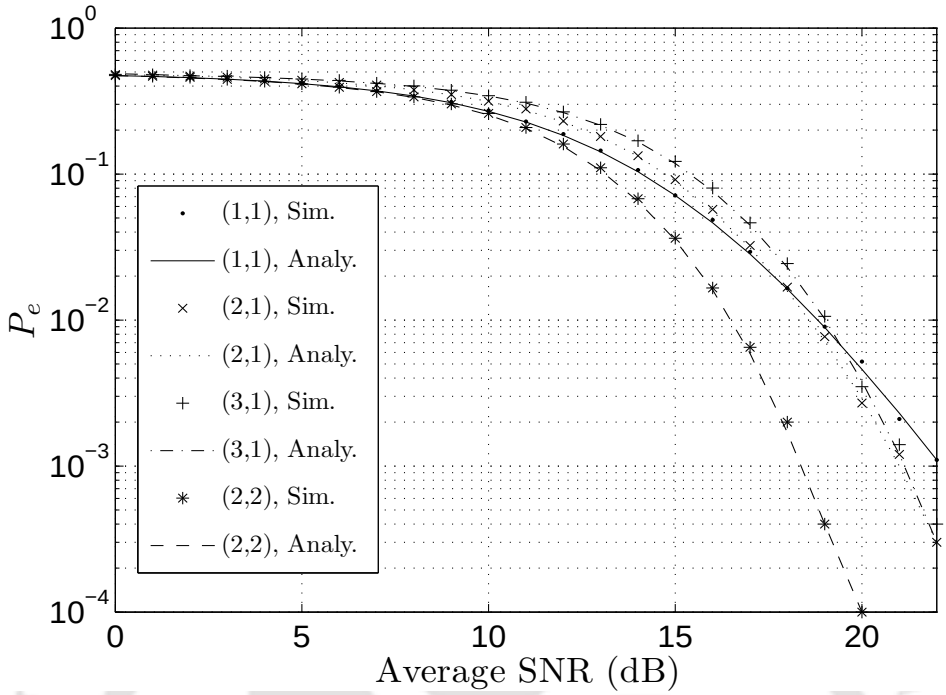

(a) BER for varying relay and destination antennas (M_R, M_D).

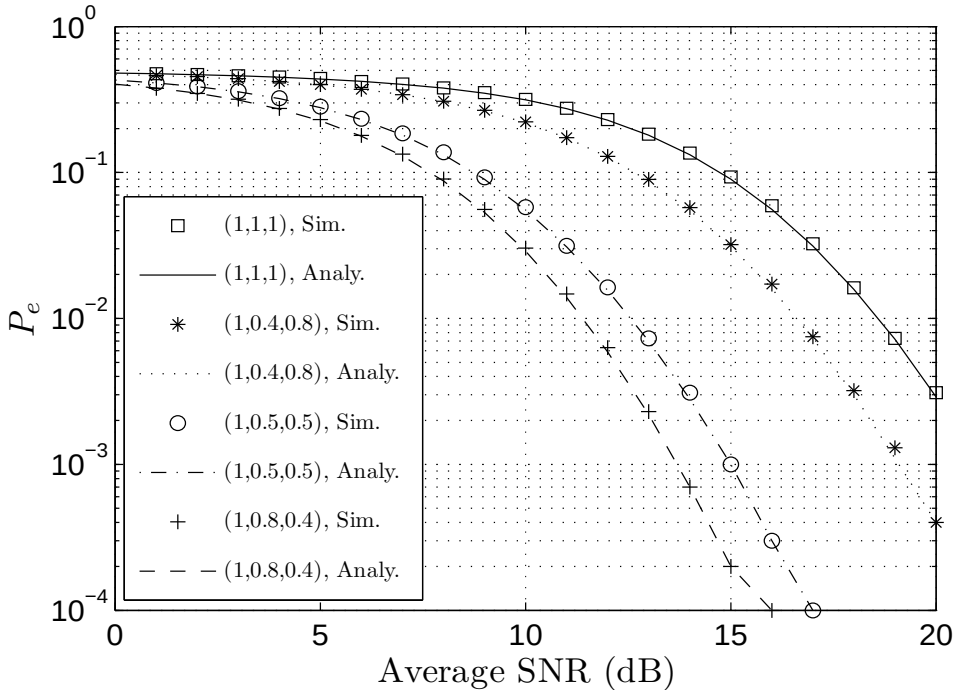

(b) BER for varying normalized distances ($d_{SD} : d_{SR} : d_{RD}$).

Figure 3.3: BER performance of the DCSK-SR scheme.

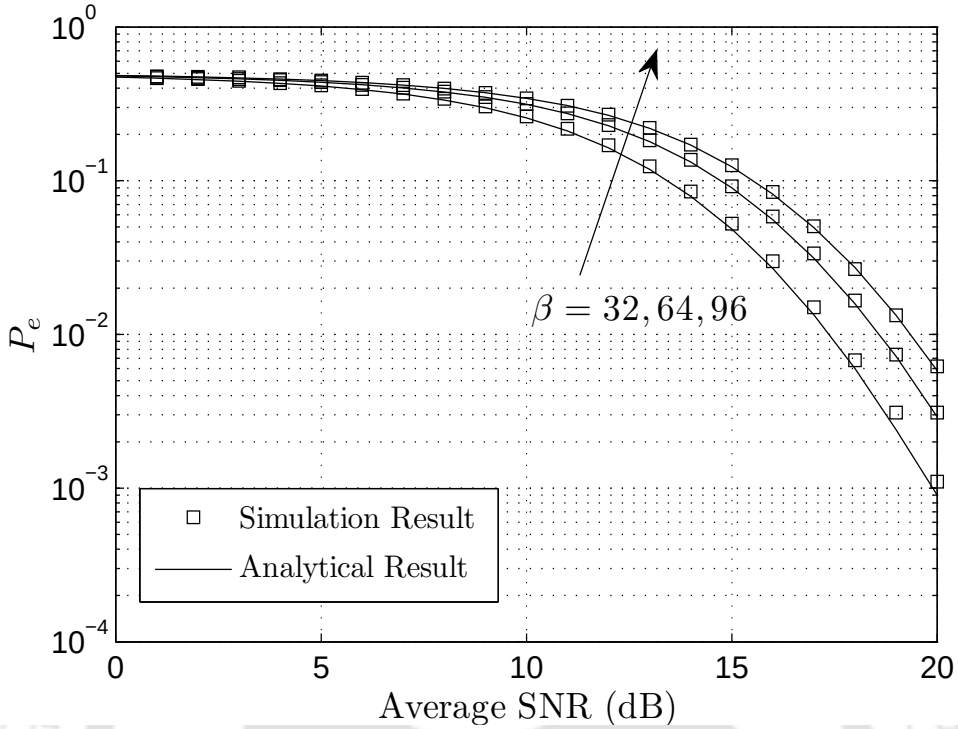

Figure 3.4: BER for different spreading factor β.

when the relays employ multiple antennas as the transmission energy of $R_b \rightarrow D$ link becomes extremely low and hence, the diversity gain is insufficient to offset the effect of deteriorated anti-noise capacity. However, At high average SNR, the relays with multiple antennas completely outperform the relays with single antenna. Further, there is a large improvement in the BER when the destination employs multiple antennas.

The effect of distance on the BER performance of the system is shown in Figure. 3.3(b). Two MIMO relays are used with $(M_R, M_D) = (2, 1)$ and $m = 1$. It can be observed from the figure that the system has a better BER when the relay cluster is close to the destination. For example, at 15 dB average SNR, the system has a BER of $\approx 9.0 \times 10^{-2}$ when the geometric position is set to $(1 : 1 : 1)$ and it improves to $\approx 3.0 \times 10^{-2}$ when the relay cluster is close to D, i.e., for $(1 : 0.4 : 0.8)$. The BER improves to $\approx 10^{-3}$ when the relay cluster is more close to the destination, i.e., $(1 : 0.5 : 0.5)$. It can be concluded from the result that the BER is more *sensitive to the distance in the second hop* as compared

Table. 3.1: BER vs normalized distance Table

$d \rightarrow$	0.5	0.6	0.7	0.8	0.9	1.0
$d_{RD} = d$ $d_{SR} = 0.5$	0.0010	0.0048	0.0143	0.0313	0.0556	0.0853
$d_{SR} = d$ $d_{RD} = 0.5$	0.0010	0.0010	0.0011	0.0013	0.0015	0.0019

to the distance in the first hop. Comparison in the BER is presented in Table 3.1 to observe the effect of hop distances. First, we fixed $d_{SR} = 0.5$ and varied d_{RD}. Similarly, d_{RD} is fixed to 0.5 and d_{SR} is varied. It can be observed from the Table that at 15 dB average SNR, the BER degrades rapidly as distance from relay to destination increases in the first case. However, in the later case, the degradation in BER is very low compared to the former one as d_{RD} is fixed. Thus, the results show that the distance in second hop dominates the system performance (in both cases) as BER changes rapidly with d_{RD} in case 1 and shows very little variation as d_{RD} is fixed in case 2.

Figure. 3.4 illustrates the effect of the spreading factor (2β) on the BER performance of the system for $\beta = 32, 64, 96$. Two MIMO relays are used with $(M_R, M_D) = (2, 1)$ and $m = 1$. The normalized distance is set to $(1 : 1 : 1)$. With fixed transmitted energy per bit, we observe from the figure that the BER at low β is better than the BER at high β since the noise component in the decision variable is proportional to β.

3.2 DCSK Bidirectional Relaying Systems

In wireless communications, cooperative transmission ensures the communication between source and destination terminals if a direct link between them is not available. In particular, a relay terminal assists source and destination terminals for communication. The relay terminal can choose different cooperative transmission protocols as transmission strategy for two-hop wireless networks [69]. Performance of DCSK modulation is evaluated using

DF protocol in [42, 43]. However, the protocols reported in [69] are spectrally inefficient since all terminals operate in half-duplex mode and hence need to use the channel twice for end-to-end communication. As it is well known, the spectral efficiency can be improved by the *two-way* communication, first studied by Shannon in [73]. Bidirectional relaying (BDR) protocols are proposed in [74] for bidirectional (two-way) communication, where two terminals exchange their information through a relay terminal.

Traditional transmission scheme requires four time slots for end-to-end communication. As shown in Figure 3.5(a), node A in the beginning transmits its information to node B through a relay node R and hence needs two time slots to complete transmission. Similarly, node B uses two time slots to transmit its information to node A. However, by using network coding at the relay [75, 76], the end-to-end communication between A and B can be achieved in three time slots. Network coded bidirectional relaying scheme [77] is shown in Figure 3.5(b), in which nodes A and B transmit their information in time slots 1 and 2, respectively. The relay performs X-OR operation on the received symbols and broadcasts the new symbol in the next time slot. At nodes A and B, the desired information can be extracted using the local information. In comparison to traditional and network coded bidirectional relaying scheme, physical-layer network coding (PNC) scheme [78, 79] is more spectral efficient since it requires only two time slots for end-to-end communication. The PNC-BDR scheme is shown in Figure 3.5(c). Specifically, instead of decoding the received symbols from A and B separately at relay node, in PNC, the combined received signal is directly mapped to a signal to be relayed.

In this section, a DCSK bidirectional relaying (DCSK-BDR) scheme is proposed in which the end-to-end communication between two source nodes is established through a relay node. The source nodes use orthogonal chaotic sequences to transmit their information and the relay node adopt DF protocol. Further, the relay node applies network coding and exploits physical-layer broadcast property to enhance efficiency. Hence, the end-to-end communication can be achieved in two time slots. Thus, this scheme is both

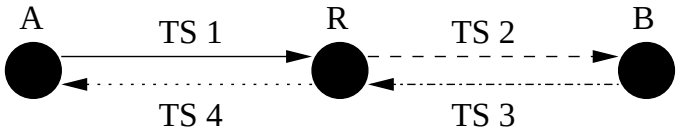

(a) Traditional transmission scheme.

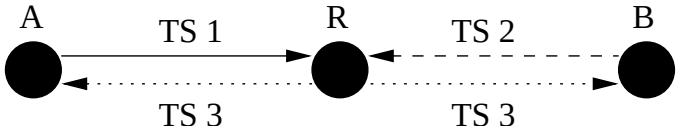

(b) Network coded BDR scheme.

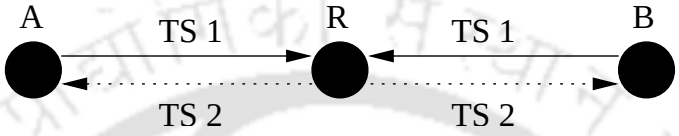

(c) PNC-BDR scheme.

Figure 3.5: Transmission schemes for end-to-end communication for conventional modulation techniques (TS=Time Slot).

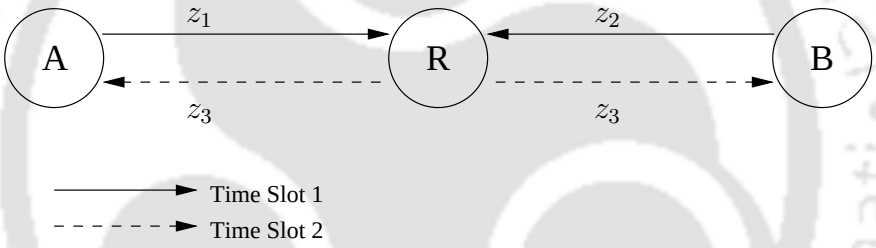

Figure 3.6: System model of bidirectional relay network.

spectral and energy efficient compared to the conventional DCSK scheme, where the relay node has to transmit two times for end-to-end communication. The end-to-end BER is evaluated for the proposed scheme in Nakagami-m fading channel.

3.2.1 System Model

A bidirectional relay network with two source nodes (A and B) and one relay node (R) is under consideration. It is assumed that each node contains one antenna and operates in half-duplex mode. The basic system model is shown in Figure 3.6, where A and B exchange their information through R, assuming there is no direct communication between

two nodes. The relay node uses DF protocol. Each transmission period is divided into two time slots. In the first time slot, the source nodes transmit their messages z_1 and z_2, respectively, to the relay node. The relay decodes both the messages and broadcasts the X-ORed version of both decoded messages in the second time slot. Mathematically,

$$z_3 = z_1 \oplus z_2, \tag{3.12}$$

where z_3 is the broadcast message by the relay in the second time slot and $\oplus$ is the bitwise X-OR operation.

After receiving the message z_3, node A extracts the message of node B by X-OR operation of z_3 and its own transmitted message z_1, i.e.,

$$\hat{z_2} = z_1 \oplus z_3 = z_1 \oplus (z_1 \oplus z_2) = z_2. \tag{3.13}$$

Similarly, B extracts the message transmitted by A.

In the first time slot, A and B transmit their signal to the relay. The received signal at the relay can be given as

$$y_R = \sum_{i=1}^{L} \sqrt{P_1 G_{AR}} \alpha_{AR,i} s_A \left(t - \tau_{AR,i}\right) + \sum_{i=1}^{L} \sqrt{P_2 G_{BR}} \alpha_{BR,i} s_B \left(t - \tau_{AR,i}\right) + n_R, \tag{3.14}$$

where n_R is AWGN at the relay node with zero mean and variance $N_0/2$, L is the number of independent fading paths in one link, G_{XY} is the path-loss of the $X \rightarrow Y$ link and $\alpha_{XY,i}$ and $\tau_{XY,i}$ are the channel coefficient and time delay of the ith path of the $X \rightarrow Y$ link, respectively. Let $d_{AR} = d$ and $d_{BR} = (1 - d)$ are the normalized distance of $A \rightarrow R$ and $B \rightarrow R$ links, respectively. Then the path-loss can be modeled as the function of normalized distance as $G_{AR} = d_{AR}^{-\eta}$ and $G_{BR} = d_{BR}^{-\eta}$, where η is the path-loss exponent. It is assumed that $\alpha_{XY,i}$ is Nakagami-m distributed with PDF given in Eq. 2.15.

In the second time slot, the relay decodes the messages received from nodes A and B, and broadcasts the X-OR of the decoded symbols, i.e., z_3. The signal received through

broadcast at node I, $I \in \{A, B\}$, can be given as

$$y_I = \sum_{i=1}^{L} \sqrt{P_3 G_{RI}} \alpha_{RI,i} s_R \left(t - \tau_{RI,i}\right) + n_I, \tag{3.15}$$

where n_I is AWGN at the node I. Using local information, the desired symbol can be extracted as given in Eq. 3.13.

In the analysis, we assume that all nodes transmit with equal power, i.e., ($P_1 = P_2 = P_3 = P$), where P_1, P_2 and P_3 are the average transmitted power of node A, B and R, respectively. The channels between $A \rightarrow R$ and $B \rightarrow R$ links are independent and subject to static block frequency-selective fading, i.e., the channel state remains constant during two time slots. Further, it is assumed that all independent channels are subjected to the same channel conditions. The delay is assumed to be negligible as compared to the bit duration, i.e., $\tau_{XY,i} \ll T_b$, to avoid ISI.

3.2.2 Performance Analysis

The instantaneous SNR for any $X \rightarrow Y$ link is $\gamma_{\mathrm{XY}} = \sum_{i=1}^{L} \gamma_{\mathrm{i}}$, where $\gamma_{\mathrm{i}} = \frac{P}{N_0} \alpha_{\mathrm{i}}^2$ is the instantaneous SNR of the ith path. Thus, using Eq. 2.37, the distribution of γ_{XY} can be given as $\gamma_{\mathrm{XY}} \sim G\left(mL, \frac{P/N_0}{mL}\right)$.

In the first time slot, nodes A and B transmit their messages to the relay R. If p_{AR} and p_{BR} are the probabilities of error of $A \rightarrow R$ and $B \rightarrow R$ links, respectively, then the error probability at R can be given as

$$p_{\mathrm{R}} = p_{\mathrm{AR}}\left(1 - p_{\mathrm{BR}}\right) + p_{\mathrm{BR}}\left(1 - p_{\mathrm{AR}}\right) = p_{\mathrm{AR}}\left(1 - 2p_{\mathrm{BR}}\right) + p_{\mathrm{BR}}, \tag{3.16}$$

where p_{AR} is the probability of error at relay R when the symbol is transmitted from node A and p_{BR} is the probability of error at R when the symbol is transmitted from node B. Mathematically, p_{AR} can be given as

$$p_{\mathrm{AR}} = \int_0^{\infty} p_{\mathrm{DCSK}}\left(\gamma\right) f_{\gamma_{\mathrm{AR}}}\left(\gamma\right) d\gamma, \tag{3.17}$$

where $p_{\text{DCSK}}(\gamma) = \frac{1}{2} erfc\left(\left[\frac{4}{\gamma} + \frac{2\beta}{\gamma^2}\right]^{-\frac{1}{2}}\right)$ is the conditional BER of DCSK over a multipath fading channel, defined in Eq. 2.23 and $f_{\gamma_{\text{AR}}}$ is the PDF of SNR γ_{AR} of $A \rightarrow R$ link. From Eq. 3.14 it can be shown that $\gamma_{\text{AR}} = \frac{P_1 G_{\text{AR}}}{N_0} \sum_{i=1}^{L} \alpha^2_{\text{AR,i}}$. An expression for $f_{\gamma_{\text{AR}}}$ can be derived using Eq. 2.37 as

$$f_{\gamma_{\text{AR}}}(\gamma) = \frac{\gamma^{mL-1} e^{-\gamma \frac{d_{\text{AR}}^{\eta\, mL}}{(P_1/N_0)}}}{\left(\frac{P_1/N_0}{d_{\text{AR}}^{\eta\, mL}}\right)^{mL} \Gamma(mL)}. \tag{3.18}$$

Thus, by substituting Eq. 3.18 in Eq. 3.17, p_{AR} can be numerically evaluated.

Similarly, p_{BR} can be given as

$$p_{\text{BR}} = \int_0^\infty p_{\text{DCSK}}(\gamma)\, f_{\gamma_{\text{BR}}}(\gamma)\, d\gamma, \tag{3.19}$$

where $p_{\text{DCSK}}(\gamma)$ is given in Eq. 3.17 and $f_{\gamma_{\text{BR}}}$ is the PDF of SNR γ_{BR} of $B \rightarrow R$ link. From Eq. 3.14, it can be shown that $\gamma_{\text{BR}} = \frac{P_2 G_{\text{BR}}}{N_0} \sum_{i=1}^{L} \alpha^2_{\text{BR,i}}$. An expression for $f_{\gamma_{\text{BR}}}$ can be derived using Eq. 2.37 as

$$f_{\gamma_{\text{BR}}}(\gamma) = \frac{\gamma^{mL-1} e^{-\gamma \frac{d_{\text{BR}}^{\eta\, mL}}{(P_2/N_0)}}}{\left(\frac{P_2/N_0}{d_{\text{BR}}^{\eta\, mL}}\right)^{mL} \Gamma(mL)}. \tag{3.20}$$

Thus, p_{BR} can be numerically evaluated by substituting Eq. 3.20 in Eq. 3.19.

At the relay, the signals received from A and B in the first time slot are decoded and an X-ORed version of decoded symbols is broadcasted by the relay in the second time slot. Nodes A and B decode the received symbol and extract their symbol from it using local information. Thus, a transmitted symbol from a source to a destination undergoes two detections in cascade. Let p_{A} is the end-to-end error probability at node A, i.e., error probability for the symbol transmitted from B to A through R and p_{B} is the end-to-end error probability at node B, i.e., error probability for the symbol transmitted from A to B through R. Hence, the end-to-end error probability at node I, $I \in \{A, B\}$, can be given as

$$p_{\text{I}} = p_{\text{R}}\big(1 - p_{\text{RI}}\big) + p_{\text{RI}}\big(1 - p_{\text{R}}\big) = p_{\text{R}}\big(1 - 2p_{\text{RI}}\big) + p_{\text{RI}}, \tag{3.21}$$

where $p_{\mathrm{RI}} = \int_0^\infty p_{\mathrm{DCSK}}(\gamma) f_{\gamma_{\mathrm{RI}}}(\gamma) d\gamma$ is the probability of error at node I, when the symbol is transmitted from node R to node I and $f_{\gamma_{\mathrm{RI}}}$ is the PDF of SNR of $R \rightarrow I$ link and can be given as

$$f_{\gamma_{\mathrm{RI}}}(\gamma) = \frac{\gamma^{mL-1} e^{-\gamma \frac{d_{\mathrm{RI}}^{\eta\, mL}}{(P_3/N_0)}}}{\left(\frac{P_3/N_0}{d_{\mathrm{RI}}^{\eta} mL}\right)^{mL} \Gamma(mL)}, \tag{3.22}$$

where P_3 is defined in the paragraph immediately below Eq. 3.15. Thus, the total average probability of error of the system can be given as

$$p_{\mathrm{tot}} = \frac{1}{2}\left(p_{\mathrm{A}} + p_{\mathrm{B}}\right). \tag{3.23}$$

By substituting Eq. 3.21 in Eq. 3.23, the total error probability of the system can be numerically evaluated.

3.2.3 Numerical and Simulation Results

The derived BER expression is numerically evaluated and compared with the MATLAB simulation results. Monte Carlo simulations are carried out to evaluate the performance of the DCSK-BDR scheme. The cubic map is used to generate the chaotic samples. In the simulation, we assume $\eta = 2$, $\beta = 64$ and $L = 2$. The two paths have equal average power gain and same path-loss model. The path delays for two paths are assumed to be $(\tau_1, \tau_2) = (0, 1)$.

BER performance of the proposed DCSK-BDR scheme is compared with that of the DCSK traditional transmission scheme in Figure 3.7(a). The error probability of both the schemes is plotted against the average SNR for $d = 0.5$ and $m = 1$. It can be observed from the figure that the performance of the proposed bidirectional relaying scheme is inferior to the traditional transmission scheme. However, by using the orthogonal chaotic signals at the source node and network coding at the relay, only two time slots are needed in the proposed scheme for end-to-end communication between A and B. Hence, the proposed scheme offers spectral efficiency. On the contrary, for end-to-end communication, the

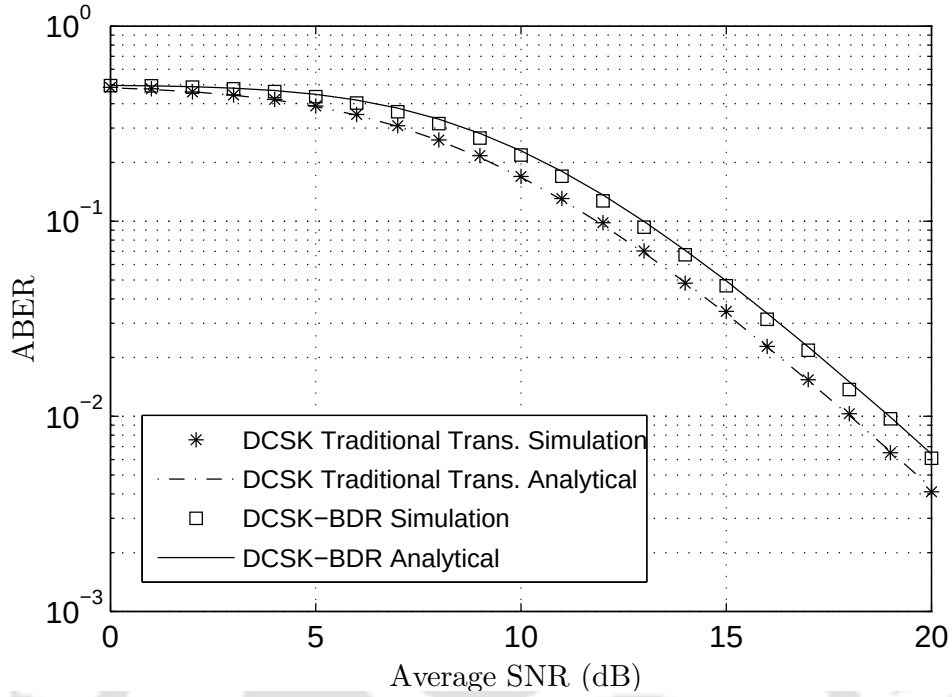

(a) BER comparison of the DCSK-BDR and the DCSK traditional transmission scheme.

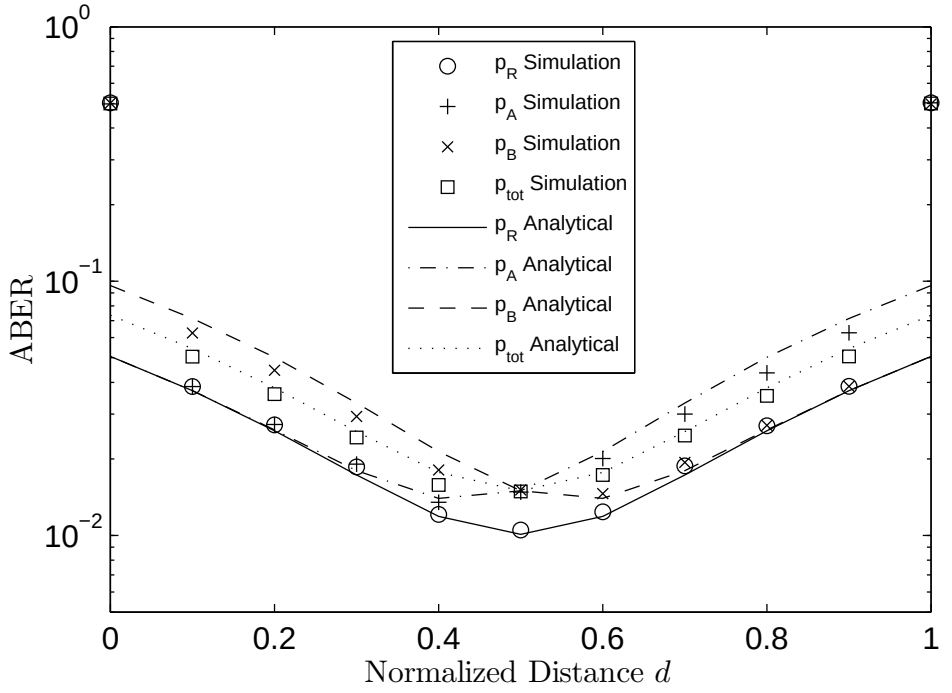

(b) BER performance of DCSK-BDR for varying normalized distance d.

Figure 3.7: BER performance of the DCSK-BDR scheme.

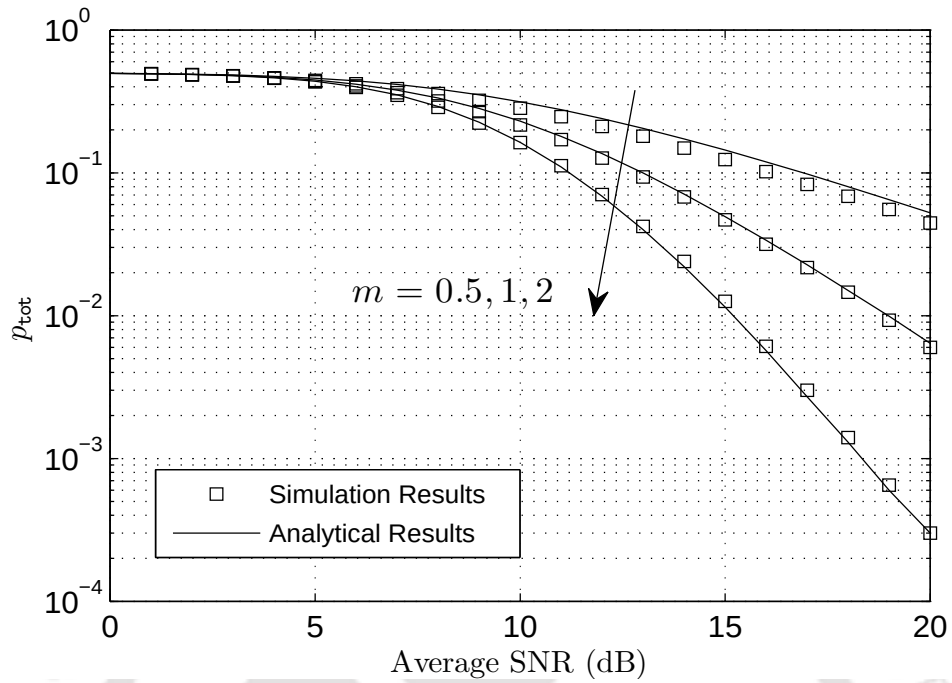

(a) BER performance of DCSK-BDR for varying m.

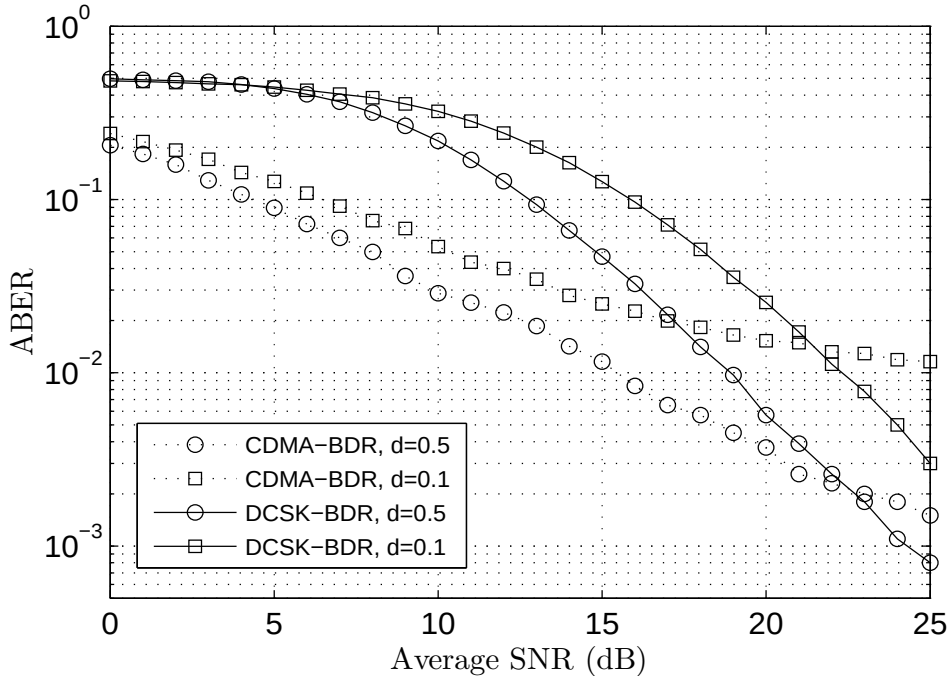

(b) BER performance comparison of the DCSK-BDR and the CDMA-BDR systems at spreading factor ($2\beta = 64$) and $m = 1$.

Figure 3.8: BER performance of the DCSK-BDR scheme.

traditional transmission scheme and the network coded BDR scheme require four and three time slots, respectively. Therefore, for a three-node wireless network, the proposed scheme improves the system throughput by a factor of 100% and 50% relative to traditional transmission scheme and network coded BDR scheme, respectively [78].

Figure 3.7(b) shows the effect of normalized distance d on p_{R}, end-to-end error probabilities (p_{A}, p_{B}) and p_{tot}, for $m = 1$. It can be observed from the figure that the system offers minimum BER when relay node is in the middle of node A and node B. The total end-to-end BER is ≈ 3 dB less than the BER at the relay. This is because the distance of the relay from any of the source nodes is always less than the end-to-end distance, i.e., $d_{\mathrm{AR}} + d_{\mathrm{RB}} = d_{\mathrm{AB}}$. However, when the relay node is close to the respective nodes, p_{A} and p_{B} have the same BER as p_{R}. The reason behind this is the higher geometric gain in the second hop. But, as shown in the figure, to obtain the best total end-to-end BER, the geometric position of relay needs to be at the middle of A and B, i.e., $d = 0.5$.

BER versus average SNR is shown in Figure 3.8(a), for $m = 0.5$, 1, and 2. The normalized distance d is set to 0.5. The figure demonstrates an improvement in BER with increase in m, as expected. For example, at 16 dB average SNR, BER improves from $\approx 1.5 \times 10^{-1}$ to $\approx 3.5 \times 10^{-2}$ when m increases from 0.5 to 1. Further, BER improves from $\approx 3.5 \times 10^{-2}$ to $\approx 6.0 \times 10^{-3}$ on the increment of m from 1 to 2.

Comparison with CDMA-BDR systems

In Figure 3.8(b), BER performance of the DCSK bidirectional relaying system is compared with that of the CDMA bidirectional relaying (CDMA-BDR) systems for $d = 0.1$, 0.5. For CDMA system simulation, Gold-sequences are adopted as spreading sequences. To ensure the same bandwidth of two systems, an extra '0' is added at the end of each Gold-sequence as the length of a Gold-sequence is always odd and the spreading factor (2β) of the DCSK system is always even. A simple correlation receiver is adopted at

the receiver. It is observed from the figure that the CDMA-BDR system has lower BER than the DCSK-BDR systems at low SNR range. However, at high SNR range, the proposed scheme completely outperforms the CDMA-BDR scheme. The reason behind the low BER of the DCSK-BDR systems at high SNR is that the DCSK system by default exploits the multipath diversity by using AcR whereas the CDMA system needs to employ a RAKE receiver to get the advantage of multipath diversity. It can be mentioned here that RAKE receiver requires the full CSI and hence increases the circuit complexity. It can also be observed from the figure that the geometric position of the relay affects the BER performance of both the systems.

3.3 DCSK Transmit Antenna Selection Systems

Wireless transmission is often affected by multipath fading. This results in the system performance degradation and hence, making reliable communication difficult. Multiple antenna system or generally called MIMO system improves the capacity and reliability of wireless communication significantly. In particular, antenna diversity is a practical, effective and thus, very popular MIMO technique to combat the effect of multipath fading. In classical antenna diversity approach, receiver uses multiple antennas and performs diversity technique operations, i.e., selection combining, maximal ratio combining (MRC), equal gain combining (EGC) or scanning diversity, to improve the robustness of the communication systems [63]. However, the receiver antenna diversity has the cost, size and power related issues, as the remote units are supposed to be small, lightweight and power efficient with low hardware complexity. Transmit antenna diversity system offers an attractive solution as it uses multiple transmit antennas at the base station and effectively mitigates fading at the remote units [80, 81]. The main drawback of any MIMO system is the multiple radio frequency (RF) chain requirement, which increases complexity and thus cost. Transmit antenna selection (TAS) offers low-cost, low-complexity solution to

achieve many of the advantages of MIMO systems or in general transmit antenna diversity systems [82]. In TAS, only selected transmit antennas are activated for transmission and hence, reduced number of RF chains are required for transmission which makes the system cost-effective and less complex. Furthermore, if only the best transmit antenna is selected and activated for transmission, there is no inter-antenna interference and consequently, transmit antenna synchronization is not required. From performance point of view, antenna selection retains the diversity order compared to the full complexity systems [83]. Though in frequency-selective channels, the antenna selection is not very effective. However, for moderately frequency-selective channels, it provides significant performance gain [84].

Among TAS schemes, TAS/MRC is popular [83, 85]. In TAS/MRC, a single transmit antenna which maximizes the total received signal power at the receiver is selected for uncoded transmission. In joint transmit and receive antenna selection, a transmit and receive antenna pair which maximizes the received SNR is selected for signal transmission [86].

In this section, DCSK modulation based transmit antenna selection schemes are proposed. First, a multiple transmit antenna and single receive antenna based DCSK-TAS scheme is proposed in which a single transmit antenna which maximizes the received SNR at the receiver is selected for DCSK transmission. Secondly, a multiple transmit and multiple receive antenna based DCSK-joint antenna selection (DCSK-JAS) scheme is proposed in which a wireless link between a transmit and a receive antenna which maximizes the received SNR is used for signal transmission. Finally, a hybrid DCSK-transmit antenna selection/equal gain combining (DCSK-TAS/EGC) scheme is proposed, in which antenna selection is performed at the transmitter and the receiver performs post-detection EGC. Specifically, a single transmit antenna which maximizes the post-detection equal gain combiner output at the receiver is selected for DCSK transmission. Mathematical expressions for the probability of error and throughput of the proposed schemes are derived

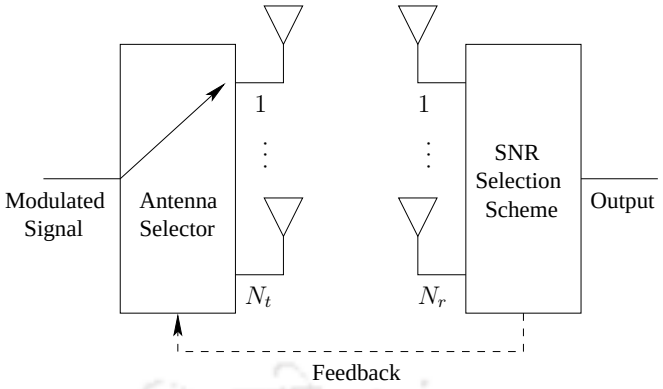

Figure 3.9: System Model for a (N_t, N_r) system.

for Nakagami-m fading channels.

3.3.1 System Model

A communication system with N_t transmitting antennas and N_r receiving antennas is under consideration. We represent this system as (N_t, N_r) system. The basic system model is shown in Figure 3.9, in which a feedback link exist between transmitter and receiver. At a time, only one transmit antenna is selected and activated for transmission. Each transmit antenna sends a pilot signal in advance at different time slots. Based on the received SNR, the best transmit antenna is selected at the receiver. Through the feedback, transmit antenna with maximum received SNR is activated for transmission.

If the jth transmit antenna is activated for transmission, the signal received at Jth receiving antenna is given by

$$y_J = \sum_{i=1}^{L} \alpha_{j,J-i} s_j \left(t - \tau_{j,J-i}\right) + n_J, \tag{3.24}$$

where $s_j(t)$ is the DCSK modulated signal, n_J is AWGN at the Jth antenna with zero mean and $N_0/2$ variance and L is the number of independent fading paths in one antenna link. The variables $\alpha_{j,J-i}$ and $\tau_{j,J-i}$ are the channel coefficient and time delay of the ith path of the $j \rightarrow J$ antenna link, respectively. It is assumed that $\alpha_{j,J-i}$ is Nakagami-m distributed with PDF given in Eq. 2.15.

The transmit antenna with maximum received SNR can be selected by the following selection criterion

DCSK-TAS

For a $(N_t, 1)$ communication system, the maximum received SNR is selected as

$$\gamma_{\text{TAS}} = \max_{1 \le j \le N_t} \{\gamma_j\}, \tag{3.25}$$

where γ_j is the received SNR when the jth transmit antenna is activated for transmission and from Eq. 3.24, it can be shown as $\gamma_j = \frac{E_b}{N_0} \sum_{i=1}^{L} \alpha_{j-i}^2$. The selected transmit antenna is activated to transmit the DCSK modulated data to the receiving end.

DCSK-JAS

If the transmitting and receiving ends have the multiple antennas, i.e., (N_t, N_r) system, the maximum received SNR can be selected by comparing all $N_t N_r$ combinations of received SNRs, as

$$\gamma_{\text{JAS}} = \max_{\substack{1 \le j \le N_t \\ 1 \le J \le N_r}} \{\gamma_{j,J}\}, \tag{3.26}$$

where $\gamma_{j,J}$ is the SNR of the jth transmit antenna and Jth receiving antenna link. The selected transmit antenna is activated to transmit the DCSK modulated data to the receiving end.

DCSK-TAS/EGC

In TAS/EGC, a single transmit antenna which maximizes the total received signal power at the receiver, is selected for transmission. TAS/EGC employs multiple antennas at transmitting and receiving end as well as a post-detection equal gain combiner at the receiver. Hence, in TAS/EGC, the signals received from each transmit antenna are post-

detection equal gain combined first and then the transmit antenna with maximum total received SNR is selected for transmission. For a (N_t, N_r) system, the maximum total received SNR can be selected as [83]

$$\gamma_{\text{TAS/EGC}} = \max_{1 \le j \le N_t} \left\{ \sum_{J=1}^{N_r} \gamma_{j,J} \right\}. \tag{3.27}$$

Through the feedback, the selected transmit antenna is activated to transmit the DCSK modulated information to the receiving end.

The channels for all transmit and receiving antenna links are assumed to be independent and subjected to static block frequency-selective fading, i.e., the channel coefficients remain constant during one frame and change independently from one frame to another. Further, all independent channels are subjected to the same channel conditions. It is assumed that the feedback works perfectly, i.e., there is no feedback error or delay. The path delay is assumed to be negligible as compared to the bit duration, i.e., $\tau_{j,J-i} \ll T_b$, to avoid ISI.

3.3.2 BER Analysis

The instantaneous SNR for any $j \to J$ antenna link is $\gamma_{j,J} = \sum_{i=1}^{L} \gamma_{j,J-i}$, where $\gamma_{j,J-i} = \frac{E_b}{N_0}\alpha_{j,J-i}^2$ is the instantaneous SNR of the ith path. Thus, from Eq. 2.26, $\gamma_{j,J}$ is gamma distributed, i.e., $\gamma_{j,J} \sim G\left(mL, \frac{E_b/N_0}{mL}\right)$, with CDF and PDF given as $F_{\gamma_{j,J}}(\gamma) = \frac{1}{\Gamma(mL)}\gamma\left(mL, \frac{mL}{E_b/N_0}\gamma\right)$ and $f_{\gamma_{j,J}}(\gamma) = \frac{\gamma^{mL-1} e^{-\frac{mL}{E_b/N_0}\gamma}}{\left(\frac{E_b/N_0}{mL}\right)^{mL}\Gamma(mL)}$, respectively.

DCSK-TAS

From Eq. 3.25, CDF of the best available SNR at the receiving end can be given using order statistics [87] as

$$F_{\gamma_{\text{TAS}}}(\gamma) = \prod_{j=1}^{N_t} F_{\gamma_j}(\gamma) = \left[F_{\gamma_j}(\gamma)\right]^{N_t}, \tag{3.28}$$

where γ_j is the instantaneous SNR of the jth link. By taking the derivative of Eq. 3.28 and substituting the values, the PDF of γ_{TAS} can be given as

$$\begin{aligned} f_{\gamma_{\text{TAS}}}(\gamma) &= N_t\Big[F_{\gamma_j}(\gamma)\Big]^{N_t-1} f_{\gamma_j}(\gamma) \\ &= N_t \frac{\gamma^{mL-1} e^{-\frac{mL}{E_b/N_0}\gamma}}{\left(\frac{E_b/N_0}{mL}\right)^{mL}\Gamma(mL)} \left[\frac{\gamma\left(mL, \frac{mL}{E_b/N_0}\gamma\right)}{\Gamma(mL)}\right]^{N_t-1}, \end{aligned} \tag{3.29}$$

where $\gamma(a,b) = \int_0^b z^{a-1}e^{-z}dz$, $\text{Re}\{a\} = 0$, is the lower incomplete gamma function [71]. Now, the average error probability of DCSK-TAS can be given as

$$P_{\text{DCSK-TAS}} = \int_0^\infty P_{\text{DCSK}}(\gamma)\, f_{\gamma_{\text{TAS}}}(\gamma)\, d\gamma, \tag{3.30}$$

where $P_{\text{DCSK}}(\gamma) = \frac{1}{2} erfc\left(\left[\frac{4}{\gamma} + \frac{2\beta}{\gamma^2}\right]^{-\frac{1}{2}}\right)$ is the conditional probability of error of DCSK over a multipath fading channel defined in Eq. 2.23.

Finally, substituting Eq. 3.29 in Eq. 3.30, the probability of error for DCSK-TAS can be numerically evaluated.

DCSK-JAS

Using Eq. 3.26, CDF of the best SNR from the N_tN_r available links between transmitter and receiver can be given as

$$F_{\gamma_{\text{JAS}}}(\gamma) = \prod_{v=1}^{N_tN_r} F_{\gamma_v}(\gamma) = [F_{\gamma_v}(\gamma)]^{N_tN_r} \tag{3.31}$$

Hence, the PDF of SNR of the joint antennas selection can be obtained by taking the derivative of Eq. 3.31 as

$$\begin{aligned} f_{\gamma_{\text{JAS}}}(\gamma) &= N_tN_r[F_{\gamma_v}(\gamma)]^{N_tN_r-1} f_{\gamma_v}(\gamma) \\ &= N_tN_r \frac{\gamma^{mL-1} e^{-\frac{mL}{E_b/N_0}\gamma}}{\left(\frac{E_b/N_0}{mL}\right)^{mL}\Gamma(mL)} \left[\frac{\gamma\left(mL, \frac{mL}{E_b/N_0}\gamma\right)}{\Gamma(mL)}\right]^{N_tN_r-1} \end{aligned} \tag{3.32}$$

Now, the average error probability of DCSK-JAS can be given as

$$P_{\text{DCSK-JAS}} = \int_0^\infty P_{\text{DCSK}}(\gamma)\, f_{\gamma_{\text{JAS}}}(\gamma)\, d\gamma, \tag{3.33}$$

where $P_{\text{DCSK}}(\gamma)$ is defined in Eq. 3.30.

Substituting Eq. 3.32 in Eq. 3.33, the probability of error for DCSK-JAS can be numerically evaluated.

DCSK-TAS/EGC

From Eq. 3.27, CDF of the best total received SNR from the N_t transmitting antennas can be given as

$$F_{\gamma_{\text{TAS/EGC}}}(\gamma) = \prod_{j=1}^{N_t} F_{\gamma_{\text{j/EGC}}}(\gamma) = \left[F_{\gamma_{\text{j/EGC}}}(\gamma)\right]^{N_t}, \tag{3.34}$$

where $\gamma_{\text{j/EGC}} = \sum_{J=1}^{N_r} \gamma_{j,J}$ is the instantaneous SNR available at the post-detection EGC output, which follows the gamma distribution, i.e., $\gamma_{\text{j/EGC}} \sim G\left(N_r mL, \frac{E_b/N_0}{mL}\right)$, with PDF $f_{\gamma_{\text{j/EGC}}}(\gamma) = \frac{\gamma^{N_r mL-1} e^{-\frac{mL}{E_b/N_0}\gamma}}{\left(\frac{E_b/N_0}{mL}\right)^{N_r mL}\Gamma(N_r mL)}$.

From Eq. 3.34, the PDF of $\gamma_{\text{TAS/EGC}}$ can be obtained as

$$\begin{aligned} f_{\gamma_{\text{TAS/EGC}}}(\gamma) &= N_t\left[F_{\gamma_{\text{j/EGC}}}(\gamma)\right]^{N_t-1} f_{\gamma_{\text{j/EGC}}}(\gamma) \\ &= N_t \frac{\gamma^{N_r mL-1} e^{-\frac{mL}{E_b/N_0}\gamma}}{\left(\frac{E_b/N_0}{mL}\right)^{N_r mL}\Gamma(N_r mL)} \left[\frac{\gamma\left(N_r mL, \frac{mL}{E_b/N_0}\gamma\right)}{\Gamma(N_r mL)}\right]^{N_t-1}. \end{aligned} \tag{3.35}$$

Now, the average error probability for DCSK-TAS/EGC can be given as

$$P_{\text{DCSK-TAS/EGC}} = \int_0^\infty P_{\text{DCSK-EGC}}(\gamma)\, f_{\gamma_{\text{TAS/EGC}}}(\gamma)\, d\gamma, \tag{3.36}$$

where $P_{\text{DCSK-EGC}}(\gamma) = \frac{1}{2} erfc\left(\left[\frac{4}{\gamma} + \frac{2N_r\beta}{\gamma^2}\right]^{-\frac{1}{2}}\right)$ is the conditional error probability of the DCSK modulation with post-detection EGC at the receiving end, defined in Eq. 2.35.

Finally, substituting Eq. 3.35 in Eq. 3.36, the probability of error for DCSK-TAS/EGC can be numerically evaluated.

3.3.3 Throughput Analysis

Throughput is defined as the number of successfully received bits per symbol and is a decreasing function of the probability of error [66, 67]. Throughput or maximum data rate for reliable communication can be given as

$$\mathrm{T_{put}}\left(\gamma\right) = 1 - H\left(P\right), \tag{3.37}$$

where $H\left(P\right)$ is the entropy of a Bernoulli random variable with parameter P [88]. The variable P is the conditional error probability which specifically depends on the modulation scheme used.

The average throughput can be obtained by averaging $\mathrm{T_{put}}\left(\gamma\right)$ over γ, as

$$\mathrm{T_{put}} = \int_{0}^{\infty} \mathrm{T_{put}}\left(\gamma\right) f\left(\gamma\right) d\gamma, \tag{3.38}$$

where $f(\gamma)$ is the PDF of γ. By substituting Eq. 3.29 and Eq. 3.37 in Eq. 3.38, the throughput for DCSK-TAS, i.e., $\mathrm{T_{DCSK-TAS}}$, can be numerically evaluated. Similarly, throughput for DCSK-JAS ($\mathrm{T_{DCSK-JAS}}$) and throughput for DCSK-TAS/EGC ($\mathrm{T_{DCSK-TAS/EGC}}$) can be numerically evaluated.

3.3.4 Numerical and Simulation Results

The derived probability of error expressions are numerically evaluated and compared with the MATLAB simulation results. Monte Carlo simulations are carried out to evaluate the performance of the proposed schemes. The cubic map is used to generate the chaotic samples. In the simulation, we assume $\beta = 64$ and $L = 2$ with path delays for two paths are $(\tau_1, \tau_2) = (0, 1)$. The two paths have identical average power gain.

In Figure 3.10(a), the probability of error of the DCSK-TAS system is plotted against the average SNR for fading parameter $m = 1$. The figure demonstrates that the error probability of the system is reduced as the number of transmit antennas increases. This is because as N_t increases, there are more available received SNRs to select the maximum

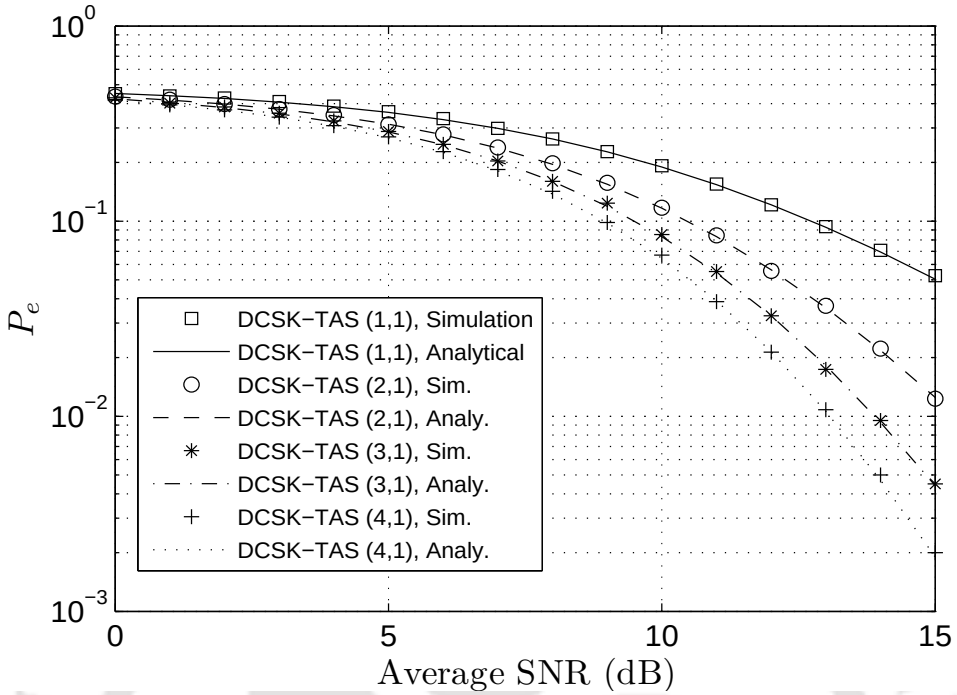

(a) Error performance of DCSK-TAS for varying N_t.

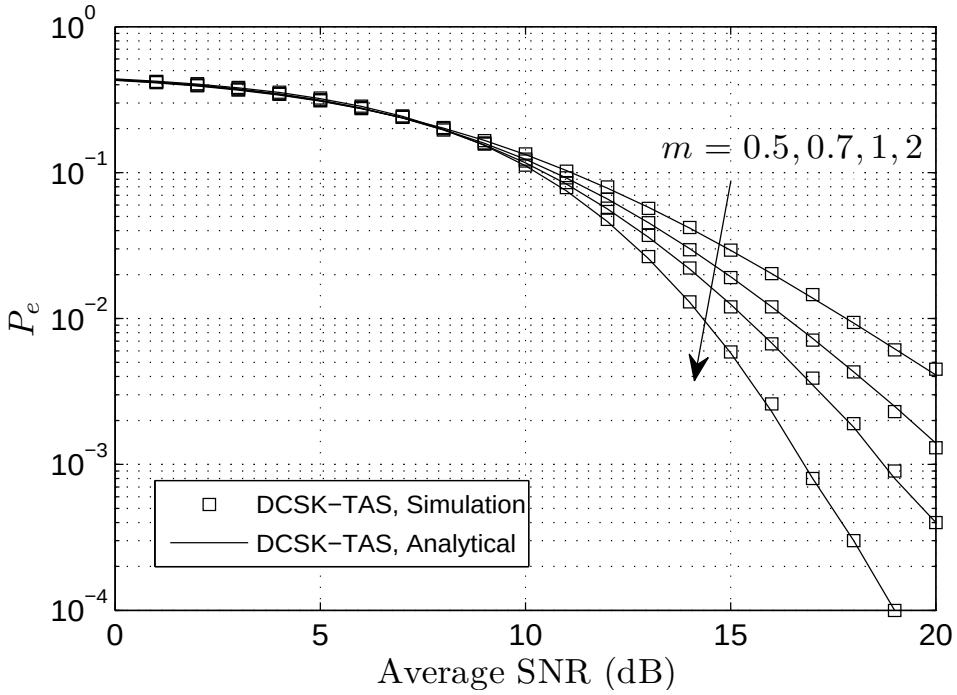

(b) Error performance of DCSK-TAS for varying m.

Figure 3.10: BER performance of the DCSK-TAS systems.

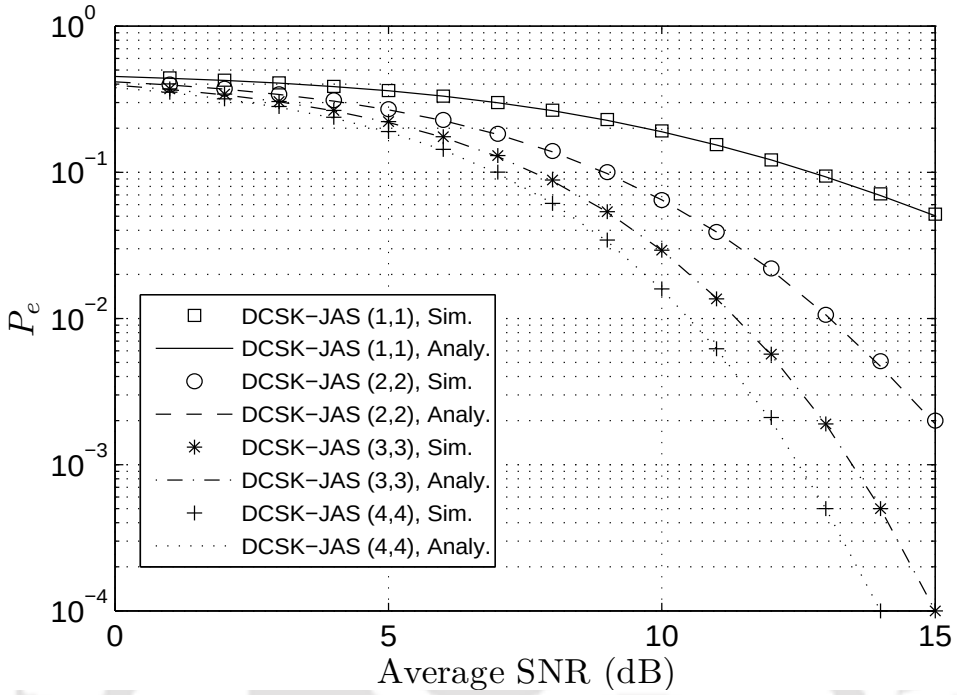

(a) Error performance of the DCSK-JAS systems.

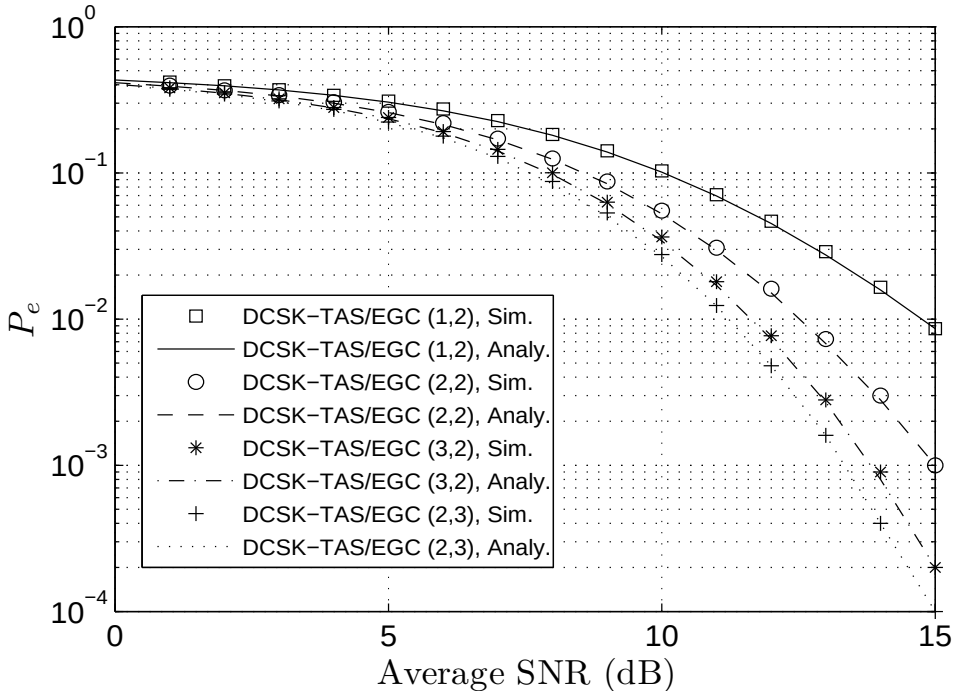

(b) Error performance of the DCSK-TAS/EGC systems.

Figure 3.11: BER performance of the DCSK-JAS and DCSK-TAS/EGC systems.

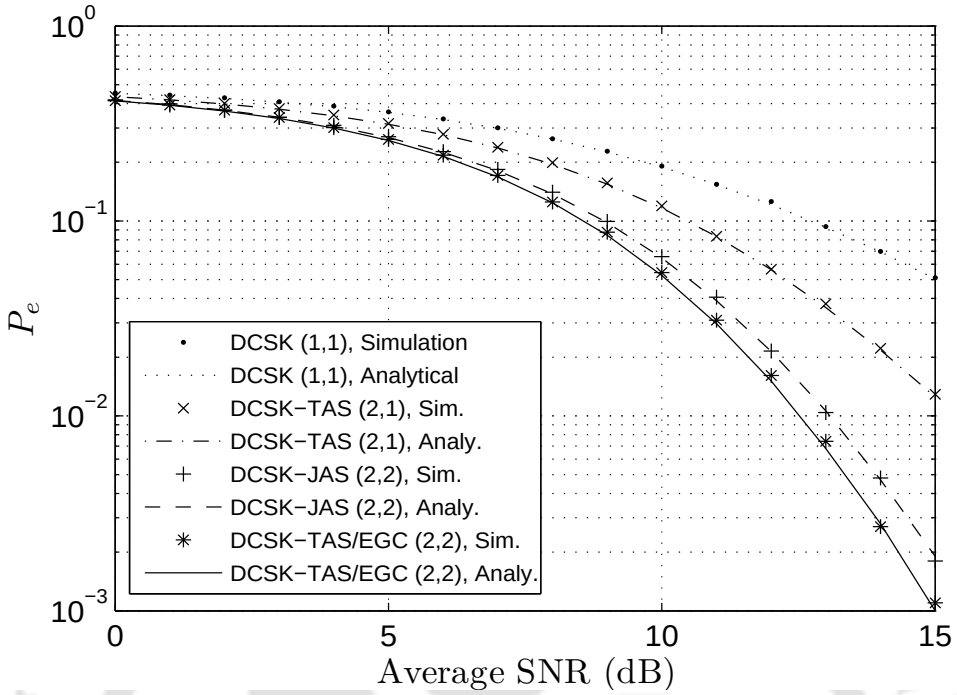

(a) Performance comparison among different TAS schemes and DCSK system for $m = 1$.

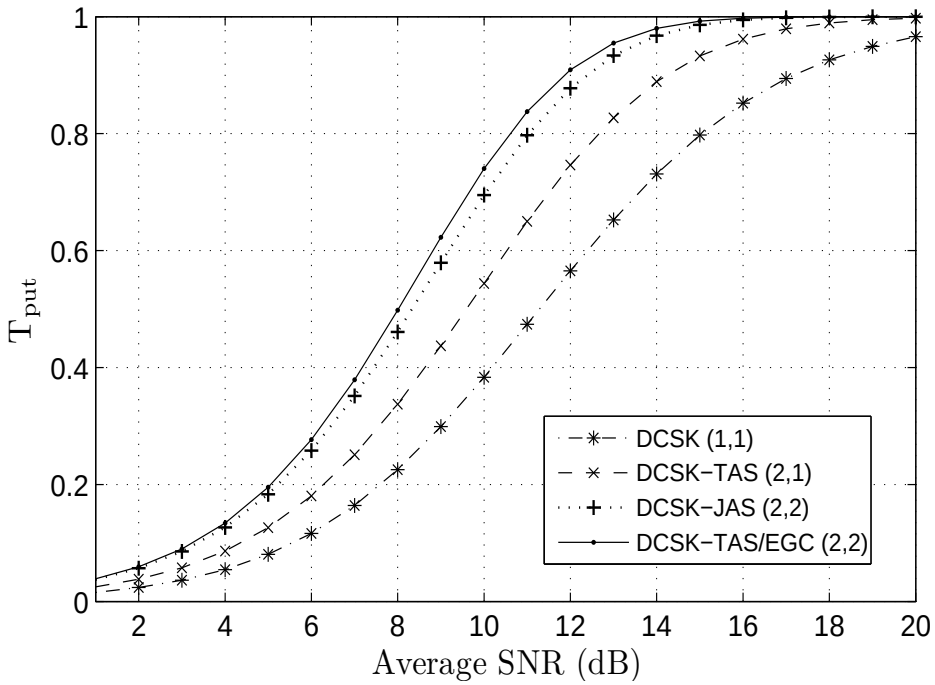

(b) Throughput performance of the transmit antennas selection schemes.

Figure 3.12: Performance comparison of DCSK transmit antennas selection systems.

received SNR. However, improvement in the error performance is deteriorated as N_t increases from 2 to 3 and so on. The improvement in $P_{\text{DCSK-TAS}}$ becomes negligible if N_t are increased beyond a certain threshold.

Error probability versus average SNR curves for DCSK-TAS $(2, 1)$ system are shown in Figure 3.10(b), for $m = 0.5$, 0.7, 1 and 2. The figure demonstrates an improvement in $P_{\text{DCSK-TAS}}$ with increase in m, as expected.

DCSK-JAS employs multiple antennas at transmitting and receiving end and hence more combination of received SNRs are available to select the maximum received SNR, as compared to DCSK-TAS. The error performance of DCSK-JAS system against the average SNR is shown in Figure 3.11(a), for $m = 1$. It can be observed from the figure that for a (N_t, N_r) system, $P_{\text{DCSK-JAS}}$ decreases as either N_t or N_r increases. For example, at 12 dB average SNR, P_e for $(1, 1)$ system is $\approx 10^{-1}$ and decreases to $\approx 2 \times 10^{-2}$ for $(2, 2)$ system. Error probability further decreases to $\approx 5 \times 10^{-3}$ for $(3, 3)$ system.

Probability of error for DCSK-TAS/EGC is plotted against the average SNR in Figure 3.11(b), for $m = 1$. In DCSK-TAS/EGC, the transmit antenna which maximizes the post-detection EGC output is selected for transmission. The figure shows the error performance of the system for different combinations of (N_t, N_r). It is observed from the figure that $P_{\text{DCSK-TAS/EGC}}$ decreases with increase in N_t or N_r. The figure demonstrates that the increasing N_r is more effective to decrease $P_{\text{DCSK-TAS/EGC}}$, compared with that of N_t. For example, at 14 dB average SNR, the error probability of DCSK-TAS/EGC is $\approx 3 \times 10^{-3}$ for $(2, 2)$ system. $P_{\text{DCSK-TAS/EGC}}$ decreases to $\approx 8 \times 10^{-4}$ when a transmit antenna is increased, i.e., for $(3, 2)$ system. However, there is a large improvement in $P_{\text{DCSK-TAS/EGC}}$ if a receiver antenna is increased, i.e., as can be seen for $(2, 3)$ system the error probability is $\approx 4 \times 10^{-4}$.

Error performance of the proposed schemes are compared in Figure 3.12(a), for $m = 1$. The figure demonstrates that the proposed schemes offer the better error performance than that of the conventional DCSK scheme with one antenna at each end. DCSK-JAS

outperforms the DCSK-TAS as it employs multiple antennas at each end and hence, more combinations of received SNRs are available to select the maximum received SNR among them. However, with same (N_t, N_r) system, the DCSK-TAS/EGC completely outperforms the DCSK-JAS but at the cost of additional post-detection EGC.

In Figure 3.12(b), throughput of the proposed schemes are presented and compared. The achievable throughput is plotted against the average SNR for $m = 1$. It can be observed from the figure that the achievable throughput for DCSK is worst than that of the proposed schemes. Among the proposed schemes, DCSK-TAS/EGC has the best throughput performance. DSCK-JAS has almost similar throughput performance as DCSK-TAS/EGC for a (N_t, N_r) system, however, the later scheme has the advantage of having post-detection EGC at the receiving end.

3.4 SM-DCSK: High Data-Rate DCSK

In DCSK, half of the bit duration is used in sending the reference sequences. This results in the reduced data rate compared to the other modulation techniques having same bandwidth. Various methods have been proposed in literature to improve the data rate of DCSK [21, 22, 46–51]. However, the proposed methods achieve high data rate at the expense of additional circuitry or computational complexity.

Spatial modulation (SM) is proposed as transmission strategy to achieve high data rate by employing multiple transmit antennas [89]. In particular, SM uses symbol modulation as well as antenna index to transmit information. In SM, at any time instant, only one antenna transmits and hence, SM is energy-efficient compared to the conventional MIMO systems. For demodulation, sub-optimal detector [89] based on maximum received signal and optimal detector [90] based on maximum likelihood (ML) detection are proposed.

In this section, a high data rate DCSK system based on spatial modulation transmission strategy, namely SM-DCSK is proposed. We use the proposed scheme with two

transmit antennas and thus double the data rate by sending two information bits simultaneously. At the receiver end, sub-optimal detector is used to retrieve the symbol. Since the proposed scheme is based on a specific transmission strategy, it does not require any complicated system hardware. Further, SM-DCSK does not need any specific frame structure for its transmission and hence, in general, by using 2^l transmitting antennas, $(l+1)$ bits can be transmitted simultaneously. Thus, the proposed scheme offers a low-complexity, energy-efficient, hight data-rate system in fading environment. Symbol-error-rate (SER) of the proposed scheme is derived. Simulation results are presented to verify the theoretical analysis of the proposed scheme.

3.4.1 System Model

A basic communication system model with two transmitting and one receiving antenna is under consideration. The transmitter uses spatial modulation as transmission strategy. A SM-mapping table with two transmitting antennas is shown in Table 3.2. The first bit is mapped into transmitting antenna number whereas the second bit is mapped into transmitting bit. For example, to transmit input bit sequence $\{10\}$, the second antenna will transmit a DCSK modulated bit '-1'. At any time instant, the received signal can be represented as

$$r = h_j \otimes s + n, \tag{3.39}$$

where s is the DCSK modulated transmitted bit, n is AWGN with zero mean and variance $N_0/2$, h_j is the time-invariant frequency-selective fading channel from antenna j, $j \in \{1, 2\}$, to receiver link and $\otimes$ is the convolution operator. The channel h_j can be represented as $h_j(k) = \sum_{i=1}^{L} \alpha_{j,i}\delta(k - \tau_{j,i})$, where $\alpha_{j,i}$ and $\tau_{j,i}$ denote the attenuation and time delay of the ith path, respectively, and L is the number of independent fading paths [61]. Thus, the dimension of the channel vector h_j is $1 \times L$.

For Spatial demodulation, the antenna number estimation and the transmitted bit

Table. 3.2: SM-mapping Table

Information Bits	**Antenna Number**	**Transmit bit**
00	1	-1
01	1	$+1$
10	2	-1
11	2	$+1$

estimation are done separately. The first step for spatial demodulation is to find the maximum received signal, which can be obtained as [89]

$$\mathrm{Z} = \mathrm{H}^* \otimes r, \tag{3.40}$$

where H^* is the complex conjugate of the channel matrix H, which is assumed to be perfectly known at the receiver. For an information bit to be transmitted, the dimension of H is $I \times L$, where I is the number of transmitting antennas. Thus, for two transmitting antennas, the dimension of $\mathrm{H} = [h_1, h_2]^T$ is $2 \times L$. Further, it is assumed that all paths of the channel are normalized, i.e., each channel path has unity gain. Taking complex valued channel coefficients and assuming all paths of the channel are independent, i.e.,

$$E\left[\alpha^*_{m,t}\alpha_{j,i}\right] = \begin{cases} 1, & \text{if } m = j \text{ and } t = i \\ 0, & \text{else} \end{cases} \tag{3.41}$$

For equal average power in all path, $\alpha_{j,i}$ needs to be multiplied by $1/\sqrt{L}$ and thus, $\alpha_{j,i}\alpha^*_{j,i} = \frac{1}{L}$.

Now, the transmit antenna number can be estimated as [89]

$$\tilde{b}_a = \arg \max_{j \in \{1,2\}} (|Z_j|) \tag{3.42}$$

And the transmitted bit can be estimated using DCSK demodulation. Note that it is well known that the DCSK demodulation does not require CSI, however, the proposed scheme needs CSI for antenna estimation purpose. The increased complexity is reasonable for higher data rate.

3.4.2 Performance Analysis

SM involves two estimation processes on the received signal; transmit antenna number estimation and transmit bit estimation. It is assumed that the two estimation processes are independent and hence the SER for SM-DCSK can be given as [89]

$$\text{SER} = P_a + P_s - P_a P_s, \tag{3.43}$$

where P_a and P_s are the probability of error for antenna number estimation and the probability of error in bit estimation, respectively. The derivations for P_a and P_s are given below. For simplicity, we consider a two-ray fading channel model ($L = 2$) to derive P_a and P_s. It is assumed that all independent channels are subjected to the same channel conditions. Further, it is assumed that the delay is negligible as compared to the bit duration, i.e., $\tau \ll T_b$, to avoid ISI.

Probability of Error in Antenna Number Estimation

Assuming a signal s_k is transmitted from antenna 1, the received signal can be given as

$$r_k = \frac{\alpha_{1,1}}{\sqrt{2}} s_k + \frac{\alpha_{1,2}}{\sqrt{2}} s_{k-\tau} + n_k, \tag{3.44}$$

where $\alpha_{1,1}$ and $\alpha_{1,2}$ are the normalized channel coefficients of antenna 1 to the receiver link, τ is the time delay between two paths and n_k is AWGN with zero mean and variance $N_0/2$. It is assumed that CSI is perfectly known at the receiver. Using the channel statistics of antenna 1 to the receiver link and from Eq. 3.40 and Eq. 3.41, it can be shown that

$$g_k^{(1)} = h_1^* \otimes r_k = \frac{1}{2} s_k + \frac{1}{2} s_{k-2\tau} + \frac{\alpha_{1,1}^*}{\sqrt{2}} n_k + \frac{\alpha_{1,2}^*}{\sqrt{2}} n_{k-\tau}. \tag{3.45}$$

Similarly, from the knowledge of channel statistics of antenna 2 to the receiver link and using Eq. 3.40 and Eq. 3.41, it can be shown that

$$g_k^{(2)} = h_2^* \otimes r_k = \frac{\alpha_{2,1}^*}{\sqrt{2}} n_k + \frac{\alpha_{2,2}^*}{\sqrt{2}} n_{k-\tau}. \tag{3.46}$$

The decision statistics for antenna j can be given as

$$Z_j = \sum_{k=(2l-1)\beta+1}^{2l\beta} \left[\left(\mathrm{Re}\{g_k^{(j)}\} \right) \left(\mathrm{Re}\{g_{k-\beta}^{(j)}\} \right) \right]. \tag{3.47}$$

Hence, the probability of selecting an antenna incorrectly is

$$P_a = P\left(|Z_1| < |Z_2| \right). \tag{3.48}$$

Let $f_1(z)$ and $f_2(z)$ is the PDF of $|Z_1|$ and $|Z_2|$, respectively. Using Eq. 3.45 and Eq. 3.46, $f_1(z)$ and $f_2(z)$ are numerically evaluated using Kernel smoothing density estimation technique and plotted in Figure 3.13. If Z is the intersection point of the two PDFs, then the probability of incorrect antenna selection can be obtained using Eq. 3.48 as

$$P_a = \int_0^Z f_2(z)\, dz. \tag{3.49}$$

Error in Transmitted Bit Estimation

Output of the correlator can be given using Eq. 2.7 as

$$y_l = \sum_{k=(2l-1)\beta+1}^{2\beta l} \left[\left(\mathrm{Re}\{g_k^{(1)}\} \right) \left(\mathrm{Re}\{g_{k-\beta}^{(1)}\} \right) \right], \tag{3.50}$$

where $g_k^{(1)}$ is given in Eq. 3.45. Assuming $\tau \ll T_b$, y_l can be simplified as

$$\begin{aligned} y_l \approx \sum_{k=(2l-1)\beta+1}^{2l\beta} \Bigg[& \left(\frac{1}{2} b_l x_{k-\beta} + \frac{1}{2} b_l x_{k-\beta-2\tau} + \frac{\alpha_{1,1_{\mathrm{R}}}}{\sqrt{2}} n_k + \frac{\alpha_{1,2_{\mathrm{R}}}}{\sqrt{2}} n_{k-\tau} \right) \\ & \times \left(\frac{1}{2} x_{k-\beta} + \frac{1}{2} x_{k-\beta-2\tau} + \frac{\alpha_{1,1_{\mathrm{R}}}}{\sqrt{2}} n_{k-\beta} + \frac{\alpha_{1,2_{\mathrm{R}}}}{\sqrt{2}} n_{k-\beta-\tau} \right) \Bigg], \end{aligned} \tag{3.51}$$

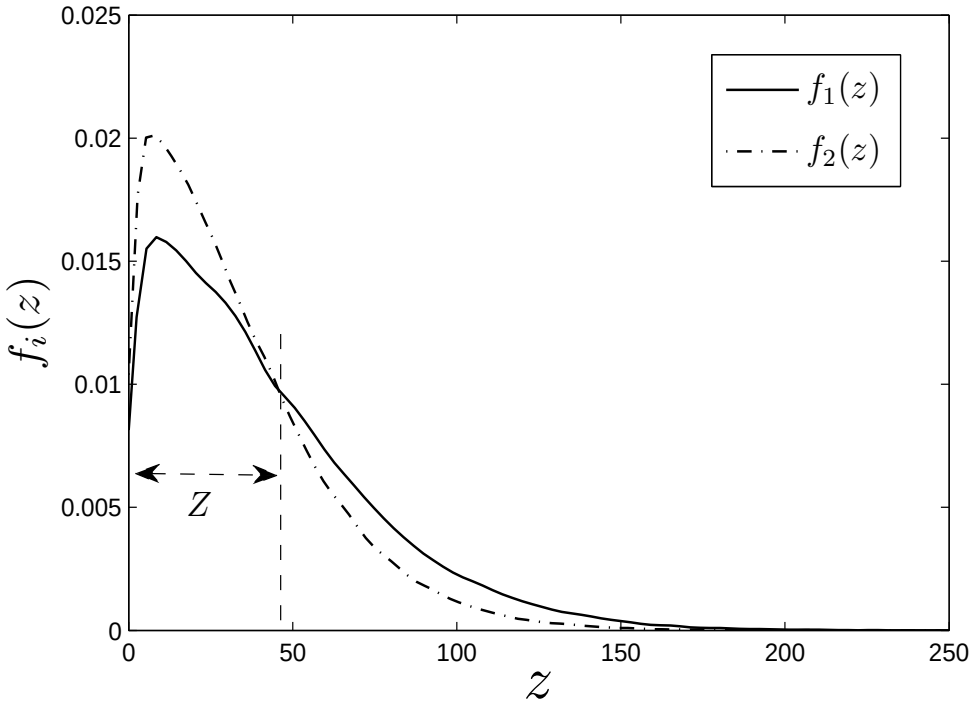

Figure 3.13: PDF of the decision statistics at 10 dB average SNR.

where, $\alpha_{1,1_{\mathrm{R}}} = \mathrm{Re}\left(\alpha_{1,1}^*\right)$ and $\alpha_{1,2_{\mathrm{R}}} = \mathrm{Re}\left(\alpha_{1,2}^*\right)$.

For large β, $\sum x_{k-\beta}x_{k-\beta-2\tau} \approx 0$. Thus, Eq. 3.51 can be further simplified as

$$\begin{aligned} y_l \approx \sum_{k=(2l-1)\beta+1}^{2l\beta} \Bigg[& \frac{1}{4}\Big\{ b_l x_{k-\beta}^2 + b_l x_{k-\beta-2\tau}^2 \Big\} \\ & + \frac{1}{2\sqrt{2}}\Big\{ \Big(x_{k-\beta} + x_{k-\beta-2\tau} \Big) \Big(\alpha_{1,1_{\mathrm{R}}} n_k + b_l \alpha_{1,1_{\mathrm{R}}} n_{k-\beta} + \alpha_{1,2_{\mathrm{R}}} n_{k-\tau} + b_l \alpha_{1,2_{\mathrm{R}}} n_{k-\beta-\tau} \Big) \Big\} \\ & + \frac{1}{2}\Big\{ \alpha_{1,1_{\mathrm{R}}}^2 n_k n_{k-\beta} + \alpha_{1,2_{\mathrm{R}}}^2 n_{k-\tau} n_{k-\beta-\tau} + \alpha_{1,1_{\mathrm{R}}} \alpha_{1,2_{\mathrm{R}}} \Big(n_k n_{k-\beta-\tau} + n_{k-\tau} n_{k-\beta} \Big) \Big\} \Bigg] \end{aligned} \tag{3.52}$$

For large spreading factor 2β, y_l can be Gaussian approximated [60]. Thus, Assuming $b_l = +1$, mean and variance of the decision variable y_l can be given as

$$\begin{aligned} E\left[y_l |_{\alpha_{1,1_{\mathrm{R}}}, \alpha_{1,2_{\mathrm{R}}}, b_l=+1} \right] &= \frac{1}{2}\beta E\left[x_k^2 \right] \\ \mathrm{var}\left[y_l |_{\alpha_{1,1_{\mathrm{R}}}, \alpha_{1,2_{\mathrm{R}}}, b_l=+1} \right] &= \frac{1}{8}\beta \mathrm{var}\left[x_k^2 \right] + \frac{1}{4}\beta \left(\alpha_{1,1_{\mathrm{R}}}^2 + \alpha_{1,2_{\mathrm{R}}}^2 \right) N_0 \mathrm{var}\left[x_k \right] \end{aligned}$$

$$+\frac{1}{4}\beta\left(\alpha_{1,1_{\mathrm{R}}}^{2}+\alpha_{1,2_{\mathrm{R}}}^{2}\right)^{2}\frac{N_0^2}{4}. \tag{3.53}$$

For logistic map being used, the conditional probability of error can be obtained as

$$\begin{aligned}
P_e &= \frac{1}{2}erfc\left(\frac{E\left[y_l|_{\alpha_{1,1_{\mathrm{R}}},\alpha_{1,2_{\mathrm{R}}},b_l=+1}\right]}{\sqrt{2\mathrm{var}\left[y_l|_{\alpha_{1,1_{\mathrm{R}}},\alpha_{1,2_{\mathrm{R}}},b_l=+1}\right]}}\right) \\
&= \frac{1}{2}erfc\left(\left[\frac{1}{2\beta}+\frac{4\left(\alpha_{1,1_{\mathrm{R}}}^{2}+\alpha_{1,2_{\mathrm{R}}}^{2}\right)N_0}{E_b}+\frac{2\beta\left(\alpha_{1,1_{\mathrm{R}}}^{2}+\alpha_{1,2_{\mathrm{R}}}^{2}\right)^{2}N_0^2}{E_b^2}\right]^{-\frac{1}{2}}\right) \\
&= \frac{1}{2}erfc\left(\left[\frac{1}{2\beta}+\frac{4\left(\gamma_{1,1}+\gamma_{1,2}\right)}{E_b/N_0}+\frac{2\beta\left(\gamma_{1,1}+\gamma_{1,2}\right)^{2}}{\left(E_b/N_0\right)^{2}}\right]^{-\frac{1}{2}}\right),
\end{aligned} \tag{3.54}$$

where E_b/N_0 is the SNR and $\gamma_{\mathrm{j,i}}=\alpha_{j,i_{\mathrm{R}}}^{2}$. Since, $\alpha_{j,i}$ is the normalized channel coefficient, $\mathrm{Re}\left(\alpha_{j,i}\right)$ can be given as $\alpha_{j,i_{\mathrm{R}}}=\cos(\theta)$, where θ is uniformly distributed in the interval $(0,2\pi]$. Thus, by applying the transformation of random variables, the PDF of $\gamma_{\mathrm{j,i}}$ can be given as

$$f\left(\gamma_{\mathrm{j,i}}\right)=\frac{1}{\pi\sqrt{\gamma_{\mathrm{j,i}}\left(1-\gamma_{\mathrm{j,i}}\right)}}, \tag{3.55}$$

where $0<\gamma_{\mathrm{j,i}}<1$.

Now, the average probability of error in bit estimation can be obtained using Eq. 3.54 and Eq. 3.55 as

$$P_s=\int_0^1\int_0^1 P_e\left(\gamma_{1,1},\gamma_{1,2}\right)f\left(\gamma_{1,1}\right)f\left(\gamma_{1,2}\right)d\gamma_{1,1}d\gamma_{1,2}. \tag{3.56}$$

Thus, substituting Eq. 3.49 and Eq. 3.56 in Eq. 3.43, the Symbol error probability of the system can be numerically evaluated.

3.4.3 Numerical and Simulation Results

The derived SER expression is numerically evaluated and compared with the MATLAB simulation results. Monte Carlo simulations are carried out to evaluate the performance of SM-DCSK system. The cubic map is used to generate the chaotic samples. In the simulation, we assume $L = 2$ and the two paths have equal average power gain. The path delays for two paths are assumed to be $(\tau_{j,1}, \tau_{j,2}) = (0, 1)$.

Symbol error rate is evaluated using Eq. 3.43, which depends on antenna number estimation error, i.e., P_a and transmitted bit estimation error, i.e., P_s. The Kernel smoothing density estimation technique is used to compute the error probability of antenna number estimation in Eq. 3.49 whereas the error probability for transmitted bit estimation in Eq. 3.56 is computed using the Gauss-Kronrod quadrature numerical integration technique. The SER is plotted against the average SNR in Figure 3.14(a), for $\beta = 64$. The analytical result matches closely with the simulation result. The estimated symbol is considered as correct only if the transmitted antenna number and the transmitted bit, both are estimated correctly. Since antenna number estimation is completely based on CSI, the contribution of error from it dominates the symbol error. The result shows an error floor in SER curve which comes from the ISI present in the channel. Note that with assumption $\tau \ll T_b$, the ISI can be neglected and hence, the expression of error probability in Eq. 3.56 is independent of τ. However, in the simulations, ISI is present which causes error floor in SER curve. Since, Eq. 3.49 is numerically evaluated using the simulation samples, the SER floor is present in analytical result also.

Simulation results presented in Figure 3.14(b) shows the effect of number of receiving antennas (A_{rx}) on the system performance. The signals received at each receiving antenna are combined using post-detection equal gain combiner [64]. The figure demonstrates an improvement in SER with increase in A_{rx}, as expected. For example, at 20 dB average SNR, SER improves from $\approx 1.0 \times 10^{-1}$ to $\approx 3.0 \times 10^{-2}$ when A_{rx} increases from 1 to 2.

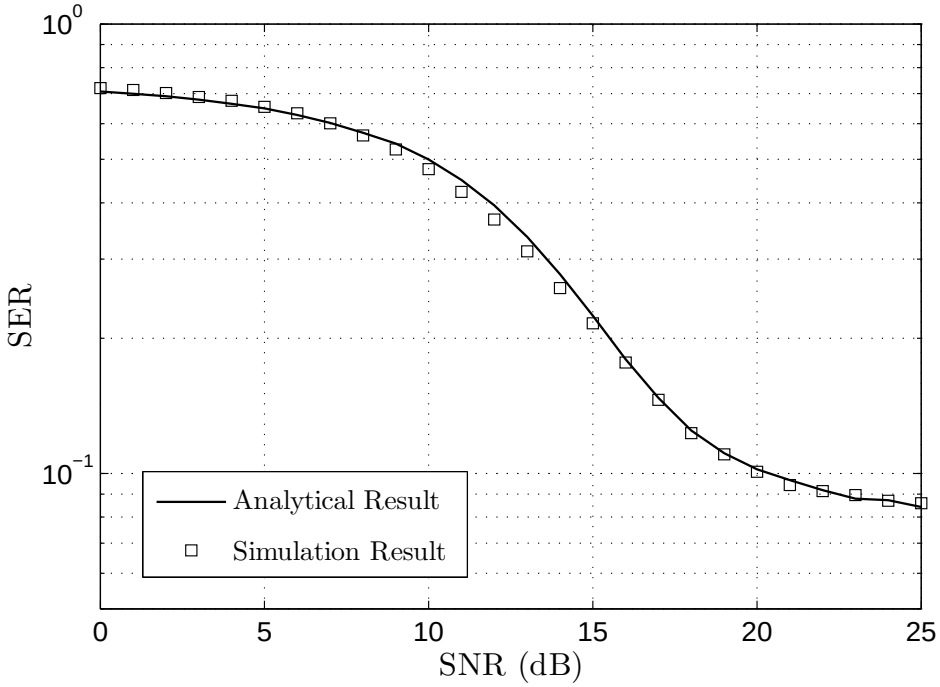

(a) SER performance of SM-DCSK scheme.

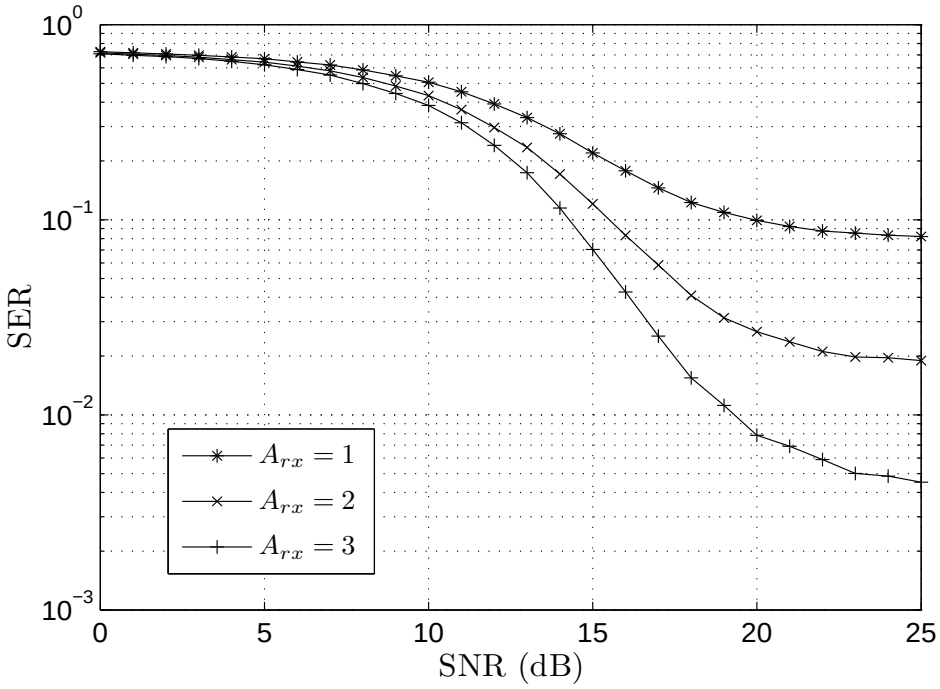

(b) SER performance of SM-DCSK with multiple receiving antennas.

Figure 3.14: SER performance of the SM-DCSK systems.

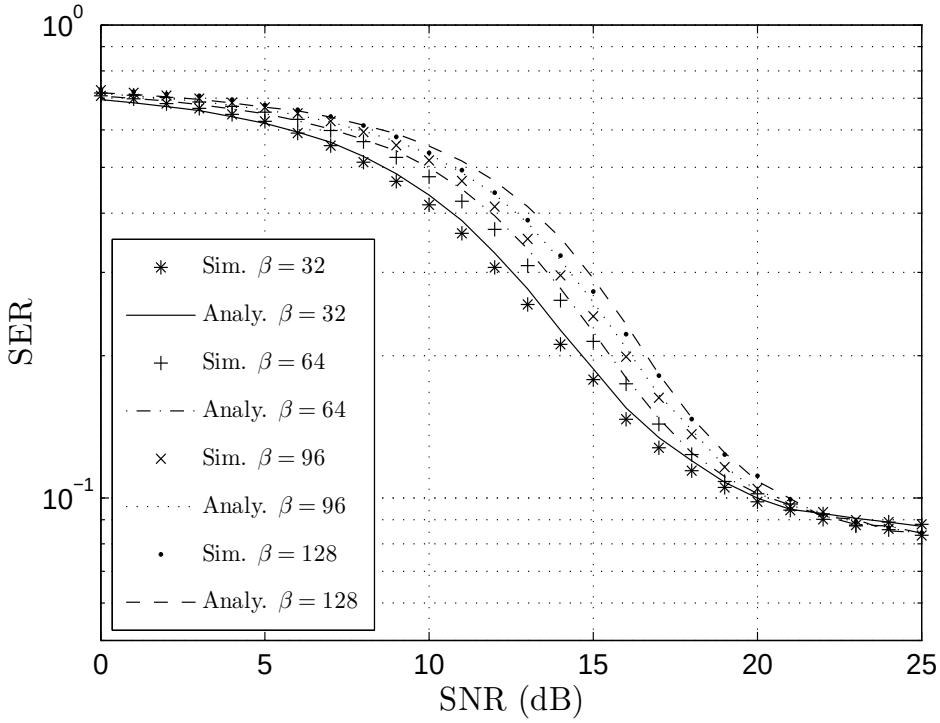

Figure 3.15: SER performance of the system for different spreading factor 2β.

Further, the SER improves from $\approx 3.0 \times 10^{-2}$ to $\approx 8.0 \times 10^{-3}$ on the increment of A_{rx} from 2 to 3.

Figure 3.15 illustrates the effect of the spreading factor (2β) on the SER performance of the system for β = 32, 64, 96 and 128. It can be observed from the figure that β does not affect widely on the SER performance of the proposed scheme. There is small improvement in SER within range of $5 - 20$ (dB) average SNR. However, at lower SNR (< 5 dB) and higher SNR (> 20 dB), there is little improvement.

3.5 Summary

In this chapter, the performance analysis of DCSK modulation in different wireless communication systems is presented. BER of the systems is plotted against the parameters of interest. The simulation results are also presented to verify the theoretical results.

First, DCSK modulation based cooperative scheme, DCSK-SR is presented. In DCSK-SR scheme, the best relay is selected from a multiple MIMO relay cluster to cooperate with the source node. The BER performance of the proposed scheme is evaluated in Nakagami-m fading environment. Mathematical expression for the PDF of SNR for each hop and end-to-end BER is derived. The results show that the proposed scheme improves the system BER significantly. It is concluded from the results that a better BER can be obtained by increasing the number of destination antennas as compared to the relay antennas. Further, the BER is more sensitive to the second hop as compared to the first hop.

Secondly, performance of bidirectional relaying system using DCSK modulation is analyzed in Nakagami-m fading environment. Orthogonal Walsh codes are adopted at the source nodes and the relay node utilizes network coding. The end-to-end communication can be achieved in two time slots and hence the proposed scheme provides spectrum and energy efficiency. Performance of the proposed scheme is compared with the DCSK traditional transmission scheme. BER of the DCSK-BDR scheme is also compared with that of the CDMA-BDR scheme and it is observed that DCSK-BDR outperforms CDMA-BDR at high SNR range.

Thirdly, DCSK modulation based TAS schemes are proposed in which transmitter utilizes transmit antenna selection diversity to make the remote unit receivers cost-effective and less hardware complex. In particular, DCSK-TAS, DCSK-JAS and DCSK-TAS/EGC schemes are proposed for different receiver structure/specifications. Probability of error and throughput of the proposed schemes are numerically evaluated for Nakagami-m fading channels. The proposed schemes completely outperform the conventional DCSK modulation with single transmit and single receive antenna. It is concluded that the error performance of the proposed schemes can be improved by employing multiple antennas at transmitter/receiver. It is also concluded that DCSK-TAS/EGC has the best performance among the proposed schemes, however, the improvement in performance of the

DCSK-TAS/EGC requires additional circuit complexity of the post-detection EGC.

Finally, a novel SM-DCSK scheme is proposed to achieve high data-rate. The data rate of DCSK improves by a factor of two by using the proposed scheme. However, with the implementation of multiple transmit antennas, higher data-rate can be achieved. Mathematical expression for SER of the proposed scheme is derived. It is concluded that the estimation in antenna error dominates the symbol error. Further, the SER performance of SM-DCSK improves if the receiver employs multiple antennas. Since, SM is a transmission strategy and it does not require changes in circuit design or in frame structure of the transmitted signal, a better data rate can be obtained if other modulation techniques such as CDSK, HE-DCSK or RM-DCSK, are used with SM transmission strategy.

Chapter 4

Conclusion and Future Work

In the past two decades, chaotic modulations have drawn a great attention in wireless communication applications due to their excellent anti-fading and anti-intercept capabilities. Of particular interest is the differential chaos shift keying (DCSK) modulation, which is considered as a very promising chaotic modulation scheme that achieves not only good error performance, but also low implementation complexity. This thesis provides an insightful survey on DCSK communication system, as well as its performance analysis in different wireless communication systems. In this chapter, the thesis is summarized in the form of conclusion and some possible future work is also presented.

A brief history of chaos-based communication is presented in the first chapter. Specifically, our attention has been restricted to the relevant chaotic digital modulation techniques. Besides, in the first chapter, the recent research works on DCSK modulation are summarized in literature survey. A comprehensive survey of DCSK communication system is presented in the second chapter. In particular, a brief discussion on chaotic signal generation, a compact overview of DCSK modulation and demodulation, and basic principle of Walsh codes based multiple-access DCSK system are presented. The performance analysis methodology of DCSK communication system is also presented in the second chapter. The analyzed DCSK modulation based communication systems are enumerated below:

1. Performance analysis of DCSK modulation over L-path fading channels is presented. Performance of the system is evaluated in Nakagami-m fading channels and plotted for the parameters of interest.

2. Performance analysis of the DCSK-EGC system is presented over Nakagami-m fading channels.

In the third chapter, the performance of DCSK modulation is analyzed in different wireless communication systems. In particular, DCSK-SR, DCSK-BDR, DCSK-TAS and SM-DCSK systems are proposed and analyzed. Focusing on the analytical approach, mathematical expressions for various performance measures such as BER/SER and throughput of the proposed systems are obtained. The mathematically obtained performance parameter expressions are numerically evaluated, plotted and the effect of different parameters on the system performance is studied. Numerically obtained results are compared with the Monte Carlo simulations results. The numerical results match closely with the simulation results. The analyzed DCSK modulation based wireless communication systems are enumerated below:

1. Performance of the DCSK-SR system is analyzed in Nakagami-m fading channels. Mathematical expressions for the PDF of received SNR for each hop and end-to-end BER are derived.

2. The end-to-end BER expression for the DCSK-BDR system over Nakagami-m fading channels is derived and the BER performance is studied.

3. BER and throughput of the DCSK modulation based transmit antenna selection schemes are derived. Performance of the DCSK-TAS, DCSK-JAS and DCSK-TAS/EGC schemes are evaluated over Nakagami-m fading channels.

4. SER of the high data-rate SM-DCSK scheme is derived and the performance is studied.

Future Work

A few research problems that can be taken up for analysis are enumerated below:

1. Investigation and analysis of DCSK selection relaying system with no CSI available.
2. Investigation and analysis of DCSK transmit antenna selection schemes with no CSI available.
3. Extension of SM-DCSK systems with more than two transmit antennas to obtain higher data-rate.
4. Performance analysis of DCSK modulation in UWB communication systems.

References

[1] J. P. Crutchfield, J. D. Farmer, N. H. Packard, and R. S. Shaw, "Chaos," *Sci. Amer.*, vol. 254, no. 12, pp. 46–57, 1986.

[2] R. C. Hilborn, *Chaos and Nonlinear Dynamics*, 2nd ed. Oxford University Press, 2009.

[3] J. C. Feng and C. K. Tse, *Reconstruction of Chaotic Signals with Application to Chaos Based Communications*. Tsinghua University Press, Singapore: World Scientific, 2008.

[4] E. N. Lorenz, "Deterministic nonperiodic flow," *J. Atmospheric Sciences*, vol. 20, no. 2, pp. 130–141, Mar. 1963.

[5] L. O. Chua, "Dynamic nonlinear networks: State-of-the-art," *IEEE Trans. Circuits Syst.*, vol. 27, no. 11, pp. 1059–1087, Nov. 1980.

[6] L. O. Chua, M. Komuro, and T. Matsumoto, "The double scroll family," *IEEE Trans. Circuits Syst.*, vol. 33, no. 11, pp. 1072–1118, Nov. 1986.

[7] M. P. Kennedy, "Three steps to chaos–Part I: Evolution," *IEEE Trans. Circuits Syst. I*, vol. 40, no. 10, pp. 640–656, Oct. 1993.

[8] ——, "Three steps to chaos–Part II: A Chua's circuit primer," *IEEE Trans. Circuits Syst. I*, vol. 40, no. 10, pp. 657–674, Oct. 1993.

[9] L. M. Pecora and T. L. Carroll, "Synchronization in chaotic systems," *Phys. Rev. Lett.*, vol. 64, pp. 821–824, 1990.

[10] J. P. Eckmann and D. Ruelle, "Ergodic theory of chaos and strange attractors," *Rev. Modern Phys.*, vol. 57, no. 3, pp. 617–656, Jul. 1985.

[11] T. S. Parker and L. O. Chua, "Chaos: A tutorial for engineers," *Proc. IEEE*, vol. 75, no. 8, pp. 982–1008, Aug. 1987.

[12] A. V. Oppenheim, G. W. Wornell, S. W. Isabelle, and K. M. Cuomo, "Signal processing in the context of chaotic signals," *Proc. IEEE ICCASP*, vol. 4, pp. 117–120, 1992.

[13] G. Kolumbán, M. P. Kennedy, and L. O. Chua, "The role of synchronization in digital communications using chaos–Part I: Fundamentals of digital communications," *IEEE Trans. Circuits Syst. I*, vol. 44, no. 10, pp. 927–936, Oct. 1997.

[14] F. C. M. Lau and C. K. Tse, *Chaos-Based Digital Communication Systems.* Heidelberg: Springer-Verlag, 2003.

[15] H. Dedieu, M. P. Kennedy, and M. Hasler, "Chaos shift keying: Modulation and demodulation of a chaotic carrier using self-synchrinized Chua's circuits," *IEEE Trans. Circuits Syst.*, vol. 40, no. 10, pp. 634–642, Oct. 1993.

[16] G. Kolumbán, M. P. Kennedy, and L. O. Chua, "The role of synchronization in digital communications using chaos–Part II: Chaotic modulation and chaotic synchronization," *IEEE Trans. Circuits Syst. I*, vol. 45, no. 11, pp. 1129–1140, Nov. 1998.

[17] G. Kolumbán and M. P. Kennedy, "The role of synchronization in digital communication using chaos–Part III: Performance bounds for correlation receivers," *IEEE Trans. Circuits Syst. I*, vol. 47, no. 12, pp. 1673–1683, Dec. 2000.

[18] G. Kolumbán, "Theoretical noise performance of correlator-based chaotic communications schemes," *IEEE Trans. Circuits Syst.*, vol. 47, no. 12, pp. 1692–1701, Dec. 2000.

[19] G. Kolumbán, B. Vizvári, W. Schwarz, and A. Abel, "Differential chaos shift keying: A robust coding for chaos communication," *Proc. NDES*, pp. 87–92, 1996.

[20] G. Kolumbán, G. Kis, M. P. Kennedy, and Z. Jákó, "FM-DCSK: A new and robust solution for chaotic communications," *Proc. NOLTA*, pp. 117–120, 1997.

[21] M. Sushchik, L. S. Tsimring, and A. R. Volkovskii, "Performance analysis of correlation-based communication schemes utilizing chaos," *IEEE Trans. Circuits Syst. I*, vol. 47, no. 12, pp. 1684–1691, Dec. 2000.

[22] Z. Galias and G. M. Maggio, "Quadrature chaos-shift keying: Theory and performance analysis," *IEEE Trans. Circuits Syst. I*, vol. 48, no. 12, pp. 1510–1519, Dec. 2001.

[23] A. J. Lawrance and G. Ohama, "Exact calculation of bit error rates in communication systems with chaotic modulation," *IEEE Trans. Circuits Syst. I*, vol. 50, no. 11, pp. 1391–1400, Nov. 2003.

[24] G. Kaddoum, P. Charge, and D. Roviras, "A generalized methodology for bit-error-rate prediction in correlation-based communication schemes using chaos," *IEEE Commun. Lett.*, vol. 13, no. 8, pp. 567–569, Aug. 2009.

[25] M. Long, Y. Chen, and F. Peng, "Simple and accurate analysis of BER performance for DCSK chaotic communication," *IEEE Commun. Lett.*, vol. 15, no. 11, pp. 1175–1177, Nov. 2011.

[26] M. P. Kennedy, G. Kolumbán, G. Kis, and Z. Jákó, "Recent advances in communicating with chaos," *Proc. IEEE ISCAS*, vol. 4, pp. 461–464, May 1998.

[27] G. Kolumbán, M. P. Kennedy, Z. Jákó, and G. Kis, "Chaotic communications with correlator receivers: Theory and performance limits," *Proc. IEEE*, vol. 90, no. 5, pp. 711–731, May 2002.

[28] F. C. M. Lau, M. M. Yip, C. K. Tse, and S. F. Hau, "A multiple-access technique for differential chaos-shift keying," *IEEE Trans. Circuits Syst. I*, vol. 49, no. 1, pp. 96–104, Jan. 2002.

[29] W. M. Tam, F. C. M. Lau, and C. K. Tse, "Analysis of bit error rates for multiple access CSK and DCSK communication systems," *IEEE Trans. Circuits Syst. I*, vol. 50, no. 5, pp. 702–707, May 2003.

[30] F. C. M. Lau, K. Y. Cheong, and C. K. Tse, "Permutation-based DCSK and multiple-access DCSK systems," *IEEE Trans. Circuits Syst. I*, vol. 50, no. 6, pp. 733–742, Jun. 2003.

[31] J. Yao and A. J. Lawrance, "Performance analysis and optimization of multi-user differential chaos-shift keying communication systems," *IEEE Trans. Circuits Syst. I*, vol. 53, no. 9, pp. 2075–2091, Sep. 2006.

[32] S. Mandal and S. Banerjee, "Performance of differential chaos shift keying communication over multipath fading channels," *IEICE Trans.*, vol. E85-A, no. 1, pp. 1–10, Jan. 2002.

[33] Z. Zhou, T. Zhou, and J. Wang, "Exact BER analysis of differential chaos shift keying communication system in fading channels," *Proc. IEEE WCNMC*, pp. 1–4, 2008.

[34] Z. Zhou, J. Wang, and Y. Ye, "Exact BER analysis of differential chaos shift keying communication system in fading channels," *Wireless Personal Commun.*, vol. 53, no. 2, pp. 299–310, 2010.

[35] Y. Xia, C. K. Tse, and F. C. M. Lau, "Performance of differential chaos-shift-keying digital communication systems over a multipath fading channel with delay spread," *IEEE Trans. Circuits Syst. II*, vol. 51, no. 12, pp. 680–684, Dec. 2004.

[36] K. Thapaliya, Q. Yang, and K. S. Kwak, "Chaotic communications in MIMO systems," *Proc. 3rd Int. Conf. Embedded Software and Systems*, pp. 708–717, 2007.

[37] H. Ma and H. Kan, "Space-time coding and processing with differential chaos shift keying scheme," *Proc. IEEE International Conference on Communications (ICC)*, pp. 1–5, 2009.

[38] G. Kaddoum, M. Vu, and F. Gagnon, "Performance analysis of differential chaotic shift keying communications in MIMO systems," *Proc. IEEE ISCAS*, pp. 1580–1583, May 2011.

[39] S. Wang and X. Wang, "M-DCSK-based chaotic communications in MIMO multipath channels with no channel state information," *IEEE Trans. Circuits Syst. II*, vol. 57, no. 12, pp. 1001–1005, Dec. 2010.

[40] P. Chen, L. Wang, and F. C. M. Lau, "One analog STBC-DCSK transmission scheme not requiring channel state information," *IEEE Trans. Circuits Syst. I*, vol. 60, no. 4, pp. 1027–1037, Apr. 2013.

[41] J. Xu, W. Xu, L. Wang, and G. Chen, "Design and simulation of a cooperative communication system based on DCSK/FM-DCSK," *Proc. IEEE ISCAS*, pp. 2454–2457, 2010.

[42] W. Xu, L. Wang, and G. Chen, "Performance of DCSK cooperative communication systems over multipath fading channels," *IEEE Trans. Circuits Syst. I*, vol. 58, no. 1, pp. 196–204, Jan. 2011.

[43] Y. Fang, J. Xu, L. Wang, and G. Chen, "Performance of MIMO relay DCSK-CD systems over Nakagami fading channels," *IEEE Trans. Circuits Syst. I*, vol. 60, no. 3, pp. 757–767, Mar. 2013.

[44] J. Huang, Z. Xu, W. Xu, and L. Wang, "Error performance analysis of opportunistic relaying system based on DCSK," *Proc. IEEE ICTSPCC*, pp. 1649–1653, 2012.

[45] G. Kaddoum, F. Parzysz, and F. Shokraneh, "Low-complexity amplify-and-forward relaying protocol for non-coherent chaos-based communication system," *IET Communications*, vol. 8, no. 13, pp. 2281–2289, Sep. 2014.

[46] W. M. Tam, F. C. M. Lau, and C. K. Tse, "Generalized correlation-delay-shift-keying scheme for noncoherent chaos-based communication systems," *IEEE Trans. Circuits Syst. I*, vol. 53, no. 3, pp. 712–721, Mar. 2006.

[47] G. Kaddoum and F. Gagnon, "Design of a high-data-rate differential chaos-shift keying system," *IEEE Trans. Circuits Syst. II*, vol. 59, no. 7, pp. 448–452, Jul. 2012.

[48] H. Yang and G.-P. Jiang, "High-efficiency differential-chaos-shift-keying scheme for chaos-based noncoherent communication," *IEEE Trans. Circuits Syst. II*, vol. 59, no. 5, pp. 312–316, May 2012.

[49] ——, "Reference-modulated DCSK: A novel chaotic communication scheme," *IEEE Trans. Circuits Syst. II*, vol. 60, no. 4, pp. 232–236, Apr. 2013.

[50] G. Kaddoum, F. Richardson, and F. Gagnon, "Design and analysis of a multi-carrier differential chaos shift keying communication system," *IEEE Trans. Commun.*, vol. 61, no. 8, pp. 3281–3291, Aug. 2013.

[51] H. Yang, G.-P. Jiang, and J. Duan, "Phase–separated DCSK: A simple delay-component-free solution for chaotic communications," *IEEE Trans. Circuits Syst. II*, vol. 61, no. 12, pp. 967–971, Dec. 2014.

[52] A. Abel and W. Schwarz, "Chaos communication–principle, schemes and system analysis," *Proc. IEEE*, vol. 90, no. 5, pp. 691–710, May 2002.

[53] C.-C. Chong and S. K. Yong, "UWB Direct chaotic communication technology for low-rate WPAN applications," *IEEE Trans. Veh. Technol.*, vol. 57, no. 3, pp. 1527–1536, May 2008.

[54] G. Kaddoum and F. Shokraneh, "Analog network coding for multi-user multi-carrier differential chaos shift keying communication system," *IEEE Trans. Wireless Commun.*, vol. 14, no. 3, pp. 1492–1505, Mar. 2015.

[55] T. Geisel and V. Fairen, "Statistical properties of chaos in Chebyshev maps," *Physics Letters A*, vol. 105, no. 6, pp. 263–266, 1984.

[56] T. Kohda and A. Tsuneda, "Even- and odd-correlation functions of chaotic Chebyshev bit sequences for CDMA," *Proc. IEEE ISSSTA*, vol. 2, pp. 391–395, Jul. 1994.

[57] G. Kolumbán, G. Kis, F. C. M. Lau, and C. K. Tse, "Optimum noncoherent FM-DCSK detector: Application of chaotic GML decision rule," *Proc. IEEE ISCAS*, vol. 4, pp. IV–597–600, 2004.

[58] T. S. Rappaport, *Wireless Communications*, 2nd ed. Prentice Hall, 2010.

[59] J. G. Proakis, *Digital Communications*, 4th ed. McGraw–Hill, 2001.

[60] N. I. Chernov, "Limit theorems and markov approximations for chaotic dynamical systems," *Probability Theory and Related Fields*, vol. 101, no. 3, pp. 321–362, 1995.

[61] M. K. Simon and M. S. Alouini, *Digital Communications over Fading Channels*. John Wiley, 2000.

[62] S. Kim, J. Bok, and H. G. Ryu, "Performance evaluation of DCSK system with chaotic maps," *Proc. IEEE ICOIN*, pp. 556–559, Jan. 2013.

[63] D. Brennan, "Linear diversity combining techniques," *Proc. IRE*, vol. 47, pp. 1075–1102, Jun. 1959.

[64] G. L. Stuber, *Principles of Mobile Communications*, 2nd ed. Kluwer, 2002.

[65] P. Chen, L. Wang, and G. Chen, "DDCSK-Walsh coding: A reliable chaotic modulation-based transmission technique," *IEEE Trans. Circuits Syst. II*, vol. 59, no. 2, pp. 128–132, Feb. 2012.

[66] A. Sendonaris, E. Erkip, and B. Aazhang, "User cooperation diversity–Part I: System description," *IEEE Trans. Commun.*, vol. 51, no. 11, pp. 1927–1938, Nov. 2003.

[67] ——, "User cooperation diversity–Part II: Implementation aspects and performance analysis," *IEEE Trans. Commun.*, vol. 51, no. 11, pp. 1939–1948, Nov. 2003.

[68] J. N. Laneman, D. N. C. Tse, and G. W. Wornell, "Cooperative diversity in wireless networks: Efficient protocols and outage behavior," *IEEE Trans. Inform. Theory*, vol. 50, no. 12, pp. 3062–3080, Dec. 2004.

[69] Y. Fan and J. Thompson, "MIMO configurations for relay channels: Theory and practice," *IEEE Trans. Wireless Commun.*, vol. 6, no. 5, pp. 1774–1786, May 2007.

[70] H. Boujemaa, "Exact and asymptotic BEP of cooperative DS-CDMA systems using decode and forward relaying in the presence of multipath propagation," *IEEE Trans. Wireless Commun.*, vol. 8, no. 9, pp. 4464–4469, Sep. 2009.

[71] I. S. Gradshteyn and I. M. Ryzhik, *Table of Integrals, Series, and Products*, 7th ed. Academic Press, 2007.

[72] O. C. Ugweje, "Selection diversity for wireless communications in Nakagami-fading with arbitrary parameters," *IEEE Trans. Veh. Technol.*, vol. 50, no. 6, pp. 1437–1448, Nov. 2001.

[73] C. E. Shannon, "Two-way communication channels," *Proc. 4th Berkeley Symp. Math. Stat. and Prob.*, vol. 1, pp. 611–644, 1961.

[74] B. Rankov and A. Wittneben, "Spectral efficient protocols for half-duplex fading relay channels," *IEEE J. Sel. Areas Commun.*, vol. 25, no. 2, pp. 379–389, Feb. 2007.

[75] R. Ahlswede, N. Cai, S.-Y. Li, and R. Yeung, "Network information flow," *IEEE Trans. Inform. Theory*, vol. 46, no. 4, pp. 1204–1216, Jul. 2000.

[76] S.-Y. Li, R. Yeung, and N. Cai, "Linear network coding," *IEEE Trans. Inform. Theory*, vol. 49, no. 2, pp. 371–381, Feb. 2003.

[77] Y. Wu, P. A. Chou, and S. Y. Kung, "Information exchange in wireless networks with network coding and physical-layer broadcast," Microsoft Research, Redmond WA, Technical Report MSR-TR-2004-78, Aug. 2004.

[78] S. Zhang, S. C. Liew, and P. Lam, "Physical-layer network coding," *Proc. ACM MobiCom*, Sep. 2006.

[79] S. Zhang, S. C. Liew, and L. Lu, "Physical layer network coding schemes over finite and infinite fields," *Proc. IEEE GLOBECOM*, pp. 1–6, Nov. 2008.

[80] S. Alamouti, "A simple transmit diversity technique for wireless communications," *IEEE J. Sel. Areas Commun.*, vol. 16, no. 8, pp. 1451–1458, Oct. 1998.

[81] A. Molisch and M. Win, "MIMO systems with antenna selection," *IEEE Microw. Mag.*, vol. 5, no. 1, pp. 46–56, Mar. 2004.

[82] S. Sanayei and A. Nosratinia, "Antenna selection in MIMO systems," *IEEE Commun. Mag.*, vol. 42, no. 10, pp. 68–73, Oct. 2004.

[83] Z. Chen, J. Yuan, and B. Vucetic, "Analysis of transmit antenna selection/maximal-ratio combining in Rayleigh fading channels," *IEEE Trans. Veh. Technol.*, vol. 54, no. 4, pp. 1312–1321, Jul. 2005.

[84] R. Irmer and G. Fettweis, "Combined transmitter and receiver optimization for multiple-antenna frequency-selective channels," *Proc. 5th Int. Symp. Wireless Personal Multimedia Communications*, pp. 412–416, 2002.

[85] Z. Chen, Z. Chi, Y. Li, and B. Vucetic, "Error performance of maximal-ratio combining with transmit antenna selection in flat Nakagami-m fading channels," *IEEE Trans. Wireless Commun.*, vol. 8, no. 1, pp. 424–431, Jan. 2009.

[86] A. F. Coskun and O. Kucur, "Performance of joint transmit and receive antenna selection in Nakagami-m fading channels," *Proc. European Wireless Conference (EW)*, pp. 314–317, Apr. 2010.

[87] H. A. David and H. N. Nagaraja, *Order Statistics*, 3rd ed. New Jersey: John Wiley, 2003.

[88] T. Cover and J. Thomas, *Elements of Information Theory*. New York: Wiley, 1991.

[89] R. Y. Mesleh, H. Haas, S. Sinanovic, C. W. Ahn, and S. Yun, "Spatial modulation," *IEEE Trans. Veh. Technol.*, vol. 57, no. 4, pp. 2228–2241, Jul. 2008.

[90] J. Jeganathan, A. Ghrayeb, and L. Szczecinski, "Spatial modulation: Optimal detection and performance analysis," *IEEE Commun. Lett.*, vol. 12, no. 8, pp. 545–547, Aug. 2008.

Publication Information

Journals

1. Atul Kumar and P. R. Sahu,"Performance Analysis of DCSK-SR Systems Based on Best Relay Selection in Multiple MIMO Relay Environment," *Int. J. Electron. Commun. (AEÜ)*, 70 (1), pp. 18–24, 2016.

2. Atul Kumar and P. R. Sahu,"Performance Analysis of Differential Chaos Shift Keying Modulation with Transmit Antenna Selection," *IET Communications*, 10 (3), pp. 327–335, 2016.

3. Atul Kumar and P. R. Sahu,"BER Analysis of DCSK Bidirectional Relaying Systems over Nakagami-m Fading Channels," *Int. J. Electron. Commun. (AEÜ)*, under review.

4. Atul Kumar and P. R. Sahu,"Spatially Modulated Differential Chaos Shift Keying Modulation Scheme and Performance Analysis," *IET Communications*, under review.

Conferences

1. Atul Kumar, P. R. Sahu, and Jibanananda Mishra,"Performance Analysis of DCSK Modulation with Diversity Combining Not Requiring Channel State Information," *Proc. IEEE National Conference on Communications (NCC)*, 2016.